Summer 8-14-2015

CCR5 and the Blood Brain Barrier During HIV-1 Infection and Cell-Cell Communications

Shawna M. Woollard
University of Nebraska Medical Center

CCR5 AND THE BLOOD BRAIN BARRIER DURING HIV-1 INFECTION AND CELL-CELL COMMUNICATIONS

By

Shawna Michelle Woollard

A DISSERTATION

Presented to the Faculty of

The Graduate College of The University of Nebraska

In Partial Fulfillment of the Requirements

For the Degree of Doctor of Philosophy

Department of Pharmacology and Experimental Neuroscience
University of Nebraska Medical Center
Omaha, Nebraska

Under the Supervision of Dr. Georgette D. Kanmogne

August, 2015

Supervisory Committee:

R. Lee Mosley, Ph.D. Pawel Ciborowski, Ph.D.

Tammy L. Kielian, Ph.D. Jialin Zheng, M.D.

Acknowledgments

It is an honor to give thanks to all the people who have helped me through this journey.

First and foremost I must thank my mentor, Dr. Georgette D. Kanmogne, without her support and guidance this work would have not been possible. I truly appreciate everything she has done for me. Under her supervision I have been able to improve my scientific and writing abilities. I am so thankful for her help in allowing me to become a better scientist and I am thankful that she never gave up on me. I also must thank my supervisory committee whose constructive criticism helped improve my project. I give my gratitude to the various people who have contributed to my project: Dr. JoEllyn McMillan's laboratory for their help with UPLC, Dr. Poluektova's laboratory for their help with the animal experiments and the use of their equipment, the Flow Cytometry core, and Dr. Joe Zhou at UNL for help with confocal microscopy.

I also need to thank both the past and present members of Dr. Kanmogne's laboratory who have assisted me in many ways. I have to thank Sangya Singh, who taught me the basic techniques performed in the laboratory and aided me in my project. I also have to thank Hong Li for her vast knowledge of immunohistochemistry and immunofluorescence, and for being my partner for the animal studies. Lastly, Dr. Biju Bhargavan, who has given me great advice and encouragement along the way, has always been a friendly face in the lab, and has always been there when I needed to vent.

I would like to thank my friends, both in Omaha and elsewhere. Specifically, I thank Dara Storm for her great friendship and for introducing me to a large group of

friends here in Omaha, including my boyfriend. I am also thankful for my professors at Capital University.

I must thank my boyfriend, Thomas Boyko, who encouraged me when my motivation waned, who comforted me when things weren't going well, and who distracted me when I needed a break. I am so grateful for everything he has done and that he is a part of my life. I thank our wonderful cats: Desmond, Graeme, Hal, and Dave. They bring me large amounts of joy everyday. I also thank Thomas's family for allowing me to become part of their family.

Finally, I thank my entire family, especially my mom, Thomasine Woollard. It has been so hard being away from her. She has always supported me in whatever I wanted to do and has never doubted me. I am so grateful that I have her in my life. I also thank my sister, Rachel Rotilio, and my brother, Eric Woollard. Lastly, I thank my grandmother Cecilia McMillan and my late grandfather, Thomas McMillan. I wish he could have been here to see what I have accomplished, but I know he would be proud of me.

CCR5 AND THE BLOOD BRAIN BARRIER DURING HIV-1 INFECTION AND CELL-CELL COMMUNICATIONS

Shawna M. Woollard, Ph.D.

University of Nebraska, 2015

Supervisor: Georgette Kanmogne, Ph.D., MPH

Human Immunodeficiency Virus (HIV-1) infection often results in blood-brain barrier (BBB) dysfunction and central nervous system (CNS) impairment. Since most viral strains that cross the BBB and enter the CNS are macrophage-tropic and use the C-C chemokine receptor type-5 (CCR5) to enter and infect target cells, we hypothesized that CCR5 plays a major role in monocytes-endothelial interactions and HIV-induced BBB dysfunction. Because the cytoskeleton is responsible for cellular morphology and motility, we further hypothesized that HIV-induced monocyte-endothelial interactions and transendothelial migration involve cytoskeletal changes and that CCR5 blockers would also affect these changes. To this end we used two small molecule CCR5 antagonists, TAK-779 and maraviroc (MVR), to evaluate the role of CCR5 on cytoskeletal changes in HIV-1-infected monocytes following monocyte-endothelial interactions. We found that HIV-1 infection of monocytes resulted in the upregulation of cytoskeletal-associated proteins following monocyte-endothelial interactions. Proteins identified included Rac1, ERK1/2, and cortactin. Rac1 phosphorylation at serine 71 (s71) was upregulated in our *in vitro* studies and this upregulation was validated in analyses of *ex-vivo* brain tissues of HIV-1-infected humans. We next examined the effect of MVR treatment on HIV-1-induced BBB injury and CNS infection *in vivo* using humanized mice. We hypothesized that MVR treatment could diminish HIV-induced BBB injury and CNS infection. HIV-1 infection resulted in decreased expression of the tight junction proteins claudin-5 and ZO-2 in the animals' brain blood vessels and MVR treatment partially attenuated these

changes. Furthermore, our data showed that MVR enters the CNS and MVR treatment reduced viral loads in brain tissues. In conclusion, this study suggests that blocking CCR5 can diminish HIV-1-induced cytoskeletal changes, diminish BBB injury and CNS infection.

Abbreviations

6-HB: Six-helix bundle

ADL: Activities of daily living

AIDS: Acquired immune deficiency syndrome

ANI: Asymptomatic neurocognitive impairment

AP-1: Activator protein 1

ARP 2/3: Actin related protein 2/3

ART: Antiretroviral therapy

AZT: Zidovudine

BBB: Blood-Brain Barrier

BH: Benjamini-Hochberg

BMVEC: Brain microvascular endothelial cells

BSA: Bovine serum albumin

CCL: Chemokine (C-C motif) ligand

CCR: C-C chemokine receptor

CCR5Δ32: 32-bp deletion in the CCR5 gene

CFDA: 5-carboxyfluorescein diacetate, acetoxymethyl ester

CNS: Central nervous system

Cortactin: CTTN

CSF: Cerebrospinal fluid

Ct: Threshold cycle

CXCR4: C-X-C chemokine receptor type 4

CYP3A: Cytochrome P450 3A

DAB: 3,3'-diaminobenzidine

DMEM: Dulbecco's modified eagles media

DMSO: Dimethyl sulfoxide

ECL: Extracellular loop

ENF: Enfuvirtide

ERK1/2: Extracellular signal-regulated kinase 1/2

FACS: Fluorescence-activated cell sorting

FAK: Focal adhesion kinase

FDA: Food and Drug Administration

GAPDH: Glyceraldehyde 3-phosphate dehydrogenase

GDP: Guanosine Diphosphate

GFAP: Glial fibrillary acidic protein

GLUT1: Glucose transporter-1

GPCR: G-protein coupled receptor

GTP: Guanosine triphosphate

HAART: Highly active antiretroviral therapy

HAD: HIV-associated dementia

HAND: HIV associated neurocognitive disorders

HBMEC: Human brain microvascular endothelial cells

HIV: Human Immunodeficiency Virus

HIVE: HIV encephalitis

HR: Heptad repeat

I.P.: Intraperitoneally

IBA1: Ionized calcium binding adapter molecule-1

IC50: Half maximal inhibitory concentration

IDV: Indinavir

IL: Interleukin

IPA: Ingenuity Pathway Anaylsis

IS: Internal standard

JAK: Janus Kinase

JAM: Junctional Adhesion Molecule

JNK: c-Jun N-terminal kinase

LTR: Long terminal repeat

MAPK: Mitogen activated protein kinase

MAP2: Microtubule-associated protein-2

MDM: Monocyte-derived macrophages

MGB: Minor groove binder

MMP: Matrix metallopeptidase

MND: Mild neurocognitive disorder

MOI: Multiplicity of infection

MOTIVATE: Maraviroc versus Optimized Therapy in Viremic Antiretroviral Treatment-Experienced Patients

MPER: Membrane-proximal external region

MVR: Maraviroc

Nef: Negative factor

NF-κB: Nuclear factor kappa-light-chain-enhancer of activated B cells

NGS: Normal goat serum

NMDAR: N-methyl-D-aspartate receptor

NSG: Non-obese diabetic, severe combined immunodeficient, IL2 receptor gamma chain deficient mice

NRTI: Nucleoside reverse-transcriptase inhibitors

OATP: Organic anion transporting polypeptide

ORF: Open reading framep.i.: post infection

PAK: p21-activated kinase

PBL: Peripheral blood lymphocyte

Pgp: P-glycoprotein

PI3K: Phosphatidylinositol-4,5-bisphosphate 3-kinase

PKB: Protein kinase B

PTM: Post translational modification

qRT-PCR: Real time quantitative reverse transcription PCR

Rev: Regulator for expression of viral proteins

RT: Reverse transcriptase

SEM: Standard error of mean

STAT: Signal transducers and activators of transcription

TAK: TAK-779

Tat: Transactivator or transcription

TCID50: Tissue culture infectious doses

TEER: Transendothelial electrical resistance

TJ: Tight Junction

TNFα: Tumor necrosis factor

Tregs: Regulatory T-cells

TTBS: Tris-Buffered Saline and Tween 20

UPLC-MS/MS: Ultra performance liquid chromatography-tandem mass spectrometry

VASP: Vasodilator-stimulated phosphoprotein

VEGFR: Vascular endothelial growth factor receptor

WNV: West Nile virus

Zonula Occludens: ZO

Table of Contents

Chapter 1

Introduction

1.1 Background

Since its discovery in the early 1980's, the human immunodeficiency virus-1 (HIV-1) has infected nearly 78 million people and killed approximately 39 million people [1]. Untreated HIV-1 infection typically results in acquired immune deficiency syndrome (AIDS). AIDS is diagnosed when a patient's CD4+ T-cell count drops to 200 cells/mm^3 or fewer or the patient presents with opportunistic infections and cancers, such as *Pneumocystis jirovecii* pneumonia, Kaposi's sarcoma, and progressive multifocal leukoencephalopathy [2, 3]. An estimated 35 million people are currently living with HIV/AIDS. Although prevalent worldwide, Sub-Saharan Africa bears the heaviest burden, with 71% of people living with HIV/AIDS located in this region [1].

HIV-1 is a lentivirus of the retroviridae family [4]. It infects cells of the immune system that express the CD4 receptor and/or the chemokine receptors CC chemokine receptor 5 (CCR5) or C-X-C chemokine receptor type 4 (CXCR-4), such as T-cells and monocytes/macrophages [4]. After HIV-1 enters the cell, the viral capsid uncoats, which allows for the release of viral RNA and proteins into the cytoplasm [4]. The viral RNA is then reverse transcribed into complementary DNA, forms the preintegration complex, and translocates to the nucleus, where the viral DNA is integrated into the host's DNA [4]. Once integrated, the virus hijacks the host cell's transcriptional machinery to synthesize viral RNA [4]. The viral RNA is then exported to the cytoplasm and translated into viral proteins [4]. Following translation, both the viral RNA and proteins are translocated to the plasma membrane, where they are packaged into immature virions [4]. The virions bud off the cell and are released into the extracellular fluid [4]. Once released, the virions undergo maturation and become infectious. These mature virions then go on to infect other cells [4].

The HIV-1 genome is approximately 9749 nucleotides in length consisting of 9 open reading frames (ORFs) encoding viral proteins [5]. The ORFs encode three

structural proteins: Gag, Pol, and Env (gp160); two regulatory proteins: transactivator of transcription (Tat) and Rev; and four accessory proteins: viral infectivity factor (Vif), viral protein R (Vpr), viral protein U (Vpu), and negative factor (Nef) [5]. Gag is proteolyzed into the matrix protein p17, the capsid protein p24, two spacer peptides, the nucleocapsid proteins p7, and p6 [5]. Pol is proteolyzed into reverse transcriptase (RT), RNase H, integrase, and HIV-1 protease [5]. The Env protein gp160 is proteolyzed into gp120 and gp41 [5].

Before the advent of antiretroviral therapy (ART) or highly active antiretroviral therapy (HAART) HIV-1 was almost always fatal. In developed countries, ART has transformed HIV-1 from a fatal infection into a chronic, lifelong illness. The first approved antiretroviral was the nucleoside analog reverse-transcriptase inhibitor (NRTI) Zidovudine/azidothymidine (AZT, Retrovir; ViiV healthcare, Brentford, London, UK) in 1987, followed shortly by several other NRTIs [6]. In 1996 two new classes of ART were introduced, the non-nucleoside reverse transcriptase inhibitors and protease inhibitors [6]. Two more classes of drugs were introduced in the 2000s, entry/fusion inhibitors and integrase inhibitors [6]. The success of ART has not come without its drawbacks, including increases in cardiovascular and metabolic diseases [7].

One of the biggest impediments to effective treatment and HIV eradication is the presence of viral reservoirs, such as the brain and lymphoid tissues. HIV enters the brain as early as 8-14 days post-infection, before most people are aware they have been infected [8]. Infection of the brain is often associated with neurocognitive impairment [9]. Poor central nervous system (CNS) penetration of many antiretroviral drugs allows for continued HIV replication in the brain [10]. Antiretroviral drugs that are able to prevent HIV entry into the brain and reduce the CNS viral load will be important in eliminating viral CNS reservoirs, which could help cure HIV-1.

1.2 CCR5

CCR5 is a member of the beta chemokine receptors found macrophages, dendritic cells, and memory T cells in the immune system; endothelium, epithelium, vascular smooth muscle and, fibroblasts; and microglia, neurons, and astrocytes in the central nervous system [11]. The *CCR5* gene is located on chromosome 3p21 and consists of 3 exons and 2 introns [12, 13]. Two promoters, one upstream and one downstream of exon 1, regulate its transcription [13]. The downstream promoter contains consensus TATA elements and potential binding sites for several transcription factors, such as signal transducers and activators of transcription (STAT), nuclear factor kappa-light-chain-enhancer of activated B cells (NF-κB), and activator protein 1 (AP-1) [13, 14]. CCR5 is a G-protein coupled receptor (GPCR) consisting of 352 amino acids, and like all GPCRs is comprised of 7 transmembrane domains with three extracellular loops and four intracellular loops [15, 16]. The N-terminal domain is extracellular, whereas the C-terminal domain is intracellular and the transmembrane domains appear to be arranged in a cluster instead of linear [17, 18]. CCR5 endogenous ligands are chemokine (C-C motif) ligand 3, 4, and 5 (CCL3, 4, and 5) [19-21].

Although the exact ligand-binding mechanism is unknown, the proposed mechanism involves the ligand first binding to the N-terminal domain followed by binding to the first and second extracellular loops [22]. The amino terminus activates the receptor via interactions with the transmembrane domains and the second extracellular loop is responsible for determining ligand specificity [22]. Following ligand binding and receptor activation, the receptor undergoes a conformational change and the receptor-bound G protein, Gi, Go, or Gq, dissociates from the receptor [23-28]. Activation of CCR5 can promote Ca2+ release and activation of phosphatidylinositol-4,5-bisphosphate 3-kinase (PI3K), mitogen-activated protein kinases (MAPK), focal adhesion kinase (FAK), proline-rich tyrosine kinase 2, extracellular signal-regulated

kinase 1/2 (ERK1/2), stress-activated protein kinase/ c-Jun N-terminal kinase (JNK), Rho GTPase, and protein kinase B (PKB) [29-33]. Following ligand binding, the receptors are internalized, which prevents further activation [34].

The major role of CCR5 is the recruitment and chemotaxis of immune cells to sites of inflammation [22]. Many other functions have been proposed. CCR5-deficient mice develop normally, but appear to have a partial defect in macrophage function [35]. Furthermore, these mice have an enhanced delayed-type hypersensitivity reaction and increased humoral responses to T cell-dependent antigenic challenge [35]. This suggests that CCR5 has a role in down-modulating T cell-dependent immune response. Interactions of CCR5 and CCL5 produce an anti-apoptotic signal in macrophages during viral infection [36]. It may also play a role In T-cell activation [37]. A 32 amino acid deletion mutation on exon 1 (CCR5Δ32) leads to decreased expression and dysfunction of CCR5 receptor [14, 38, 39].

CCR5 is known for its role as a co-receptor for HIV and is important in HIV transmission and disease progression. Individuals with the CCR5Δ32 mutation have delayed HIV-1 disease progression or are resistant to HIV-1 infection [14, 38-41]. Besides HIV-1, CCR5 can play a role, either beneficial or harmful, in other viral infections. CCR5 is critical for the survival of mice infected with West Nile virus (WNV) and humans with the CCR5Δ32 mutation appear to have a higher risk of death during WNV infection [42, 43]; absence of the CCR5 gene is also associated with increased prevalence and severity of tick-borne encephalitis [44]. On the other hand, absence of CCR5 may provide protection against smallpox infection and the bubonic plague [45]. In addition to viral infections, due to its role in chemotaxis and inflammation, CCR5 is suspected to play a part in several types of cancer. And as with viral infections this can be either beneficial or harmful. Strong expression of CCR5 is associated with non-metastatic colorectal cancer and weak CCR5 expression is associated with lymph node

metastasis and advanced disease [46]. Stromal cells that express CCR5 have been shown to increase pulmonary metastasis [47]. Interaction of CCL5 and CCR5 can enhance the migration of chondrosarcoma cells and human oral cancer cells [48, 49]. In gastric cancer, CCL5/CCR5 is highly expressed in the cancers with lymph node metastasis [50]. Furthermore, CCL5/CCR5 was shown to promote proliferation of gastric cancer cells and increase the tumor burden in mice transplanted with gastric cancer cells [51].

1.3 HIV Entry

HIV cellular entry is a complex, multiple step process. Entry begins by the virus binding to the cell surface [52]. This can be facilitated by attachment factors such as heparin sulfate or dendritic cell–specific intercellular adhesion molecular 3-grabbing non-integrin (DC-SIGN), although they are not required and differ between cell type and viral strain [52]. Attachment occurs through non-covalent interactions with the HIV Env and the attachment factor, and accelerates the interactions between the virus and the cell by bringing Env closer to CD4 and the co-receptor [52]. Attachment is often the rate-limiting step of viral infection [52]. Entry involves Env binding to two cellular receptors in a sequential pattern. Env is composed of trimers of two subunits: gp120 and gp41 [52]. The gp120 subunit, which is responsible for the receptor and co-receptor binding, contains five conserved domains (C1-C5) and five variable loops (V1-V5) [52]. The gp41 subunit, which is responsible for viral fusion, is a transmembrane protein composed of an N-terminal fusion peptide followed by N and C terminal heptad repeat (HR) regions and lastly a membrane-proximal external region (MPER) [53].

The initial binding step in HIV entry involves gp120 binding to CD4 [54]. CD4 is an immunoglobulin superfamily member found on the surface of immune cells such as T helper cells, macrophages, and dendritic cells [55]. The primary function of CD4 is to

assist the T-cell receptor in communicating with antigen-presenting cells, but also appears to enhance Fc region of IgG responses in other cell types [56]. CD4 contains four immunoglobulin domains (D1-D4), with D1 and D3 resembling immunoglobulin variable domains and D2 and D4 resembling immunoglobulin constant domains [57]. In T-cell-antigen presenting cell binding, the D1 domain of CD4 interacts with the β_2-domain of MHC class II molecules [57]. In HIV entry, gp120 binds to CD4 via the CD4 binding site, resulting the rearrangement of V1/V2, which in turn causes the rearrangement of V3 [58]. Rearrangement of the V3 loop leads to exposure of the co-receptor-binding site and positions the stem for co-receptor binding and exposure of the gp41 N-HR region [52]. Formation of the bridging sheet, the second co-receptor-binding site, also occurs during CD4 binding [59]. The bridging sheet is a four-stranded beta sheet comprised of two beta sheets from the inner domain and two beta sheets from the outer domain of gp120 [60].

Following V3 rearrangement and formation of the bridging sheet, co-receptor binding occurs [52]. The two most common co-receptors are the chemokine receptors CCR5 and CXCR4, with CCR5-using viruses (R5 viruses) being the predominant forms during the early stages of infection, while CXCR4-using viruses (X4 viruses) are associated with disease progression and AIDS [52]. The N-terminal domain and the extracellular loops of the co-receptors are important for gp120 binding [59]. During co-receptor binding, the V3 loop of gp120, which had previously undergone rearrangement during CD4 binding, binds to the second extracellular loop (ECL2) of the co-receptor [59]. Following gp120 binding to the ECL2, four sulfated tyrosine residues, at positions 3, 10, 14, and 15, in the N-terminal domain of the co-receptor interact with the base of the V3 loop and the bridging sheet [59].

Following co-receptor binding, the viral membrane fuses to the host cell membrane. The viral Env, a class I fusion protein, mediates viral fusion using a trimer-of-

hairpins pathway of membrane fusion [61]. When gp120 binds to CD4, gp41 undergoes a conformational change to its pre-hairpin orientation [59]. In this state, a trimer of helices is formed from the N-terminal peptides. The C-terminal helices remain attached to the viral membrane [62]. The rearrangement of the N-terminal peptides into a trimer allows the fusion peptide to be inserted into the cell membrane [62]. Once binding to the co-receptor occurs, gp120 dissociates from the viral Env, freeing gp41 and allowing it to engage with the cellular membrane [62]. During fusion gp41 undergoes further conformational change to form the hairpin fusion-active state, called the six-helix bundle (6-HB), in which the C-terminal HRs wrap around the N-terminal HRs in an antiparallel manner [63]. Each of the N-terminal HRs contains a hydrophobic deep pocket which helps to stabilize 6-HB formation and membrane fusion [64]. The 6-HB brings the viral membrane in close proximity to the cellular membrane resulting in fusion and the viral core entrance into the cell [65, 66]. HIV-1 entry is summarized in Figure 1-1.

Although it was previously thought that HIV-1 only enters the cell by fusing with the plasma membrane, it is now known that it can enter the cell via endocytosis [67]. HIV-1 has been shown to fuse with endosomes [68, 69]; and increasing the endosomal pH increases HIV-1 fusion and infection [70]. Inhibition of clathrin- and dynamin-dependent endocytosis or micropinocytosis reduces HIV-1 infection [71, 72]. Endocytic entry offers several advantages, such sheltering HIV-1 from antibodies and inhibitors targeting intermediate conformations of Env [71].

1.4 HIV tropism

Viral tropism is determined by co-receptor binding. Most clinically relevant strains use CXCR4 or CCR5 [73]. However, it has been demonstrated that some HIV strains can use other co-receptors. These co-receptors include CCR3, which has been implicated in the infection of microglia [74, 75], CCR2b [76], and CCR8 [77]. These other co-receptors

do not appear to play a major role in HIV-1 pathogenesis [78]. CCR5 appears to be the main co-receptor in HIV-1 transmission and pathogenesis, with viruses that use CXCR4 occurring during the later stages of infection [79, 80]. R5 viruses are typically macrophage-tropic (M-tropic) viruses due to their ability to infect macrophages, in addition to being able to infect CD4+ T-cells [81]. However, some R5 viruses cannot efficiently infect macrophages [79, 82, 83]. R5 viruses do not normally induce syncytia and are typically the main source of viral reservoirs [79]. On the other hand, X4 viruses are typically T-tropic and mainly infect CD4 T-cells [81]. However, some X4 viruses can also infect macrophages [84]. X4 viruses normally induce syncytia and can directly kill CD4 T-cells [85]. Viruses that can use both co-receptors are called dual-tropic viruses [86].

Co-receptor usage is determined by genetic variations in the viral Env, with the V3 loop playing a major role [86]. Therefore, genotypic methods can be used to predict viral tropism. The 11/25 rule is a genotyping method for predicting co-receptor use [87]. This rule states that a virus is more likely to be X4–tropic if the amino acid residues at positions 11 and 25 are arginine, histidine, or lysine, all positively charged amino acids [87]. While the 11/25 rule is highly sensitive for predicting syncytia-inducing viruses (~96%), it is not as sensitive for predicting X4-tropic viruses (~58%) [87]. However, this rule is a good clinical predictor of disease progression [88, 89]. Treatment experienced patients had significantly lower CD4 counts and poorer immunological restoration while receiving ART when they were predicted to have X4-tropic viruses using the 11/25 rule [88, 89]. In general, the V3 loop of R5 viruses have a net charge of +3 to +5, whereas the V3 loop of X4 viruses have a net charge of +7 to +10 [87]. Interactions with the co-receptor N-terminal domain, in general, is necessary for R5 viruses [90]; whereas X4 viruses interact with the co-receptor ECL2 domain, with little-to-no interactions with the N-terminal domain [91, 92]. The electrostatic charge of the virus also plays a role in

determining tropism. The N-terminal domain of CCR5 is negatively charged, containing three acidic amino acids and the sulfated tyrosine residues, and can interact with the positively charged bridging sheet of gp120 [92]. The ECL2 domain of CXCR4 carries a negative charge, containing five acidic amino acids, and can interact with the positively charged V3 loop [92].

Clinically, viral tropism is determined phenotypically by the Trofile assay (Monogram Biosciences, Inc., South San Francisco, CA) [93]. In this assay the viral *Env* gene is amplified from plasma, cloned into a vector, and co-transfected with an *Env*-deficient HIV-1 genomic vector into HEK293 cells [94]. The HIV-1 particles are harvested and used to infect U87:CXCR4 and U87:CCR5 cells [94]. The *Env*-deficient HIV-1 genomic vector carries a luciferase reporter gene, which will produce a signal in the U87:CXCR4 cells when X4-tropic viruses are present or in the U87:CCR5 cells when R5-tropic viruses are present [94]. If a signal is produced in both cell types, the virus is considered to be dual-tropic [94]. Tropism is further confirmed by the use of inhibitors for CCR5 or CXCR4 [93]. This assay is typically performed when a patient is being considered for CCR5 antagonists or exhibiting virological failure with CCR5 antagonists [93]. Earlier versions of the assay did not detect low levels of X4 viruses; it could fully detect X4 variants present at 10% of the viral population, but only had a detection rate of 85% when X4 variants constituted 5% of the viral population [94]. However, a newer version of this assay, with enhanced sensitivity, is able to detect X4 variants present at 0.3% of the viral population with 100% sensitivity [95].

1.5 History of HIV-1 entry inhibitors

The development of inhibitors to block the entry of HIV-1 had been a topic of interest for many years before approval of enfuvirtide (ENF, Fuzeon; Hoffman-La Roche, Nutley, NJ, USA) in 2003 by the Food and Drug Administration (FDA) [96]. Enfuvirtide binds to

the viral gp41 to prevent the formation of the entry pore [96]. This would remain the only entry inhibitor available until the FDA approval of maraviroc (MVR; Selzentry, ViiV Healthcare). MVR is unique in its mechanism of action compared to other antiretroviral agents in that it targets the host cell instead of the virus [97].

Some of the earliest attempts to block the entry of the virus were through the development of soluble CD4 (sCD4) molecules [98]. These molecules lack the transmembrane and cytoplasmic domains of CD4 but are able to bind to viral gp120 and prevent it from binding to the cellular CD4 [98]. *In vitro* they were able to inhibit HIV-1 entry at high doses [98]. However, in clinical trials sCD4 molecules were not effective in decreasing the viral loads of HIV-1-infected patients [98]. The small molecule gp120 inhibitors BMS-378806 and BMS-448043 were discontinued during clinical trials [99]. BMS-626529 and its prodrug BMS-663068, two small molecule gp120 inhibitors, are currently in phase II clinical trials and have demonstrated good efficacy and safety [100]. Ibalizumab is a monoclonal antibody that binds to CD4 and has completed phase I and II clinical trials [101]. Ibalizumab does not prevent gp120 binding to CD4, but can decrease the flexibility of CD4 and inhibit gp120 access to the co-receptors [101]. Other agents, often called fusion inhibitors, have been developed that prevent fusion of gp41 to the cellular membrane. ENF, a 36 amino acid synthetic peptide corresponding to the HR2 region of gp41, prevents the association of HR1 and HR2 [102]. Due to its low oral bioavailability, ENF must be injected subcutaneously twice daily [103]. For this reason ENF is often used only for salvage therapy [96].

In 1996 the HIV-1 co-receptors, CCR5 and CXCR4, were discovered and became ideal candidates for the development of drugs blocking HIV-1 infection [99]. AMD3100, a small molecule CXCR4 antagonist, was one of the first co-receptor inhibitors identified, and displayed antiviral activity against X4-tropic strains [104]. Further development for the treatment of HIV-1 infection was discontinued due to lack of

efficacy and cardiac abnormalities [105]. However, AMD3100 found a new life for the treatment of non-Hodgkin's lymphoma [106]; and is used to mobilize hematopoietic stem cells [106]. Of particular interest as a drug target is CCR5, as it was previously shown that its natural ligands CCL3, CCL4, and CCL5 could block HIV-1 infection [107]. N-terminal domain modifications of CCL5 have been developed to enhance the antiretroviral activity of natural CCL5, including MET-RANTES and AOP-RANTES [108, 109]. Several small molecule CCR5 antagonists have been discovered and four have made it to at least phase II clinical trials: aplaviroc, vicriviroc, INCB009471, and maraviroc [110]. Aplaviroc displayed good efficacy in clinical trials, but development was terminated due to hepatotoxicity in phase IIb and III trials [111]. Development of vicriviroc was discontinued during phase III clinical trials due to a lack of efficacy [110]. INCB009471 showed good efficacy in a phase II study and also has a half-life of 60 hours, making once-a-day dosing an option [110]. However, the company developing this drug decided to discontinue further studies [110]. The FDA approved MVR in 2007 for use in treatment-experienced HIV-1-infected individuals with R5-tropic infection, and it was subsequently approved for treatment-naïve HIV-1-infected individuals with R5-tropic infection [112].

1.6 The CCR5 inhibitor Maraviroc

MVR, originally called UK-427,857 (empirical formula: $C_{29}H_{41}F_2N_5O$), was developed by Pfizer in their efforts to discover small molecule CCR5 ligands [113]. MVR binds allosterically to the CCR5 receptor on the cell surface and prevents binding of the viral gp120 to the receptor [114]. MVR has a molecular weight of 513.67 g/mol. It is moderately lipophilic, with a distribution constant at pH 7.4 (log $D_{7.4}$), and is a weak base, with a logarithmic acid dissociation constant (pKa) of 7.3 [97, 115]. It is highly soluble across the pH range of 1 to 7.5 [112]. MVR is bound to plasma proteins at 76%

[97]. The half-life of MVR is approximately 16 hours and maximum plasma concentrations occur 2 hours after dosing [115]. For a 300 mg/kg dose, the maximum concentration in plasma is 800 ng/g and exposure is 4497 ng*h/l [115]. The absolute oral bioavailability of 300 mg MVR is 33% [115]. MVR is widely distributed throughout the body, with detectable levels being found in the seminal plasma, vaginal tissue and cervicovaginal fluid, rectum, and cerebrospinal fluid (CSF) [112, 116-125].

MVR is metabolized by cytochrome P450 (CYP) 3A4 (CYP3A4) and CYP3A5 and is a substrate for P-glycoprotein-1 (Pgp1) [112]. In the plasma, MVR remains largely unchanged, accounting for 42% of the circulating forms [115]. The most abundant metabolite present in the plasma is a secondary amine product of N-dealkylation [112]. MVR is excreted mainly through feces (76.4%), but also can be excreted through urine (19.6%) [115]. Most of the excretion through feces occurs within 96 hours and most of the excretion through urine occurs within 36 hours [115].

A Phase II trial in asymptomatic humans infected with R5-tropic HIV-1 receiving 300 mg/kg twice daily of MVR showed a decrease in HIV-1 RNA levels of 1.6 $\log_{10}$ copies/ml compared to a decrease of 0.02 $\log_{10}$ copies/ml in infected humans receiving placebo [126]. The efficacy of MVR was further confirmed in a pair of phase III trials, the Maraviroc versus Optimized Therapy in Viremic Antiretroviral Treatment-Experienced Patients (MOTIVATE) 1 and 2 [127]. Eligible subjects had evidence of resistance to drugs from three antiretroviral classes or were triple-class experienced, had plasma HIV-1 RNA levels >5,000 copies/mL, and exclusively had R5 virus at screening [127]. Patients received oral MVR or placebo once or twice daily, with doses being adjusted for the other drugs in the patient's ART regimen [127]. Treatment with MVR decreased viral RNA load by week 48, compared to placebo, with a viral RNA load decrease of −1.84 $\log_{10}$ copies/ml in patients receiving MVR compared to −0.79 $\log_{10}$ copies/ml in patients receiving placebo [127].

In addition to reducing viral load, MVR has been shown to be involved in immune restoration during HIV infection. In the MOTIVATE trials CD4 cell counts increased to 124 cells/mm^3 in the MVR arms compared with 61 cells/mm^3 in the placebo arms [127]. This was true even after adjusting for the greater virologic potency of MVR-containing regimens [128]. Short-term MVR treatment of patients with persistent virological failure resulted in increased levels of CD4+ and CD8+ T-cells and was positively correlated with improved antiviral activity [129]. HIV-1-infected patients who received MVR intensification therapy had accelerated recovery of CD4+ T cell counts and maintained higher CD4+ T cell counts after MVR discontinuation [130]. In patients with suppressed viremia MVR treatment was associated with modest increases in CD4+ and CD8+ T cell counts and reduction in the percentages of regulatory T cells (Tregs) [131]. Reductions in Tregs with MVR treatment have been shown in other studies of treatment-naïve patients and can become evident as early as 8 days after treatment initiation [132].

MVR has been successfully used in clinical settings, resulting in decreased viral loads and increased CD4 cell counts [133, 134]. Treatment failure is often due to the outgrowth of previously undetectable X4-tropic viruses [135, 136]. In addition, MVR has also been suggested as a candidate for pre- or post-exposure prophylaxis [137-140], for use in dual therapy regimens (protease inhibitor and nucleoside/nucleotide reverse transcriptase inhibitors sparing regimens) [141-144], and in the treatment of immune reconstitution inflammatory syndrome [145, 146]. Outside of HIV-1 infection, MVR has also shown efficacy in the treatment of cancer by preventing metastasis of cancer cells [51, 147, 148], graft-versus-host disease by inhibiting lymphocyte trafficking [149, 150], and pulmonary arterial hypertension by reducing inflammation [151].

1.7 The Blood-Brain Barrier (BBB)

The BBB acts as a barrier between peripheral circulation and the CNS [152]. Functions of the BBB include controlling the influx and efflux of substances into and out of the brain, regulating ion homeostasis, and immune surveillance [152]. The BBB is composed of brain microvascular endothelial cells (BMVECs), basement membranes, pericytes, and astrocytic end-feets (Figure 1-2) [152]. BMVECs form a monolayer and provide a continuous cellular barrier between the blood and the interstitial fluid; they are involved in the transport of micronutrients and macronutrients, receptor-mediated signaling, leukocyte trafficking, and osmoregulation [152]. Astrocytes are glial cells that encircle the endothelium, provide a cellular link to the neurons, and promote the formation of endothelial tight junctions (TJs) [152]. They may also be involved in the maintenance of BBB tightness and function [152]. On the brain side of the barrier there is a basement membrane composed of fibronectin and laminin that is embedded with pericytes, which partially wrap the endothelial cells [152]. Pericytes help stabilize the BBB and regulate blood flow and BMVEC proliferation [152]. Pericytes also display macrophage-like activity such as taking up small and soluble molecules by pinocytosis to clean the extracellular fluid of the BBB and act as phagocytes in response to inflammation [153].

BMVECs are connected together via adherent junctions, gap junctions, and TJs proteins. TJs are responsible for the barrier function of these cells (Figure 1-3) [154]; and include the integral membrane proteins: occludin, claudins, junctional adhesion molecules (JAMs); and the accessory proteins: zonula occludens (ZOs) [154]. Occludin, a 65-kDa protein, detected in the cellular margins of BMVECS, is involved in TJ stabilization and optimal barrier function, as well as signal transduction [154]. While occludin does not appear to be essential for the formation of TJs, decreased expression is associated with BBB dysfunction [154]. Located in a similar membrane area as occludin, claudins are a large family of proteins, 20 to 27 kDa, comprising 27 members

with high sequence similarities in humans [155, 156]. Claudins can interact with each other in either a homophilic or heterophilic manner and are responsible for forming the primary seal of TJs [156]. Claudin-5 is the dominant claudin in BMVECs, although claudins-1, 3, and 12 are also expressed [156]. The JAM family consists of JAM-A, B, and C; they form homotypic cell-cell contacts between endothelial cells and regulates cell polarity, BBB stability, and leukocyte transmigration through BBB [157]. ZOs are membrane-associated guanylate kinase proteins containing multiple binding domains for protein-protein interactions [154]. The ZO proteins connect the transmembrane TJ proteins to the actin cytoskeleton [154]. In the BBB the most highly expressed ZO proteins are ZO-1 and ZO-2 [154].

1.8 HIV-associated neurocognitive disorders (HAND)

1.8.1 Pathogenesis of HAND

HAND is a spectrum of neurological disorders that occurs as the result of HIV infiltration into the brain and injury to brain cells, including neurons [158]. HAND is classified into three categories, depending on disease severity: asymptomatic neurocognitive impairment (ANI), mild neurocognitive disorder (MND), and HIV-associated dementia (HAD) [155]. Patients with ANI display acquired impairment in cognitive functioning in at least two ability domains during neuropsychological testing, but do not have impairment in activities of daily living (ADLs) and any delirium or dementia [155]. Patients with MND display mild and acquired impairment in at least two cognitive ability domains during neuropsychological testing and at least some mild impairment in their ADLs, but have no delirium or dementia [155]. HAD is the most severe form, with patients displaying acquired, moderate-to-severe cognitive impairment involving at least two ability domains during neuropsychological testing, with accompanying motor and behavioral

impairments, marked impairments in their ADLs, and dementia [155]. Although the prevalence of HAD has decreased with the introduction of ART, the levels of ANI and MND have increased [155]. The CNS HIV Antiretroviral Therapy Effects Research Group, the largest study to date examining HIV cognitive impairment, showed that 52% of HIV-seropositive patients had cognitive impairment [159]. Other studies estimate that 20 to 70% of HIV-1-infected individuals with access to antiretroviral therapy have neurocognitive deficits [160-166]. This increased prevalence of HAND can be partially explained by the increased lifespan of HIV-1-infected patients [158].

HIV-1 neuropathogenesis results from a combination of cellular and viral factors [167]. Current knowledge based on *in vivo* and *in vitro* studies provides a general outline of how HIV-1-CNS infection and the eventual progression to HAND occur: HIV-1-infected monocytes and macrophages infiltrate the brain and establish residence, as well as productively infecting microglia, the resident immune cells of the brain (Figure 1-4) [167]. The infected cells become activated and mount an immune response causing the release of cytokines and chemokines. Infected cells also secrete viral proteins and toxic factors [168]; and the combination of cytokines, chemokines, and viral proteins leads to further activation of brain immune cells [168]. Although HIV-1 does not infect neurons, the constant barrage of viral proteins and inflammatory molecules and toxic factors results in encephalitis, neuronal injury, damage, and apoptosis, which eventually leads to neurocognitive impairment [168]. The hallmark of chronic CNS inflammation during HIV infection, termed HIV encephalitis (HIVE), is characterized by the presence of multinucleated giants cells, microgliosis, microglial nodules, astrogliosis, and neuronal loss [155].

1.8.2 The blood-brain barrier and HAND

BBB alterations occur early after peripheral HIV-1 infection occurs [169]. HIV-1 is thought to enter the brain via infiltration of HIV and infected cells through the BBB, known as the “Trojan horse” mechanism [170]. HIV-1 virions and viral proteins, such as gp120, Tat, Nef, and Vpr induce BBB inflammation and dysfunction, and this is associated with increased expression and secretion of proinflammatory cytokines and chemokines such as tumor necrosis factor alpha (TNFα), interleukin (IL)-6, IL-8, and CCL2 by infected and/or activated cells [171, 172]. This results in damage to endothelial cells, enabling further cellular infiltration [168]. Additionally, secretion of cytokines and chemokines results in increased clustering of integrin receptors to facilitate monocyte binding and increased expression of adhesion molecules to facilitate monocyte adhesion [173].

Viral proteins that cause BBB damage and increase permeability include Tat, gp120, and Nef [173]. These viral proteins can increase endothelial permeability by decreasing the expression of claudins, ZO1, ZO2, and occludin [174-180]. Tat can induce adhesion to the extracellular matrix via focal adhesions and can cause apoptosis of BMVECs by the induction of caspases [177, 181]. Tat can also induce oxidative stress by dysregulating nitric oxide production and decreasing the levels of intracellular glutathione in BMVECs [177, 182]. Exposure of BMVECs to Tat results in upregulation of matrix metallopeptidase-3 (MMP3), which in turn can further degrade occludins [175]. Exposure of BMVECs to gp120 can induce the passage of HIV across the BBB by induction of adsorptive endocytosis [183-185]. Additionally, exposure of BMVECs to gp120 can increase the expression of adhesion molecules such as intercellular adhesion molecule-1 and vascular cell adhesion molecule-1, which increases monocyte adhesion and migration across the BBB [186-188]. HIV-1 gp120 can also induce MMP2 and MMP9 and decrease laminin in the BBB basement membrane [189]. Nef is expressed in

astrocytes of HIV-1 patients, especially in patients with dementia [190], and increases the sensitivity of astrocytes to hydrogen peroxide [191]. Like gp120, Nef can increase MMP9 expression and induce BBB disruption [192].

1.8.3 Neurons and HAND

Once HIV-1-infected cells set up residence in the brain, a combination of viral and cellular factors causes neuronal dysfunction, damage, and eventual neuronal death [167]. Cytokines and chemokines, released from activated macrophages, microglia, and astrocytes, are elevated in the brains and CSF of HAND patients [158]. These include TNFα, IL-6, CCL2, CCL3, CCL4, and CCL5 [155]. These cytokines and chemokines can induce monocyte/macrophage migration and accumulation in the CNS [155]. There is evidence that TNFα, more than HIV-1 infection itself, is one of the major inducers of monocyte migration into the CNS [193]. In addition, TNFα can cause direct neuronal damage [158, 194]. Besides cytokines and chemokines, other cellular factors involved in HAND include neurotoxins such as quinolinic acid and nitric oxide, which can be neurotoxic when produced in excess [155].

Furthermore, several HIV-1 proteins shed from infected cells, such as Nef, gp120, and Tat, are known to be neurotoxic [155]. Gp120 can bind directly to N-methyl-D-aspartate receptor (NMDAR) and cause a lethal influx of calcium ions in neurons [195]. Gp120 binds to CCR5 or CXCR4, without the presence of CD4, on neurons and promotes apoptosis [196, 197]. Gp120 has also been associated with oxidative stress [198, 199]. Similarly, Tat can activate NMDAR to cause a toxic influx of calcium ions and promote oxidative stress in neurons [200, 201]. Tat can also activate caspases, cause mitochondrial dysfunction, and induce unfolded protein response leading to apoptosis [202]. Gp120, Tat, and Nef can upregulate inflammatory molecules to cause neuronal

dysfunction and death [155]. These include MMPs, TNFα, IL-6, nitric oxide, and CCL5 [155].

1.8.4 Monocytes/macrophages in HAND

Monocytes and macrophages play a major role in the pathology of HAND. HIV-1-infected monocytes can traverse the BBB, and macrophages are the principal HIV-1-infected cell type in the brain [203, 204]. Even with ART, monocytes/macrophages often remain infected and constitute long-term viral reservoirs. In fact, HIV-1 DNA levels in monocytes is associated with persistent HAND and peripheral infection of monocytes is correlated with HAND in ART-treated individuals [205]. Furthermore, the accumulation of macrophages in the CNS appears to be a more accurate predictor of HAND than CNS infection itself [206].

Monocytes can be categorized into three main subsets: CD14++CD16- (high CD14 expression, no CD16 expression), CD14++ CD16+ (high CD14 expression, low CD16 expression), and CD14+CD16++ (low CD14 expression, high CD16 expression); also known as classical resting monocytes, intermediate monocytes, and non-classical activated monocytes, respectively [207]. Typically the non-classical CD16++ monocytes only represent 5-10% of the total monocyte population [207]. However, the population of these cells can expand to approximately 40% in HIV-1-infected individuals and higher amounts are found in the brains of patients with HIV-1 encephalopathy [207, 208]. Non-classical activated monocytes become infected with HIV-1 more easily and support increased levels of viral replication [207]. Furthermore, they are able to migrate across the BBB more efficiently compared to their classical counterparts [207]. These studies provide evidence of the importance of monocytes in HIV-1-infection.

1.8.5 Mouse models of HAND

Mouse models have become a tool in understanding and treating HAND. These models have several advantages compared to other models of HAND, such as SIV-infected rhesus macaques; including the ease of handling, relative low cost, and well-established and easy-to-use methods for manipulating the mouse genome [209]. Mouse models to study HAND include transgenic mice, in which mice are genetically modified to express HIV-1 genes. In these models HIV expression can be ubiquitous or tissue/cell-specific. Once such model is the Tg26 mouse line, in which mice carry an HIV-1 construct containing a 3.0-kb deletion of the gag-pol region in the pNL4-3 proviral genomic construct [210]. These mice show expression of HIV-1 mRNA in skin, skeletal muscle, kidneys rain, eye, gastrointestinal tract, spleen, and thymus. Another transgenic mouse model involves the insertion of the viral Tat or Env gene into the mouse genome under the control of a glial fibrillary acidic protein (GFAP) promoter, resulting in gp120 or Tat protein expression by brain astrocytes [209]. Other transgenic models have been developed for HIV-1 gene expression in immune cells, macrophages, and podocytes [210].

More recently, humanized mouse models have become prevalent. Humanized mice are immune deficient mice reconstituted with a human immune system, allowing for long-term chronic HIV-1 replication [209]. One such mouse model involves the engraftment of non-obese diabetic, severe combined immunodeficient, IL2 receptor gamma chain deficient (NSG) mice with human peripheral blood lymphocytes (PBL) [209]. These mice become engrafted rapidly with human immune cells, with particularly strong T cell engraftment [209]. This model allows for a rapid and efficient method for studying HAND. NSG mice reconstituted with CD34+ human hematopoietic stem cells from human fetal liver allows for chronic HIV-1 infection, and subsequently long-term studies. These mice develop a near-complete human immune system by 20-22 weeks of

age [211]. Limitations of these humanized mice include variable levels of human cell engraftment [212]. This can affect the pathology seen in the mice during HIV-1 infection. In addition, the mice have incomplete peripheral immunopathology, due to a lack of human stromal elements [212].

1.9 Study hypothesis

Most HIV strains that enter the CNS are R5-tropic [213, 214]. Studies in our laboratory have previously shown that human brain microvascular endothelial cells (HBMEC) express CCR5 and implicate CCR5 in HIV-1-induced BBB damage [179, 215]. CCR5 antibodies diminished HIV-1-induced activation of STAT1 and STAT3 and prevented HIV-1-induced monocyte adhesion and migration in an *in vitro* BBB model [215]. HIV-1 activates STAT1 signaling in endothelial cells, which induces the transcription and expression of proinflammatory cytokines and downregulates the expression of TJ proteins [216]. CCR5 antibodies prevented gp120-induced intracellular calcium release [179]. MVR treatment of HIV-1-infected patients increased cerebral metabolite markers of neuronal integrity [122]. In addition, HIV-1-infected patients on MVR containing regimens showed a trend towards improvement in neurocognitive status and reduced TNF-α concentrations in the CSF [217].

Given the role of CCR5 in HIV-1 infection and the fact that most HIV-1 strains that cross the BBB, enter the CNS, and cause HAND are CCR5-tropic, we set out to further elucidate the role of CCR5 in BBB dysfunction following HIV-1 infection and monocyte/macrophages interactions with HBMEC. We hypothesized that CCR5 plays a major role in monocytes-BBB communications and CNS entry. HIV-1 infection increases monocyte adhesion and migration through the BBB, and this can be prevented by CCR5 neutralizing antibodies [215]. Because the cytoskeleton is responsible for cellular motility, we hypothesized that HIV-1 would induce cytoskeletal changes in monocytes

following infection and monocyte-endothelial communications and that blocking CCR5 would prevent those changes. We further hypothesized that CCR5 inhibition could reduce HIV-1-induced BBB damage and reduce viral loads in the brain. In the present study we used a combination of *in vitro* and *in vivo* techniques to determine the role of CCR5 in HIV-1-induced BBB injury and HAND.

1.10 Figures

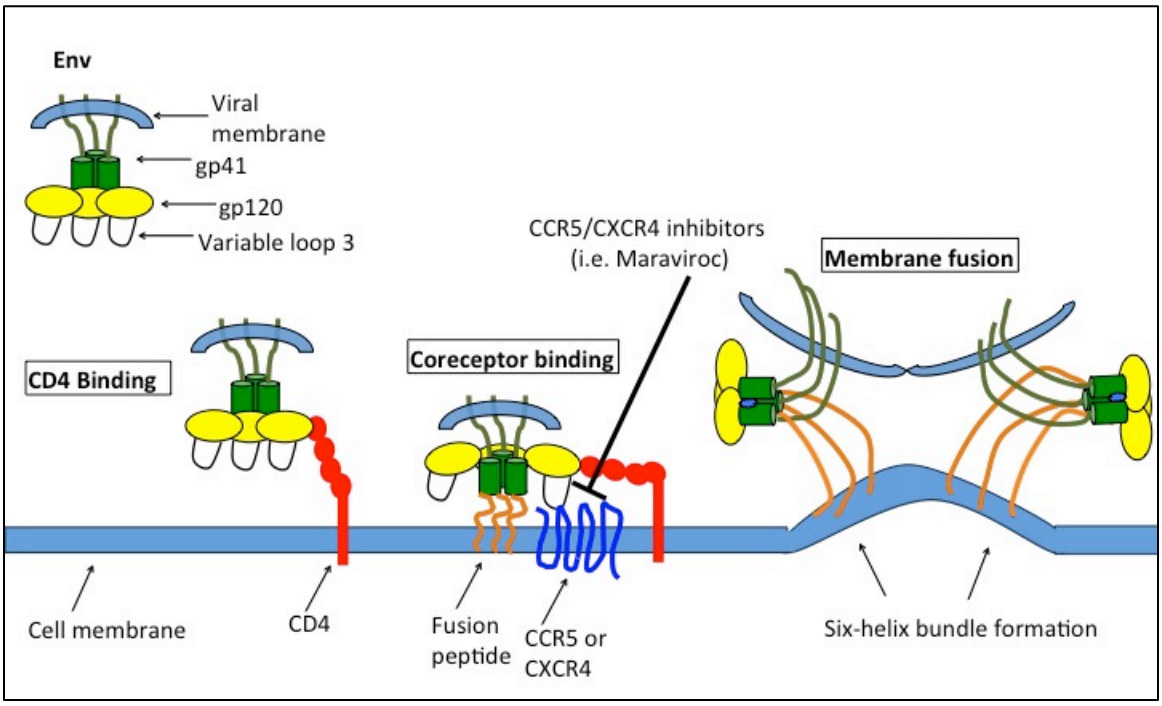

Figure 1-1: HIV-1 receptor and co-receptor binding. The viral Env is composed of three gp120 and three gp41 subunits. Gp120 binds to CD4 on the cell surface, causing a conformational change in the Env protein. This conformational change allows for co-receptor binding, which is partially mediated by the V3 loop of Env. Following co-receptor binding, the fusion peptide of gp41 inserts into the cell membrane, followed by formation of the six-helix bundle and membrane fusion. CCR5 or CXCR4 antagonists can inhibit co-receptor binding and subsequent HIV-1 entry.

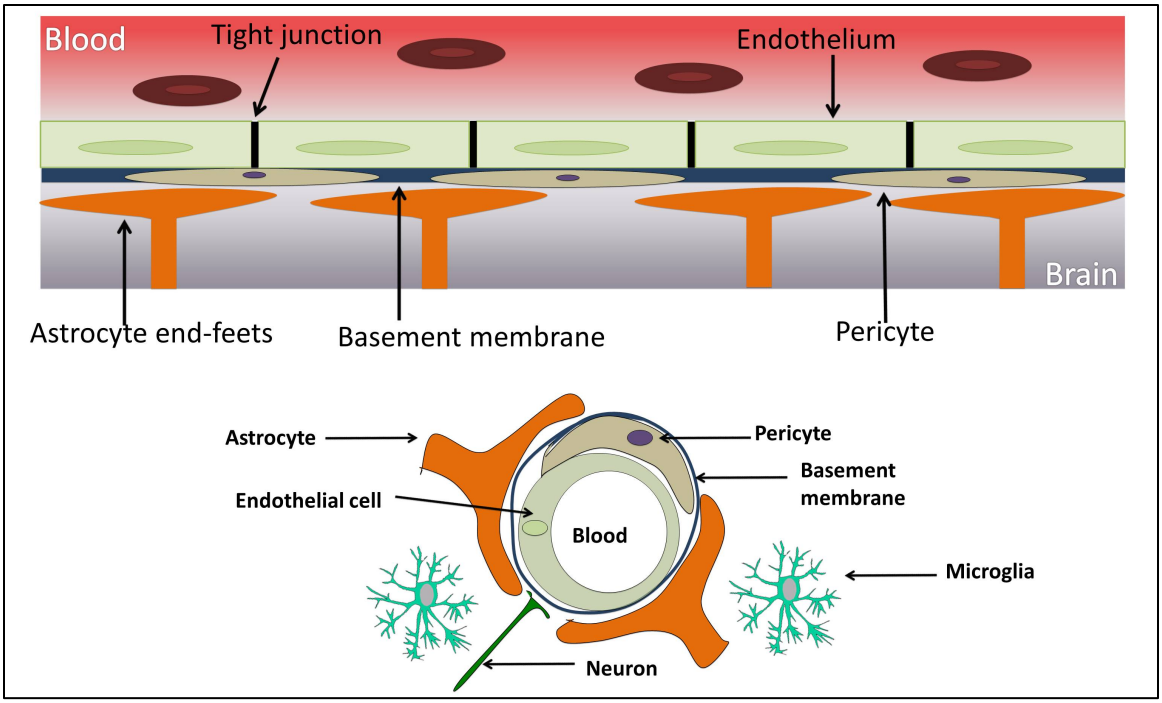

Figure 1-2: The blood-brain barrier structure. The blood-brain barrier consists of vascular endothelial cells connected via tight junctions, which regulate the passage of molecules across the barrier. Pericytes, which partially surround the endothelium on the side of the brain, provides support to the vessels and regulate capillary blood flow. The endothelial cells and pericytes are enclosed by a basement membrane. The basement membrane is involved in vessel development, stability, and has a barrier function. Astrocytic end-feets surround the endothelium and provide a connection to neurons.

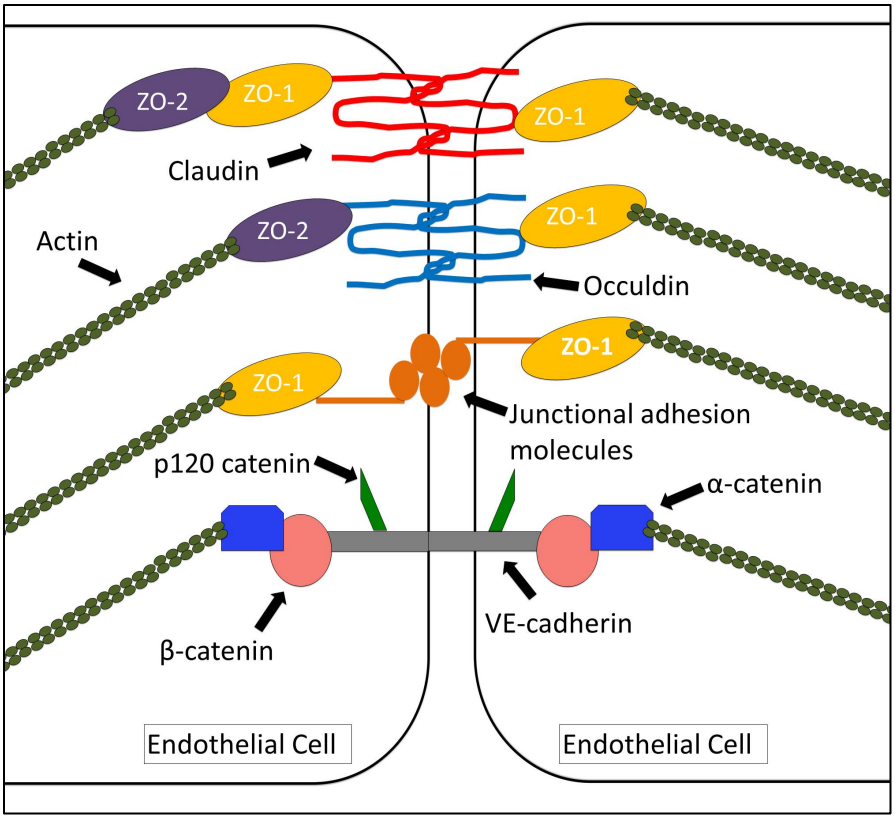

Figure 1-3: Molecular components of tight junctions and adherens junctions in the BBB. Tight junctions are composed of claudins, occludin, and junctional adhesion molecules at the cell surface, all of which mediates cellular contact. These molecules bind to ZO-1 or ZO-2, which bind tight junctions to the actin cytoskeleton. Adherens junctions are composed of VE-caderhin at the cell surface. VE-cadherin binds to a complex of catenin proteins, which bind to the cytoskeleton.

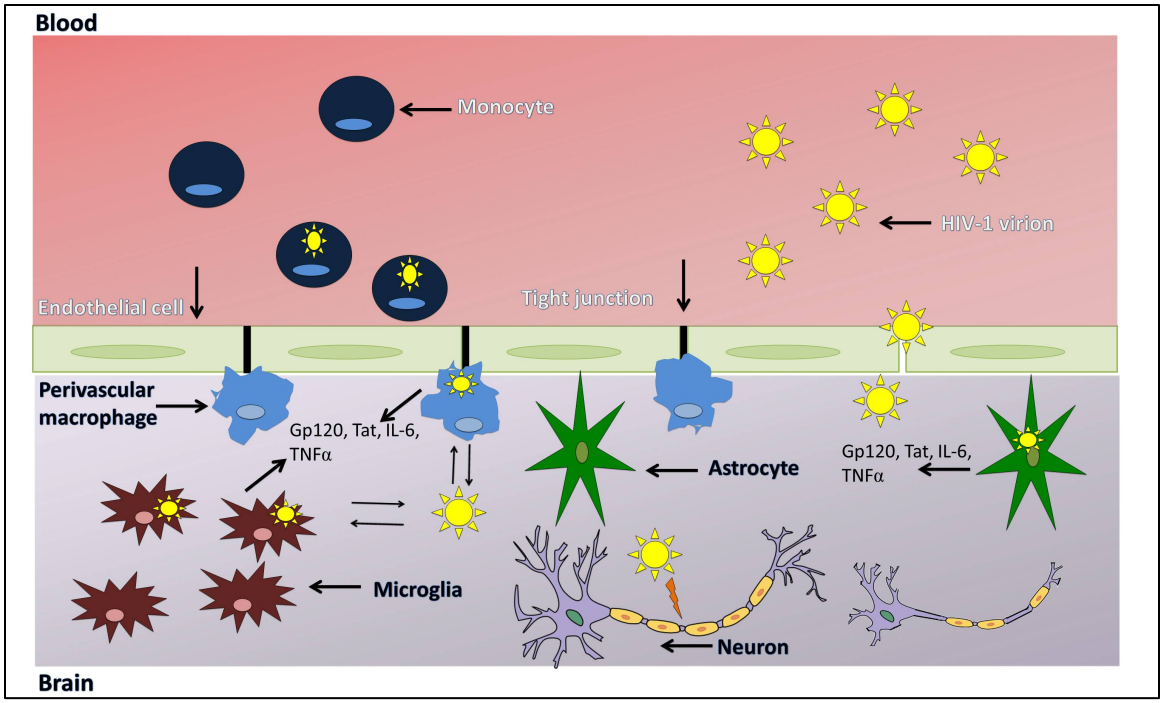

Figure 1-4: HIV-1 neuroinvasion. HIV-1 enters the brain via the migration of infected monocytes through the blood-brain barrier. Once inside the brain, these cells differentiate into perivascular macrophages. Infected macrophages release viral particles that productively infect microglia and can also infect astrocytes, and proinflammatory molecules and viral proteins, which can damage cells. HIV-1 infection causes damage to the endothelium, which allows for the passage of more infected cells and viral particles. Although, HIV-1 does not infect neurons its virions, viral proteins, and cellular factors can induce neuronal injury and damage, resulting in HAND.

Chapter 2

CCR5 antagonists diminish HIV-1 infection, HIV-1-induced monocyte migration, and HIV-1-induced cytoskeletal changes in monocytes during monocyte-endothelial interactions

2.1 Background

Most HIV-1 strains that cross the BBB, enter the brain, and infect CNS cells use CCR5 to enter and infect target cells [213, 214]. HIV-1 infection is associated with increased monocyte adhesion and migration through the BBB, during which the cellular cytoskeleton undergoes major changes and reorganization [218, 219]. GPCRs, including CCR5, are associated with cytoskeletal reorganization [220, 221]. In macrophages, activation of CCR5 by its natural ligands CCL3, CCL4, and CCL5 induce actin reorganization and lamellipodia formation, sheet-like membrane protrusions found at the leading edge of motile cells [221]. CCR5 is able to bind to alpha-catenin, which is known to function in cell–cell adhesion and can act as a connector that attaches the plasma membrane-associated cadherin adhesion-complex to the matrix of the cellular cytoskeleton in PM1 T-lymphocytes, a cell line susceptible to a wide variety of HIV isolates [220].

Small molecule CCR5 antagonists, such as MVR and TAK-779 (TAK), have become a new avenue for the treatment of HIV-1 infection [65]. Not only does MVR prevent viral entry, but it has also been reported to have several immunological benefits, including decreased migration of immune cells [222-225]. We therefore hypothesized that CCR5 plays a major role in monocyte-brain endothelium interactions and HIV-1 entry into the CNS, and that CCR5 antagonists would diminish these effects. We also hypothesized that HIV-1-induced monocyte-endothelial interactions and trans-endothelial migration involve cytoskeletal changes, and that CCR5 blockers would also affect these changes. To test these hypotheses, we used a cytoskeleton phospho-antibody array to investigate changes in the expression and activation of cytoskeleton-associated proteins in monocytes following HIV-1 infection and endothelial interaction (summarized in Figure 2-1 and 2-2). We further used CCR5 antagonists (TAK and MVR) and CCR5 neutralizing antibodies to determine the role of CCR5 on HIV-1 infection of

monocytes-derived macrophages (MDM), monocyte-endothelial interaction, and cytoskeletal changes. In addition, we examined the expression of cytoskeleton-associated proteins in the brain tissues of HIV-1 infected individuals.

2.2 Materials and Methods

2.2.1 Cell culture

Human monocytes were obtained from HIV-1-, HIV-2, and hepatitis B-seronegative donors undergoing leukopheresis by countercurrent centrifugal elutriation of mononuclear leukocyte-rich fractions. Monocytes were re-suspended in complete Dulbecco's Modified Eagles Media (DMEM) containing 2 mM L-glutamine (Life Technologies, Grand Island, NY, USA), 10% heat-inactivated human serum, 100 µg/ml gentamicin, and 10 µg/ml ciprofloxacin (Sigma, St. Louis, MO). MDM were obtained from monocytes by culture for 7 days in complete DMEM containing 1,000 U/ml macrophage colony-stimulating factor. Every two days, half of the medium was removed and replaced with fresh medium.

Primary human brain microvascular endothelial cells (HBMEC) were isolated from the temporal cortex of brain tissue obtained during surgical removal of epileptogenic cerebral cortex in adult patients, under an Institutional Review Board-approved protocol at the University of Arizona (Tucson, AZ). Routine evaluation for von Willebrand factor, *Ulex europaeus* lectin, and CD31 showed that cells were >99% pure. Freshly isolated HBMEC were plated on collagen-coated flasks or culture plates and cultured using DMEM/F12 media (Life Technologies) containing 10% fetal bovine serum (Atlanta Biologicals, Flowery Branch, GA, USA), supplemented with 10 mmol/l L-glutamine (Life Technologies), 1% heparin (Thermo Fisher Scientific, Pittsburgh, PA, USA), 1% endothelial cell growth supplement (BD Bioscience, San Jose, CA, USA), 1% penicillin-streptomycin (Life Technologies), and 1% fungizone (MP Biomedicals, Solon,

OH, USA). Cells at passage 2 to 4 were used for all studies. All cells were maintained at 37°C in 95% oxygen and 5% CO2.

2.2.2 Cell treatment and HIV-1 infection

Monocytes were infected with HIV-1_{ADA}, a clade-B M-tropic viral isolate, at a multiplicity of infection (MOI) of 0.01 and cultured overnight (12 hours). After the 12 hours culture, monocytes were washed 3 times with PBS to remove free viral particles and used for co-culture experiments. For experiments testing the effects of CCR5 antagonists, monocytes and MDM were treated with 5 μM TAK or 5 μM MVR for 30 min prior to viral exposure. Both TAK and MVR were obtained from the NIH AIDS Research and Reference Reagent Program. All reagents were prescreened for endotoxin (<10 pg/ ml, Associates of Cape Cod, Woods Hole, MA) and mycoplasma contamination (Gen-probe II, Gen-probe, San Diego, CA).

2.2.3 Trans-endothelial electrical resistance (TEER)

For TEER measurements, HBMEC were seeded on gold-film electrode surface (Applied BioPhysics Inc., Troy, NY) and cultured to confluence. Confluent HBMEC were exposed to 5 to 20 μM of TAK or MVR; TEER live-recorded readings were made before and after exposures. Controls consisted of non-treated HBMEC and cells treated with 0.1% saponin as non-resistant control. To determine whether any effect of the CCR5 blockers on the BBB was reversible, HBMEC were washed after 48 hours to remove TAK or MVR and TEER live-recorded readings were made for an additional 20 to 24 hours.

2.2.4 Co-culture of monocytes with HBMEC

HIV-1-infected monocytes were added to confluent monolayers of HBMEC in 100-mm culture plates (5 monocytes for each HBMEC) and co-cultured for 2 hours. Controls consisted of mock-infected monocytes co-cultured with HBMEC, as well as infected and

mock-infected monocytes not cultured with HBMEC. Following the 2-hour co-culture, monocytes were harvested by washing the HBMEC monolayer 3 times with PBS. Adherent HBMEC were checked by microscopy to ensure maximal removal of monocytes before harvesting endothelial cells by scrapping. Each cell type was pelleted by centrifugation at 3,000 rpm for 10 min followed by protein extraction.

2.2.5 Protein extraction and cytoskeleton antibody microarray

The Cytoskeleton-II protein arrays and all reagents used for protein microarray analysis were from Full Moon Biosystems (Sunnyvale, CA), except Cy3-conjugated streptavidin, which was from GE Healthcare Life Sciences (Piscataway, NJ). Each Cytoskeleton-II protein array contained 141 well-characterized phosphorylated antibodies of the cytoskeletal pathway and corresponding total antibodies. To ensure reliability and consistency of results, each array included 6 replicates of each antibody and phospho-antibody. Additional controls on each array included 6 positive controls consisting of Cy-3 labeled antibodies, 6 negative controls containing bovine serum albumin (BSA), and empty spots containing no antibody, with the 6 replicates scattered throughout the array. Cells were lysed and protein extracted using the Protein Extraction Kit (Full Moon Biosystems). For protein extraction, one tube of Lysis Beads was added to the cell pellet followed by 200 µl of extraction buffer. This mixture was vortexed for 30 seconds and incubated on ice for 10 minutes. The mixture was incubated another 60 minutes on ice and vortexed for 30 seconds every 10 minutes. Following extraction, protein lysate was purified and the lysis buffer was replaced with the labeling buffer. Spin columns, containing a dry gel, were reconstituted by adding 650 µl of Labeling buffer, vortexed for 5 seconds, allowed to rest for 30 minutes at room temperature, and vortexed in wash tubes at 7,500 x g for 2 minutes to remove excess fluid. In a spin column, 100 µl of protein extract was added directly to the center of the gel bed. The spin column was

placed in a collection tube and centrifuged at 7,500 x g for 2 minutes. Protein lysate was quantified and checked for quality control by UV absorbance, with absorbance greater than 4 OD with two separate peaks at 200-230 nm and 240-280 nm. Proteins were labeled with biotin. For labeling, biotin was dissolved in N,N-dimethylformamide to give a concentration of 10 µg/ul, mixed with 80 OD of protein lysate, and incubated at room temperature for 1 hour on a rocking platform at setting 2 (VWR International, Radnor, PA). Following incubation, stop reagent was added and samples were incubated for 30 minutes at room temperature on a rocking platform.

For the antibody array, slides were first blocked with blocking solution for 30 minutes at room temperature on orbital shaker and washed 10 times for 10 seconds each with mili-Q water. Biotin-labeled proteins were mixed with coupling solution, poured onto the slide, incubated on an orbital shaker for 1 hour at room temperature, washed 3 times with 1x wash solution, and washed 10 times for 10 seconds each wash, with mili-Q water. Slides were incubated with 0.5 mg/ml of Cy3-Streptavidin, incubated on an orbital shaker for 20 minutes at room temperature in the dark, washed 3 times for 10 minutes each with 1x wash solution, washed 10 times for 10 seconds each wash with mili-Q water, and dried by centrifugation. Slides were scanned using Full Moon Biosystems Scanning Array Service. The protein array procedure is summarized in Figure 2-1.

2.2.6 Array data analysis

Each spot throughout the array was scanned to provide its signal intensity value, including positive (spots containing Cy-3 labeled antibodies) and negative (empty spots and spots containing BSA) controls. For background correction, the median value of the negative control signal was subtracted from the values of each antibody and phospho-antibody. The background corrected signal was log2 transformed and normalized to the mean value of beta-actin signal. For each phosphorylated antibody, the background-

corrected signal was normalized to the mean value of the corresponding total antibody. The fold changes between treatment groups were derived from ratios of geometric mean signal intensities. Treatment groups included: control non-infected monocytes co-cultured with HBMEC (control), HIV-1 infected monocytes co-cultured with HBMEC (HIV-1), and HIV-1 infected monocytes treated with CCR5 blockers and co-cultured with HBMEC (HIV-1 + TAK). ANOVA with heterogeneous variance was used for statistical analyses of protein expression between groups, and the Tukey-Kramer method used for multiple comparisons. The Benjamini-Hochberg (BH) method was then used to control the false discovery rate. Proteins with BH adjusted p-value less than 0.05 were considered to be differentially expressed.

2.2.7 Ingenuity pathway analysis (IPA)

Differentially expressed and phosphorylated proteins identified in HIV-1-infected monocytes co-cultured with HBMEC compared to non-infected monocytes co-cultured with HBMEC or infected monocytes treated with CCR5 blockers and co-cultured with HBMEC, were analyzed using the Ingenuity Pathways Analysis 3.0 (Ingenuity Systems, Redwood City, CA). The networks obtained through IPA software describe functional relationships between protein products based on known interactions, biological functions, and canonical pathways. Using a false discovery rate of 0.05, only phospho-proteins upregulated or downregulated by at least 1.5-fold were considered; and for non-phosphorylated proteins, only those upregulated or downregulated by at least 2-fold were considered.

2.2.8 Monocyte adhesion to an in vitro BBB model

HBMEC were plated on 96-well collagen-coated black plates with clear bottoms and cultured to confluence. Infected monocytes (2.5×10^5 cells) treated or non-treated with CCR5 blockers or CCR5 antibodies were labeled with 5-carboxyfluorescein diacetate,

acetoxymethyl ester (CFDA), 10 μM/1 × 10^6 cells for 1 hour, and co-cultured with HBMEC for 15 min. HBMEC were then washed 3 times with PBS, and the number of adherent monocytes were quantified by spectrophotometry (excitation: 492 nm, emission: 517 nm), with a standard curve derived from a serial dilution of a known number of CFDA-labeled monocytes.

2.2.9 RNA isolation from human brain tissues

Brain tissues (cortex) from nine HIV-1-seropositive patients without neurocognitive impairment, ten HIV-1-seropositive patients with neurocognitive impairment, and twelve HIV-seronegative controls were obtained from the National NeuroAIDS Tissue Consortium and our Department of Pharmacology and Experimental Neuroscience brain bank. The clinical and demographic histories of all brain tissue donors are detailed in Table 2-1. Total RNA was extracted from human brain tissues using Trizol reagent (Life Technologies). One-milliliter of Trizol reagent was added to 50 mg of brain tissue and tissues were homogenized using the TissueRuptor homogenizer (Qiagen, Valencia, CA). Homogenized samples were incubated at room temperature for 5 minutes and after incubation, 200 μl of chloroform was added to each sample, shaken by hand for 15 seconds, and incubated at room temperature for 15 minutes. Samples were centrifuged at 12,000 x g for 15 minutes at 4℃. During centrifugation the mixture separates into three layers: a bottom red phenol-chloroform phase, an interphase, and a colorless top aqueous phase. The aqueous phase was transferred to a new tube and mixed with 500 μl of 100% isopropanol to precipitate RNA. Samples were incubated at room temperature for 10 minutes followed by centrifugation at 12,000 x g for 10 minutes at 4℃. Supernatant was removed from the tubes and 1 ml of 75% ethanol was added to each sample, vortexed, and centrifuged at 7,500 x g for 5 minutes at 4℃. Supernatant was removed and samples were air dried for 5 minutes at room temperature. Pellets

were re-dissolved in 30 µl of RNase-free water and incubated on a heat block set at 55℃ for 10 minutes. RNA was further cleaned using Total RNA cleanup kit (Qiagen). RNA yield and quality were checked using a NanoDrop spectrophotometer (NanoDrop Technologies, Wilmington, DE) and for all samples absorbance ratio of 260/280 was ≥ 2.

2.2.10 Reverse transcription and quantitative real-time PCR (qRT-PCR)

For each sample, cDNA was generated from 2 µg RNA using the High Capacity cDNA Reverse Transcription Kit (Life Technologies). For each sample, 2 µg of RNA in 10 µl of RNase-free water was mixed with 2 µl 10X RT buffer, 0.8 µl 25X deoxynucleotides (dNTPs), 2 µl 10X reverse transcription random primers, 1 µl MultiScribe™ reverse transcriptase, 1 µl RNase inhibitor, and 3.2 µl nuclease-free water. Cycling conditions were: 10 minutes at 25℃, 120 minutes at 37℃, 5 minutes at 85℃, and hold at 4℃.

A TaqMan gene detection system was used and quantification performed using the Applied Biosystems StepOnePlus™ system (Life Technologies). For each sample, the cDNA obtained was diluted in nuclease free water at a ratio of 1:20; a 20 µl reaction mixture containing 9 µl of each diluted cDNA sample, 10 µl of 2X TaqMan Fast Universal PCR Master Mix (containing the polymerase enzyme, dNTPs and MgCl2), and 1 µl of primer-probe [containing 900 nM of each forward and reverse primer and 250 nM TaqMan minor groove binder (MGB) probe]. Twenty-microliters of reaction mixture wasloaded into the wells of an optical 96-well fast plate (Life Technologies). The plate was loaded into the StepOnePlus system and cycling conditions were: 20 second hold at 95℃ followed by 40 cycles of 1 second at 95℃ and 20 seconds at 60℃. All reagents and primer-probes (900 nM of each primer and 250 nM TaqMan MGB probe) were obtained from Applied Biosystems and for endogenous controls, each gene expression was normalized to GAPDH. Primer IDs were Rac1: Hs01902432_s1, cortactin: Hs01124225_m1, and GAPDH Hs99999905_m1.

Data was analyzed using the delta-delta Ct method. The threshold cycle (Ct) of each sample's GAPDH target gene was subtracted from the Ct of each sample to give delta Ct. The delta Ct of HIV-1 samples were subtracted from the delta Ct of the control sample to give delta-delta Ct. Fold change was calculated by the equation: 2^-delta-delta Ct.

2.2.11 Protein extraction and western blot analyses

Cells were lysed in a mammalian total protein extraction reagent (Thermo Fisher) containing 1x Protease Inhibitor Cocktail (Sigma) and 1x phosphatase inhibitor cocktail. Lysates were kept on ice for 20 mins and centrifuged for 30 mins 13,000 RPM to remove insoluble materials. Total protein concentration in the resulting supernatant was measured using the bicinchoninic acid assay (Thermo Fisher). Proteins (40 µg) were separated by sodium dodecyl sulfate polyacrylamide gel electrophoresis (80 volts for 1.5 hours) and transferred to nitrocellulose membrane (65 volts for 4 hours). Membranes were blocked with SuperBlock™ blocking buffer (Thermo Fisher) for 1 hour at room temperature on a rocking platform followed by incubation with primary antibodies overnight at 4℃ on a rocking platform. Membranes were washed 5 times for 5 minutes each with 1x western blot wash buffer containing 40 g Dulbecco's phosphate buffered saline (DPBS, Corning) and 0.001% Tween20 (Sigma), and then incubated with either anti-mouse or anti-rabbit HRP conjugated antibodies for 1 hour at room temperature on a rocking platform. Membranes were washed 5 times for 5 minutes each with 1x western blot wash buffer, incubated with Immobilon Western Chemiluminescent HRP Substrate (Millipore, Temecula, CA), and developed on x-ray film. ERK1/2 antibodies were from Cell Signaling (Danvers, MA), while all other antibodies were from Full Moon Biosystems. All antibodies were used at a 1:1000 dilution. Following Western blot with phosphorylated antibodies, membranes were stripped using Restore Western Blot

Stripping Buffer (Thermo Fisher) and re-blotted with the corresponding total antibody, then stripped again and re-blotted with β-actin antibody to confirm equal loading. Results were expressed as ratios of relative intensity of the phospho-protein to total protein, or β-actin.

2.2.12 Immunofluorescence and confocal microscopy

Sections of human brain tissue were embedded in optimal cutting temperature (OCT) compound (Sakura Finetek, Torrance, CA). Five-micrometer sections were cut from each human brain tissue using a Leica CM1860 cryostat (Buffalo Grove, IL) and mounted on glass slides. Tissue sections were fixed in 4% paraformaldehyde for 20 minutes at room temperature, dried, washed with 1X PBS for 5 minutes at room temperature, and incubated 1 hour in PBS containing 3% BSA to block for non-specific binding. Tissue sections were incubated at 4 ℃ overnight with antibodies to phospho-Rac1(S71) (1:100), CD163 (1:00), ionized calcium binding adapter molecule-1 (IBA1, 1:50), GFAP (1;100), microtubule-associated protein-2 (MAP2, 1:300), or glucose transporter-1 (GLUT1,1:100) diluted in PBS containing 3% BSA and 0.1% Triton X-100. All antibodies were purchased from Abcam (Cambridge, MA). After incubation with primary antibodies, tissues were washed with 1X PBS 3 times for 5 minutes and stained with secondary antibodies coupled with Alexa Fluor-488, or −635 (Life Technologies) at 1:500 dilutions for 1 hour in the dark at room temperature. Stained tissues were washed 5 times with 1X PBS and mounted in Prolong Gold anti-fade reagent containing DAPI (Molecular Probes, Grand Island, NY). For confocal microscopy, stained tissues were examined under an Olympus FV500-IX 81 confocal laser scanning imaging system. The triple laser lines excitation were 405 nm for nucleus-stains; 488 nm for CD163, GFAP, MAP2, IBA1, or GLUT1, and 635 nm for pRac1(S71). A 4th laser line (excitation: 543 nm. Emission: 595-nm) was used to detect auto-fluorescent pigments.

2.2.13 Statistical analyses

Data were analyzed by t-test (two-tailed) for two-group comparisons and one-way ANOVA followed by Tukey's multiple-comparisons tests using GraphPad Prism 5.0b. (GraphPad Software, La Jolla, CA). Threshold of significance level was 0.05.

2.3 Results

2.3.1 CCR5 blockers prevent HIV-1 infection of macrophages

MVR and TAK are both small molecule CCR5 antagonists that are able to inhibit HIV-1 infection *in vitro* in a variety of cell types and *in vivo* [114, 133, 226-229]. To confirm the effects of CCR5 blockers in human MDM, we infected these cells with HIV-1 in the presence of TAK or MVR and viral replication was assessed by quantifying viral reverse transcriptase activity. From day-5 to day-18 post-infection (p.i), MVR diminished MDM infection by 7.2- to 44-fold (Figure 2-3), while TAK diminished MDM infection by 4.8- to 15.3-fold (Figure 2-4). All data was statistically significant, with $p < 0.001$.

2.3.2 CCR5 blockers do not affect brain endothelial cell integrity

Several antiretrovirals, including AZT and indinavir have been associated with BBB dysfunction, which could exacerbate HIV-induced BBB injury [230]. To determine whether CCR5 blockers could alter endothelial cell integrity, we assessed their effects on the brain TEER. Exposure of HBMEC to concentrations of 5 μM to 20 μM TAK (Figure 2-5A) or MVR (Figure 2-5B) did not alter TEER at any time through 48 hours. Saponin (0.1%) was used as a non-resistant control and was associated with the loss of endothelial integrity.

2.3.3 CCR5 blockers decrease HIV-1-induced monocyte adhesion

HIV-1 infection has been shown to increase monocyte adhesion to brain endothelial cells [215]. To determine if CCR5 antagonists could diminish this, we quantified the adhesion of infected and non-infected monocytes to the BBB, in the presence or absence of CCR5 antagonists, using an *in vitro* BBB model. HIV-1 infection increased monocyte adhesion to HBMEC and TAK (5 μM), MVR (5 μM), and CCR5 neutralizing antibodies (25 μg/ml) significantly decreased HIV-1-induced monocyte adhesion (Figure 2-6).

2.3.4 Increased expression of cytoskeletal proteins in HIV-infected monocytes following monocyte-endothelial interactions

During migration a monocyte's cytoskeleton undergoes major reorganization to facilitate its movement across the endothelium [231]. To determine the changes in cytoskeleton-associated proteins in infected and non-infected monocytes during monocyte-endothelial interactions, we co-cultured infected or non-infected monocytes with HBMEC in the presence or absence of the CCR5 antagonist, TAK (5 μM). Co-culture of HIV-1 infected monocytes with HBMEC induced the upregulation of cytoskeleton-associated proteins in monocytes compared to uninfected monocytes co-cultured with HBMEC. Of the 141 proteins in the array, 13 proteins were upregulated by 2-fold or more (Table 2-2). The remaining 128 cytoskeleton-associated proteins were not significantly changed or did not meet the 2-fold change cut-off. Treatment of monocytes with TAK prevented HIV-1-induced upregulation of cytoskeleton-associated proteins during monocyte-endothelial interactions (Table 2-2).

2.3.5 Altered phosphorylation of cytoskeleton-associated proteins in HIV-1 infected monocytes during monocyte-endothelial interactions

Phosphorylation is known to play a major role in the regulation of protein function, protein-protein interactions, and cellular functions [232]. Because minor changes in

protein phosphorylation levels can have functional significance, we used a 1.5-fold change cut-off to analyze proteins differentially phosphorylated in HIV-1 infected monocytes following monocyte-endothelial co-culture compared to infected monocytes treated with TAK and non-infected monocytes co-cultured with HBMEC. Normalization of each phospho-protein to the expression of its corresponding total protein showed an increase in the phosphorylation of 9 proteins and a decrease in the phosphorylation of 12 proteins. Thirty-three proteins had no significant change in phosphorylation level. When proteins were normalized to the sample's actin levels, 33 proteins showed an increase in phosphorylation, 7 proteins showed a decrease in phosphorylation, and 25 proteins had no significant change in phosphorylation levels. We then determined the cytoskeleton-associated proteins that were differentially expressed when normalized to both their corresponding total proteins and the sample actin levels. Eight proteins showed significantly increased phosphorylation and 3 proteins showed significantly decreased phosphorylation when using both normalization methods (Table 2-3). HIV-1 infection and endothelial-monocyte interactions increased the phosphorylation of Merlin (Ser518), vasodilator-stimulated phosphoprotein (VASP) (Ser157), Rac1 (S71), cortactin (Tyr421), and ERK1/2 (Tyr204/202) by 4.5 to 6.3-fold, 4-fold, 2.3- to 3.6-fold, 2 to 3-fold, and 2.4 to 2.6-fold, respectively (Table 2-3). TAK prevented HIV-1-induced phosphorylation of these cytoskeleton-associated proteins during monocyte-endothelial interactions (Table 2-3, 2-4). IPA of differentially expressed and phosphorylated proteins showed that the major biological functions associated with these cytoskeleton-associated proteins and phosphorylation network included cellular assembly and organization, cellular movement, cell morphology, post-translational modification, cell cycle, and cell-to-cell signaling (Table 2-5). Canonical pathways activated in HIV-1 infected monocytes co-cultured with HBMEC included chemokine and integrin signaling and cell junction signaling (Table 2-6).

2.3.6 Validation of HIV-1-induced activation of Rac1 and ERK1/2 following monocytes-endothelial interactions, and CCR5 modulation

Rac1 is a cytoskeletal protein that regulates cell polarity and the formation of lamellipodia, and thus plays an important role in leukocyte transendothelial migration [233]. ERK1/2 also regulates cellular proliferation, differentiation, and transcriptional regulation [234]; and both Rac1 and ERK1/2 have been previously implicated in HIV-1 infection [235-238]. Therefore, we performed additional Western blot experiments to confirm whether HIV-1 infection and monocyte-endothelial interactions induced Rac1 and ERK1/2 activation and to confirm the role of CCR5. The data confirmed our protein microarray results and showed that HIV-1 infection increased phosphorylation of Rac1 at S71 and phosphorylation of ERK1/2 in human monocytes following monocyte-endothelial communication, and the CCR5 antagonists MVR and TAK diminished HIV-1-induced phosphorylation of Rac1 and ERK1/2 (Figure 2-7).

2.3.7 Increased transcription of cortactin (CTTN) and Rac1 in brain tissues of HIV-1-infected patients

To determine whether our *in vitro* findings correlated with changes in HIV-1-infected humans and to determine if our translational results could be correlated with transcription, we analyzed the brain tissues of 12 HIV-1 seronegative control subjects, 9 HIV-1-seropositive patients without evidence of HIVE, and 10 HIV-1-seropositive patients with HIVE and HAND (Table 2.1). All brain tissues were from the cortex region, with 28 of the 31 samples from the frontal cortex, 2 samples from the parietal cortex, and 1 sample from the temporal cortex. The average age for all individuals was 45.5 years ± 11.15 (range: 27-72 years). The average age was 52 years, 41.78 years, and 41.4 years for HIV-seronegative, HIV-seropositive, and HIV-seropositve with neurocognitive impairment, respectively. The average post-mortem interval for all individuals was 7.4

hours ± 4.31 (range: 2.75-21 hours). The average post-mortem interval was 4.62 hours, 8.53 hours, and 9.72 hours for HIV-seronegative, HIV-seropositive, and HIV-seropositve with neurocognitive impairment, respectively. RAC1 transcription was upregulated by 3-fold and 4-fold in the brain tissues from HIV-1-infected patients compared to brain tissues from seronegative controls ($p<0.01$) and HIVE patients ($p<0.01$), respectively (Figure 2-8A, B). In addition to RAC1, we examined CTTN transcription. Cortactin promotes the formation of lamellopodia and subsequent cellular migration [239]; Rac1 can activate cortactin, resulting in the formation of lamellipodia [240]. CTTN transcription was upregulated by 2.4-fold ($p < 0.001$) and 1.6-fold ($p < 0.01$) in the brain tissues from HIV-1-infected patients compared to brain tissues from seronegative controls and HIVE patients, respectively (Figure 2-8C, D).

2.3.8 Rac1 phosphorylation at S71 is increased in the brain tissues of HIV-1-infected patients

Using the brain tissues described in section 2.2.7, we analyzed Rac1 phosphorylation in human brain tissues. In the first experiment, 4 brain tissue samples were used for each group: seronegative controls (HIV neg), HIV-1-infected individuals without evidence of neurocognitive impairment (HIV pos), and HIV-1-infected individuals with HIVE. In HIV-1-infected patients there was significant upregulation of phosphorylated Rac1(S71) in brain tissues compared to brain tissues from seronegative controls ($p<0.01$) and HIVE patients ($p<0.001$; Figure 2-9A,B). An additional western blot experiment with 6 brain tissue samples from HIV-1-negative and HIV-1-positive individuals further confirmed that phosphorylated Rac1(S71) is increased in HIV-1-positive individuals ($p<0.05$; Figures 2-9C,D).

2.3.9 Phospho-Rac1 (S71) is expressed in brain macrophages and blood vessel tight junctions

To determine which cell types in the human brain expresses phospho-Rac1 (S71), we analyzed brain tissue sections from seronegative controls and HIV-1-infected patients with and without HIVE by confocal microscopy. Tissues showed high expression of pRac1 (S71) in brain macrophages (Figure 2-10A-C, white arrows) and blood vessels, with pRac1(S71) mostly expressed on vessels tight junction strands (Figure 2-10A, C, G, J-M, orange arrows). Most samples did not show pRac1 expression in microglia (Figure 2-10D, E); however, some HIVE patients did show pRac1 expression in microglia (Figure 2-10F, white arrows). There was no observed pRac1(S71) expression in astrocytes (Figure 2-10G-I) or neurons (Figure 2-10J, K) in any of the samples analyzed. Because lipofuscin-like pigments can accumulate in the human brain and autofluoresce over a broad excitation and emission spectra [241], we used a 4th laser line (excitation: 543-nm, emission: 595-nm) to differentiate autofluorescent pigments from antibody staining. These autofluorescent pigments are shown in white (Figure 2-10, yellow arrows).

2.4 Discussion

In this study, we showed, using a cytoskeleton-associated protein array and western blot analysis, that HIV-1 infection of monocytes increases the expression of cytoskeleton-associated proteins during interactions with HBMEC and treatment with CCR5 antagonists attenuated these effects. HIV-1 induced phosphorylation of cytoskeleton-associated proteins, including Rac1 at S71 in monocytes during interactions with HBMEC. This appears to be mediated by CCR5, since CCR5 antagonists attenuated HIV-1-induced Rac1 S71 phosphorylation. We further showed that HIV-1 infection in humans is associated with increased transcription of RAC1 and CTTN in brain tissues.

Rac1 phosphorylation at S71 is increased in the brain tissues of HIV-1 infected individuals compared to non-infected individuals and those with HAND. We showed by immunofluorescence analysis of brain tissues that Rac1 phosphorylation at S71 occurred mostly in brain macrophages and blood vessels. Furthermore, CCR5 blockers reduced the HIV-1-induced increase in monocyte adhesion to the BBB and prevented viral infection.

Rac1, a member of the Rac subfamily of Rho GTPases, is a small signaling G protein and a modulator of the cytoskeleton functions; it is involved in cytoskeletal reorganization, cell-cell adhesion, and motility [242]. Rac1 is ubiquitously expressed and is the predominant Rac family member found in monocytes, accounting for 90% of Rac expression [243]. Like most Rho GTPases, Rac1 behaves as a molecular switch fluctuating between inactive and active states [233]. In its active state, guanosine triphosphate (GTP) binds Rac1 and in its inactive state it is bound by guanosine diphosphate (GDP) [233]. Two proteins are involved in regulating the switch between Rac1 activation and inactivation: Guanine nucleotide Exchange Factors activate Rac1 by promoting the change of GDP to GTP and GTPase-Activating Proteins inactivate Rac1 by hydrolysis of the bound GTP back into GDP [233]. Rac1 can be activated by a variety of extracellular stimuli, including GPCRs and integrins [244, 245]. Once activated, Rac1 can activate a variety of molecules, such as ERK1/2, PKB, and STAT [246]. Activation of these pathways via Rac1 is associated with cell growth and chemotaxis.

Rac1 plays a major role in cell adhesion and migration [233]. In lymphocytes, activated Rac1 promotes adhesion by cell spreading and this was accompanied by actin polymerization, cytoskeletal rearrangements, and clustering of integrins [247]. Rac1 can promote the formation of membrane ruffles and lamellipodia and subsequent migration in multiple ways. Activation of Rac1 stimulates the actin related protein 2/3 (ARP2/3) complex through activation of WASP-family verprolin-homologous protein via its

effectors non-catalytic region of tyrosine kinase adaptor protein-1 (NCK1) associated protein-1 and cytoplasmic fragile X mental retardation 1 interacting protein-2 (FMR1) or brain-specific angiogenesis inhibitor 1 associated protein-2 (BAIAP2) [233]. Through its effector, p21-activated kinase (PAK), Rac1 can induce activation of the actin binding protein, filamin, a protein important in cross-linking actin filaments [233]. In addition, PAK can activate LIM (Lin11, Isl-1 & Mec-3 domain) kinase, which in turn inactivates cofilin. Inactivated cofilin stabilizes actin filaments and filament arrays [233]. The result of these pathways is the polymerization of new actin filaments and the formation of a branched network of actin characteristic of lamellipodia and membrane ruffles [233]. Furthermore, Rac1 S71 phosphorylation has been shown to increase filopodial structures and enhance cell motility and migration [248]. This suggests that activation of Rac1 in HIV-1-infected monocytes following monocyte-endothelial interactions could result in increased migration of infected monocytes across the blood-brain barrier leading to HIV-1 CNS infection.

In addition to its role in cell adhesion and migration, there is some evidence that Rac1 may be involved in inflammatory responses. In macrophages, prostaglandins can activate the inflammatory molecule cyclooxygenase-2 via Rac1 [249]. Rac1 activity can promote the activation of NADPH oxidase and the production of reactive oxygen species, which both can act as proinflammatory mediators [250]. Thus, in addition to its role in HIV-1-induced monocyte migration, Rac1 may also be involved in oxidative stress and the inflammatory response during HIV-1 infection.

Previous studies have also suggested a role for Rac1 in HIV-1 infection. Nef activates PAK1 through association with Rac1, and a dominant-negative form of Rac1 decreased viral production levels [237, 251]. Nef activation of PAK1 via Rac1 resulted in cytoskeletal rearrangements, such as increased lamellipodia [252, 253]. In addition, Rac1 appears to be necessary for CD28-dependent HIV-1 transcription in T-cells and

internalization of the Tat protein transduction domain, a small region of Tat that is responsible for translocating Tat across the cellular membrane [236, 254]. Lastly, activated Rac1 is involved in Gag plasma membrane localization and viral particle production [255].

CCR5 can interact with Rac1 and these interactions are involved in HIV-1 infection and migration. Binding of viral Env to the CD4 receptor and CCR5 or CXCR4 co-receptors induces a signaling cascade through Gαq that results in Rac1 activation, actin cytoskeletal reorganizations, and membrane fusion, which are necessary for efficient viral infection [27, 256, 257]. HIV-1 infection of macrophages via endocytosis requires Rac1 [235]. In addition, activation of CCR5 in macrophages results in Rac1 activation, cytoskeletal reorganization, and formation of lamellipodia; and a Rac dominant–negative mutation blocked these effects [221].

Cortactin, which was identified in our protein array and further shown to be transcriptionally upregulated in the brains of HIV-1-infected individuals, is a cytoskeletal protein that is localized to the sites of actin assembly and play a crucial role in the formation of lamellipodia [258]. Rac1 activates cortactin, allowing cortactin to bind and activate the ARP2/3 complex, leading to the formation of lamellipodia [240]. Overexpression of cortactin is associated increased invasiveness of several types of cancers, including head and neck squamous cell carcinoma, breast cancer, colorectal cancer, and melanoma [239]. Cortactin overexpression in cancer is thought to alter cellular migration [239]. Although not previously implicated in HIV-1-infection, increased expression of cortactin in infected cells could lead to increased migration of these cells.

HIV-1 induced transcriptional regulation of Rac1 and cortactin likely occurs during the earlier stages of infection, as our data showed increased Rac1 and cortactin transcription in the brain tissues of HIV-1 infected individuals without evidence of neurocognitive impairment compared to seronegative controls or HIV-1 infected

individuals with HAND/HIVE. This likely correlates with BBB breach and increased trafficking of monocytes into the CNS, which is known to precede HAND/HIVE [259]. Previous studies by our laboratory have shown increased transcriptional upregulation of proinflammatory cytokines in brain tissues of HIV-1+/nonencephalitic patients compared to brain tissues of seronegative controls and HAND/HIVE patients, further confirming that increased inflammation and inflammation-induced damages that leads to HIVE and HAND often precede the onset of HIVE/HAND [215]. Rac1 activation is associated with clustering of cell adhesion molecules, leukocyte migration, and increased production of reactive oxygen species [233]. These events are all associated with HIV-1 CNS dysfunction and occur prior to the onset of HAND/HIVE [260]. In accordance with these studies, we suggest that gp120 binding to CCR5 in monocytes and the interactions of these infected monocytes with the brain endothelium results in activation of Rac1 and cortactin, which in turn increases monocyte adhesion and migration through the BBB, resulting in increased infiltration of infected monocytes into the CNS. Furthermore, activation of Rac1 could result in increased expression of proinflammatory molecules, causing further damage to the BBB and CNS.

2.5 Summary

HIV-1 infection of monocytes is associated with increased adhesion to the brain endothelium. This adhesion, as well as viral replication in macrophages, can be blocked by the use of CCR5 antagonists. On their own, CCR5 blockers are not toxic to monocytes/macrophages and do not affect BBB integrity. Using a cytoskeleton-associated protein array we found that HIV-1 infection of monocytes increased the expression and phosphorylation of cytoskeleton-associated proteins, including phosphorylation of Rac1 at S71 and cortactin, during interactions with brain endothelial cells. These proteins are involved in cellular assembly, cellular movement, and cell

morphology; and blocking HIV-1 infection in monocytes by the use of CCR5 antagonists prevented these changes. Rac1 mRNA expression and phosphorylation at S71 was increased in human brain tissues from HIV-1-infected individuals, compared to seronegative controls and HIV-1-infected individuals with HAND/HIVE. Lastly, we found that phosphorylated Rac1 S71 was expressed mainly in brain macrophages and blood vessel tight junctions. We suggest that HIV-1 binding to CCR5 in monocytes and the interactions of these infected monocytes with the brain endothelium results in activation cytoskeletal-associated proteins, which in turn increases monocyte adhesion and migration through the BBB, resulting in increased infiltration of infected monocytes into the CNS.

2.6 Figures and tables

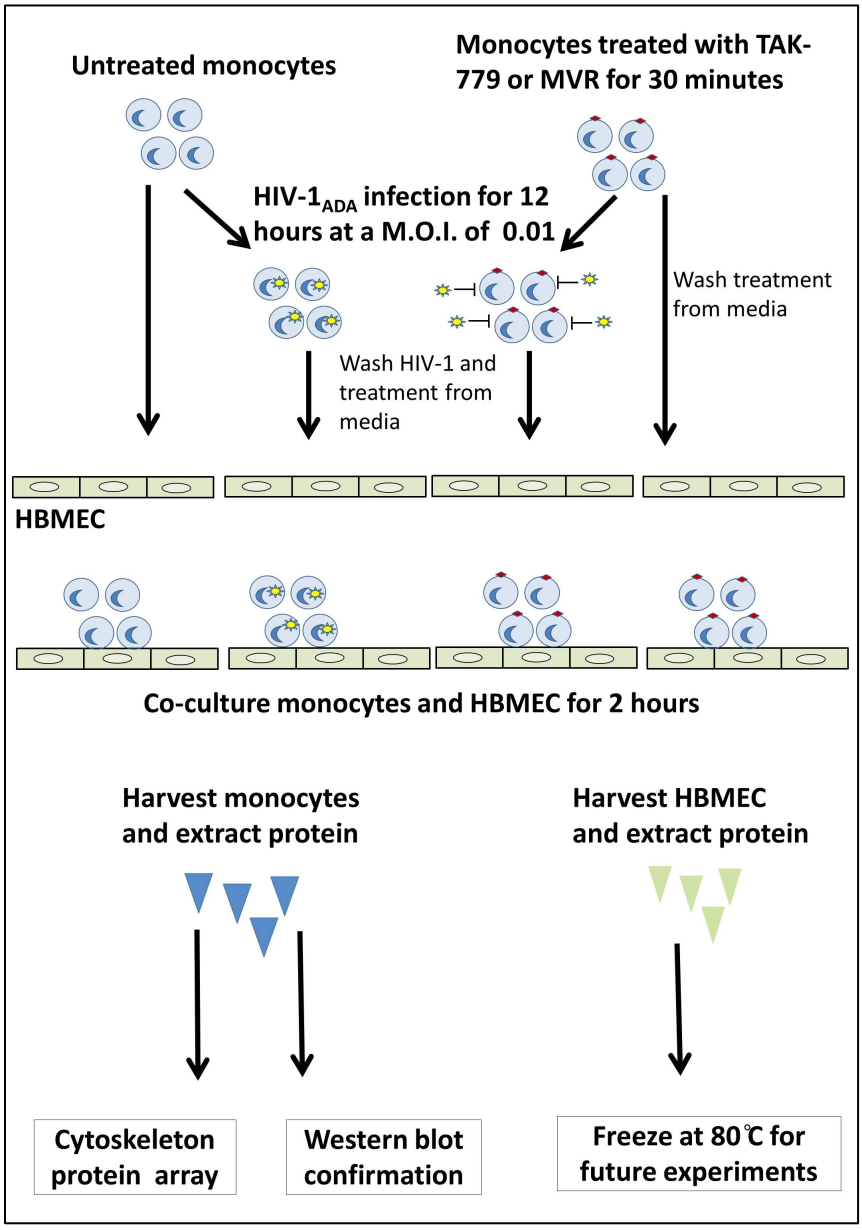

Figure 2-1: Summary of co-culture experiments. Freshly elutriated monocytes were treated with 5 μM TAK or MVR for 30 minutes followed by infection with HIV-1_{ADA} for 12 hours and were washed three times with PBS to remove free virions. Monocytes were then resuspended in fresh media and co-cultured with HBMEC for 2 hours in a 5:1 ratio. Treatment conditions were: Untreated, uninfected monocytes; treated (5 μM TAK or MVR), uninfected monocytes; untreated, infected monocytes; and treated (5 μM TAK or

MVR), infected monocytes. Cells were harvested separately and protein was extracted and quantified as described in Methods (**2.2.5** and **2.2.11**). Monocyte protein lysates were used for cytoskeleton-associated protein array and western blot experiments as described in Methods (**2.2.5** and **2.2.11**), and HBMEC protein lysates were frozen for future experiments.

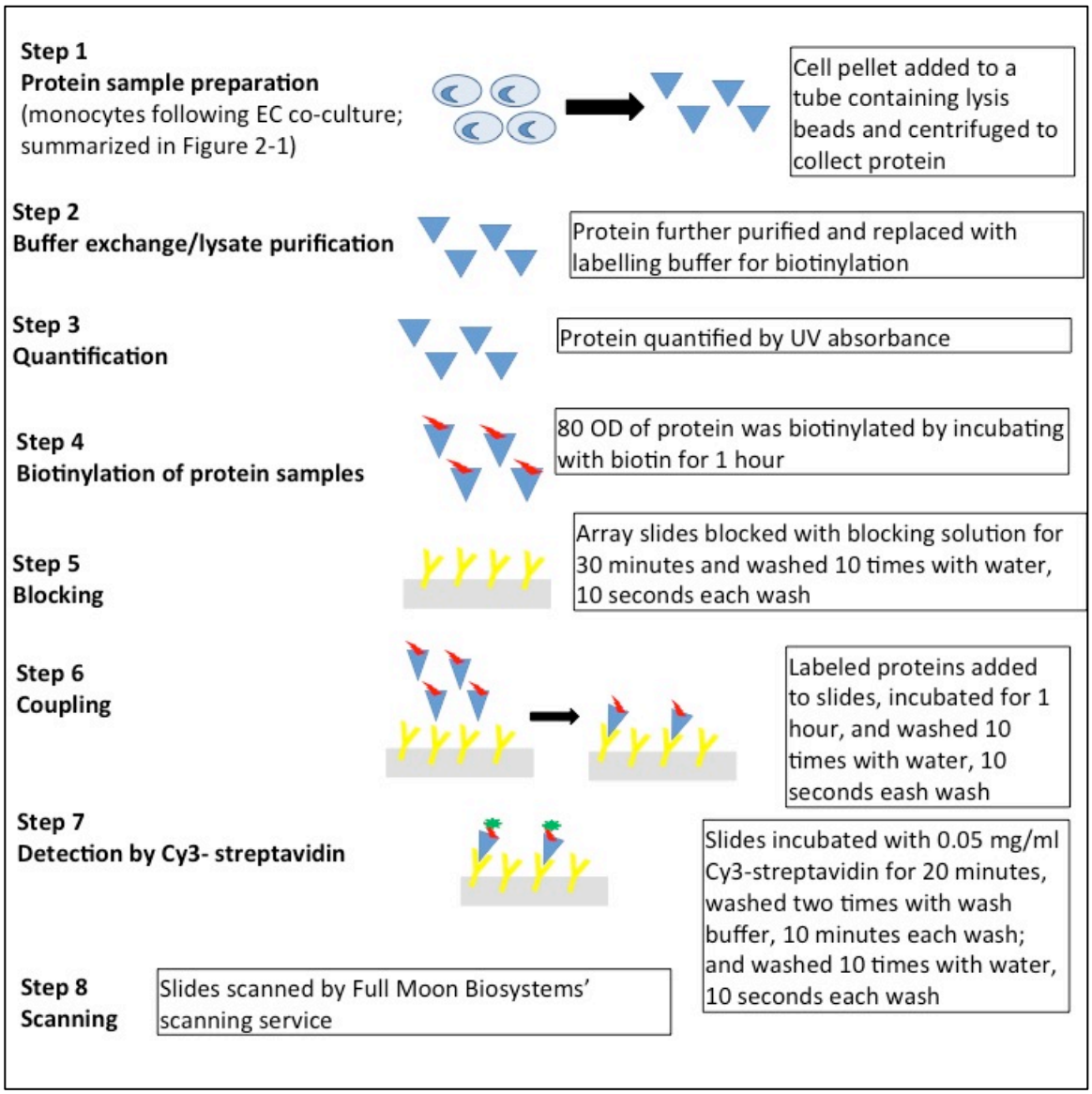

Figure 2-2: General outline of the antibody array. Monocytes were lysed and protein extracted following co-culture with HBMEC using the Full Moon protein extraction kit. Samples were biotinylated for 1 hour. Array slides were blocked for 30 minutes followed by washing and labeled proteins were incubated with array slides for 1 hour followed by washing. Slides were incubated with Cy3-streptavidin for 20 minutes, washed with

washing buffer, and then washed with water. Slides were scanned using Full Moon Biosystems Scanning Array Service.

HIV-1 Status	ID	Gender/ Age (y)	PMI (h)	Neurocognition/ Neuropathology	Other autopsy diagnosis
Neg	N1	M/35	8.5	Normal/None	Mild Alzheimer gliosis
Neg	N2	N/A	N/A	Normal/None	N/A
Neg	N3	F/38	5.75	Normal/Not significant	Mild gliosis, lung and bile duct carcinoma
Neg	N4	M/32	4.25	Normal/Not significant	Cystic fibrosis, and multiorgan failure
Neg	N5	F/46	4	Normal/Not significant	Mild fibrosis, mild patchy gliosis
Neg	N6	F/49	4.5	Normal/Not significant	Hepatic cirrhosis, liver failure
Neg	N7	M/52	5.25	Normal/None	Hypertension, renal failure
Neg	N8	M/72	3	Normal/None	Hypertension, COPD
Neg	N9	M/64	3.3	Normal/None	Hepatic carcinoma
Neg	N10	M/56	3	Normal/Not significant	Lung adenocarcinoma, mild nonspecific cortical atrophy
Neg	N11	M/67	3.5	Normal/None	COPD, TB
Neg	N12	M/61	5.75	Normal/Not significant	Cardiomyopathy, mild gliosis
Pos	P1	?/46	2.75	Normal/None	N/A
Pos	P2	?/27	8	Normal/None	N/A
Pos	P3	?/37	5	Normal/None	N/A
Pos	P4	M/39	11	Normal/None	Minimal non-diagnostic abnormalities
Pos	P5	M/35	6.5	Normal/None	Non-Hodgkins lymphoma, AIDS
Pos	P6	M/54	6.5	Normal/None	AIDS
Pos	P7	M/48	15	Normal/None	Liver disease
Pos	P8	M/52	8	Normal/None	AIDS
Pos	P9	M/38	14	Normal	Pneumonia, hemophilia A, AIDS
Pos	HAD1 /D1	M/30	6	HAD/HIVE	Minimal terminal anoxia
Pos	HAD2 /D2	?/50	21	HAD/HIVE	N/A
Pos	HAD3 /D3	?/39	12	HAD/HIVE	N/A
Pos	HAD4 /D4	?/40	12	HAD/HIVE	N/A
Pos	HAD5 /D5	M/47	11	HAD/HIVE	Encephalopathy, microglial nodule encephalitis, meningoencephalitis with microvascular damage
Pos	HAD6	M/40	5	HAD/HIVE	Non-Hodgkin’s

	/D6				lymphoma, AIDS, lymphocytic meningitis
Pos	HAD7 /D7	M/44	4	HAD/HIVE	Microglial nodules, astrocytosis, widespread gliosis, AIDS
Pos	HAD8 /D8	M/52	5	HAD/HIVE	Atherosclerosis
Pos	HAD9 /D9	M/34	11.5	HAD/HIVE	AIDS
Pos	HAD1 0/D10	M/38	7	HAD/HIVE	HIV encephalopathy / Leukoencephalopathy, AIDS

Table 2-1: Clinical history of brain tissues donors. Neg indicates HIV seronegative; Pos, HIV seropositive; HAD, HIV-associated dementia; HIVE, HIV encephalitis; y, years; M, male; F, female; ? or N/A, not available; and PMI, postmortem interval; AIDS, acquired immunodeficiency syndrome; COPD: chronic obstructive pulmonary disease; TB, tuberculosis. Modified from Woollard, S.M., Li, H., Singh S., Yu F., and Kanmogne G.D. (2014) HIV-1 induces cytoskeletal alterations and Rac1 activation during monocyte-blood-brain barrier interactions: modulatory role of CCR5. *Retrovirology. 11:20 [261].* Reprinted with permission under the Creative Commons Attribution License or equivalent.

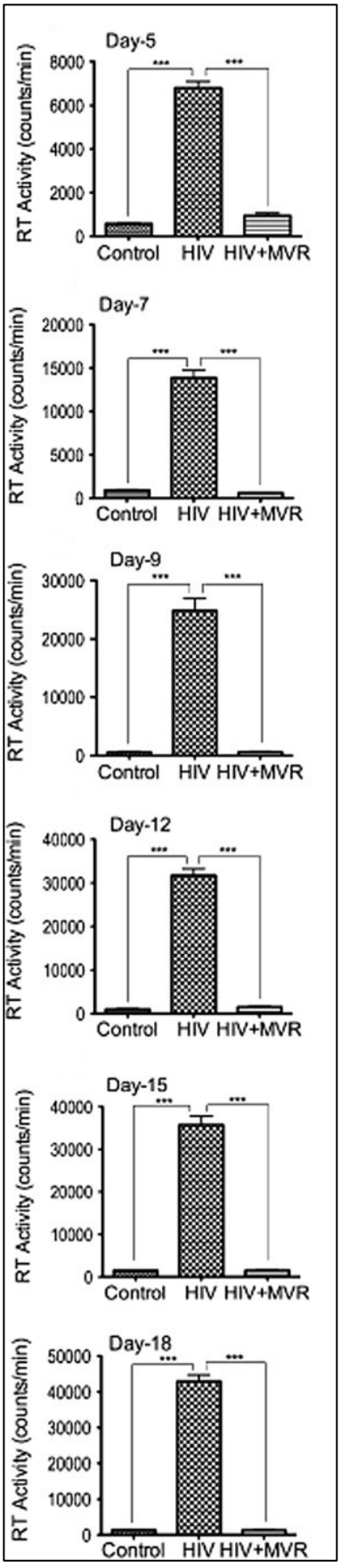
Day-5
RT Activity (counts/min)
8000
6000
4000
2000
0
***
***
Control
HIV
HIV+MVR
Day-7
RT Activity (counts/min)
20000
15000
10000
5000
0
***
***
Control
HIV
HIV+MVR
Day-9
RT Activity (counts/min)
30000
20000
10000
0
***
***
Control
HIV
HIV+MVR
Day-12
RT Activity (counts/min)
40000
30000
20000
10000
0
***
***
Control
HIV
HIV+MVR
Day-15
RT Activity (counts/min)
40000
30000
20000
10000
0
***
***
Control
HIV
HIV+MVR
Day-18
RT Activity (counts/min)
50000
40000
30000
20000
10000
0
***
***
Control
HIV
HIV+MVR

Figure 2-3: The CCR5 antagonist, MVR, inhibits HIV-1 infection in MDM. MDM were infected with the macrophage tropic HIV-1_{ADA} with or without MVR (5 μM) in the media. Controls consisted of mock-infected cells. Culture supernatants were collected every 2 or 3 days from day-5 to day-18 p.i and viral replication estimated by quantifying the reverse transcriptase activity. MVR inhibited HIV-1 infection from as early as day-5 and up to day-18 p.i. This is a representative data from 3 independent experiments using 3 different human donors, with each donor tested in triplicate. One-way ANOVA followed by Tukey's multiple-comparisons tests was performed using GraphPad Prism 5.0b to determine significance. Threshold of significance level was 0.05. ***$P < 0.001$. Error bars represent standard error of mean (SEM). Modified from Woollard, S.M., Li, H., Singh S., Yu F., and Kanmogne G.D. (2014) HIV-1 induces cytoskeletal alterations and Rac1 activation during monocyte-blood-brain barrier interactions: modulatory role of CCR5. *Retrovirology. 11:20 [261].* Reprinted with permission under the Creative Commons Attribution License or equivalent.

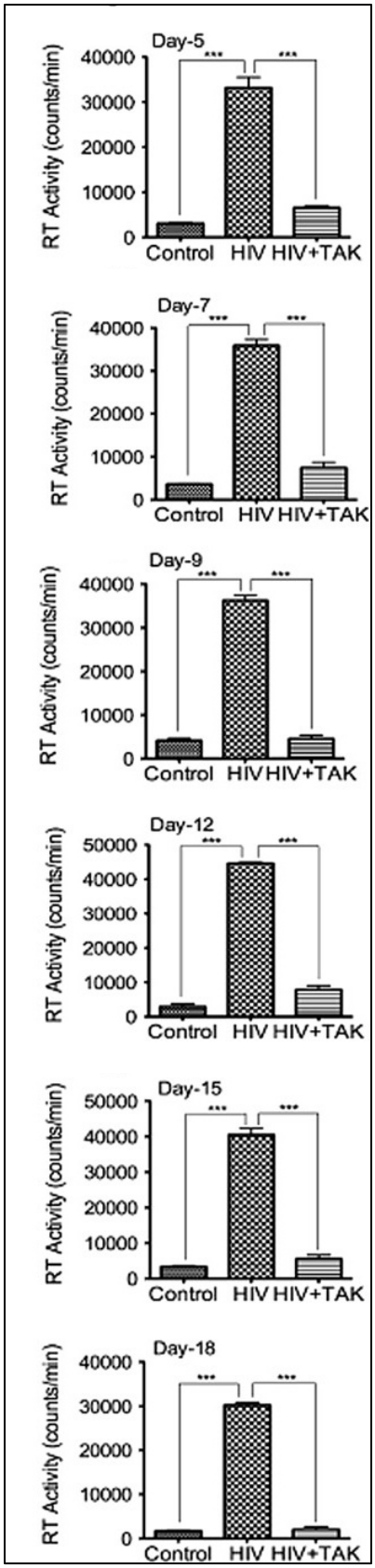
Day-5
RT Activity (counts/min)
40000
30000
20000
10000
0
***
***
Control
HIV
HIV+TAK
Day-7
RT Activity (counts/min)
40000
30000
20000
10000
0
***
***
Control
HIV
HIV+TAK
Day-9
RT Activity (counts/min)
40000
30000
20000
10000
0
***
***
Control
HIV
HIV+TAK
Day-12
RT Activity (counts/min)
50000
40000
30000
20000
10000
0
***
***
Control
HIV
HIV+TAK
Day-15
RT Activity (counts/min)
50000
40000
30000
20000
10000
0
***
***
Control
HIV
HIV+TAK
Day-18
RT Activity (counts/min)
40000
30000
20000
10000
0
***
***
Control
HIV
HIV+TAK

Figure 2-4: The CCR5 antagonist, TAK, inhibits HIV-1 infection in MDM. MDM were infected with the macrophage tropic HIV-1_{ADA} with or without TAK (5 μM) in the media. Controls consisted of mock-infected cells. Culture supernatants were collected every 2 or 3 days from day-5 to day-18 p.i. and viral replication estimated by quantifying the reverse transcriptase activity. TAK inhibited HIV-1 infection from as early as day-5 and up to day-18 p.i. This is representative data from 3 independent experiments using 3 different human donors, with each donor tested in triplicate. One-way ANOVA followed by Tukey's multiple-comparisons tests was performed using GraphPad Prism 5.0b to determine significance. Threshold of significance level was 0.05. ***$P < 0.001$. Error bars represent SEM. Modified from Woollard, S.M., Li, H., Singh S., Yu F., and Kanmogne G.D. (2014) HIV-1 induces cytoskeletal alterations and Rac1 activation during monocyte-blood-brain barrier interactions: modulatory role of CCR5. *Retrovirology. 11:20 [261].* Reprinted with permission under the Creative Commons Attribution License or equivalent.

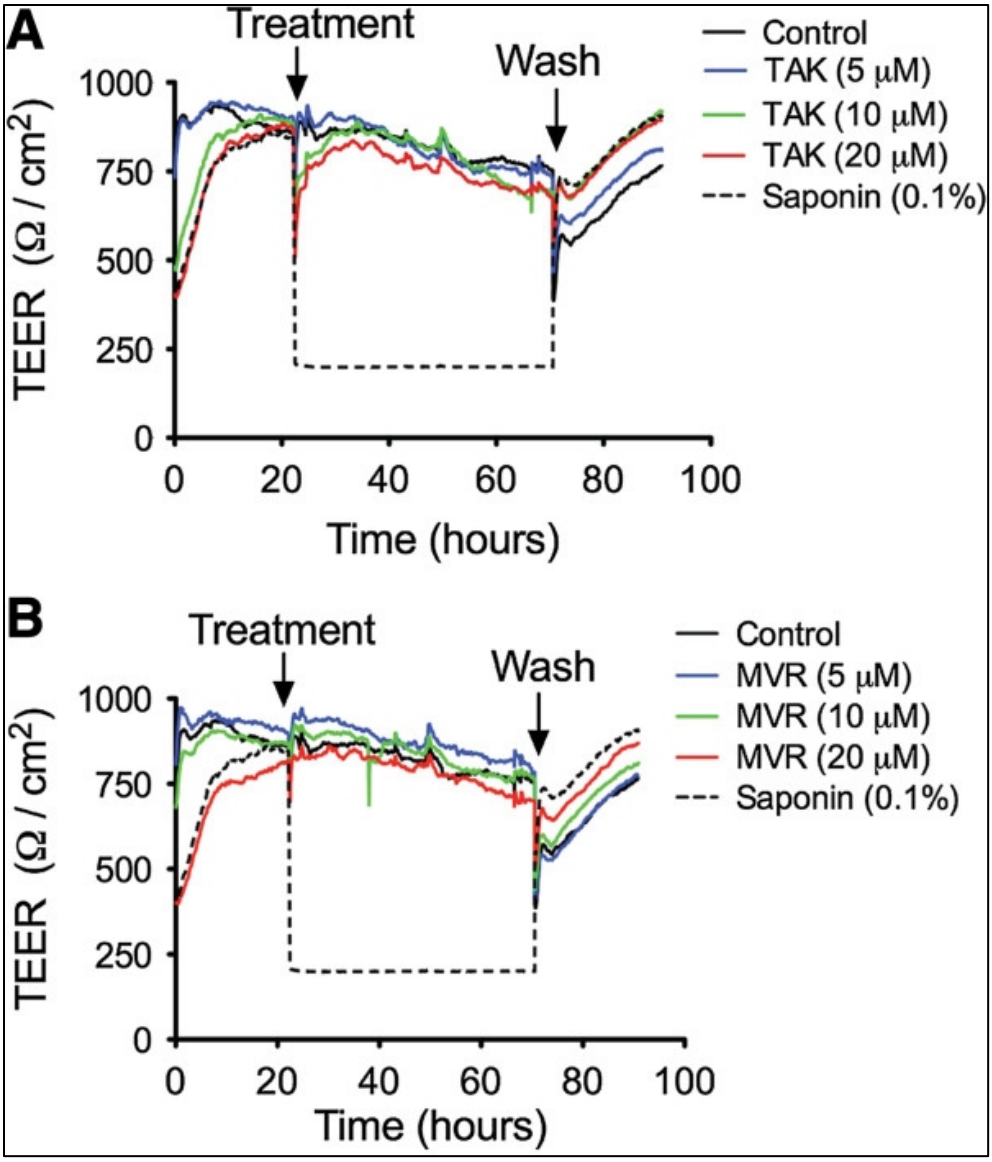

Figure 2-5: Effects of CCR5 antagonists on the BBB integrity. Confluent HBMEC monolayers were treated with TAK (**A**) or MVR (**B**) at concentrations of 5, 10, or 20 μM and TEER was measured in real-time before and after exposures. Neither TAK-779 nor MVR altered TEER. TEER values were similar during treatment and when cells were washed to remove CCR5 antagonists. Controls consisted of mock-treated cells and cells treated with 0.1% saponin. Saponin-induced decrease in TEER was reversed upon removal of saponin from the media. Modified from Woollard, S.M., Li, H., Singh S., Yu F., and Kanmogne G.D. (2014) HIV-1 induces cytoskeletal alterations and Rac1

activation during monocyte-blood-brain barrier interactions: modulatory role of CCR5. *Retrovirology. 11:20 [261].* Reprinted with permission under the Creative Commons Attribution License or equivalent.

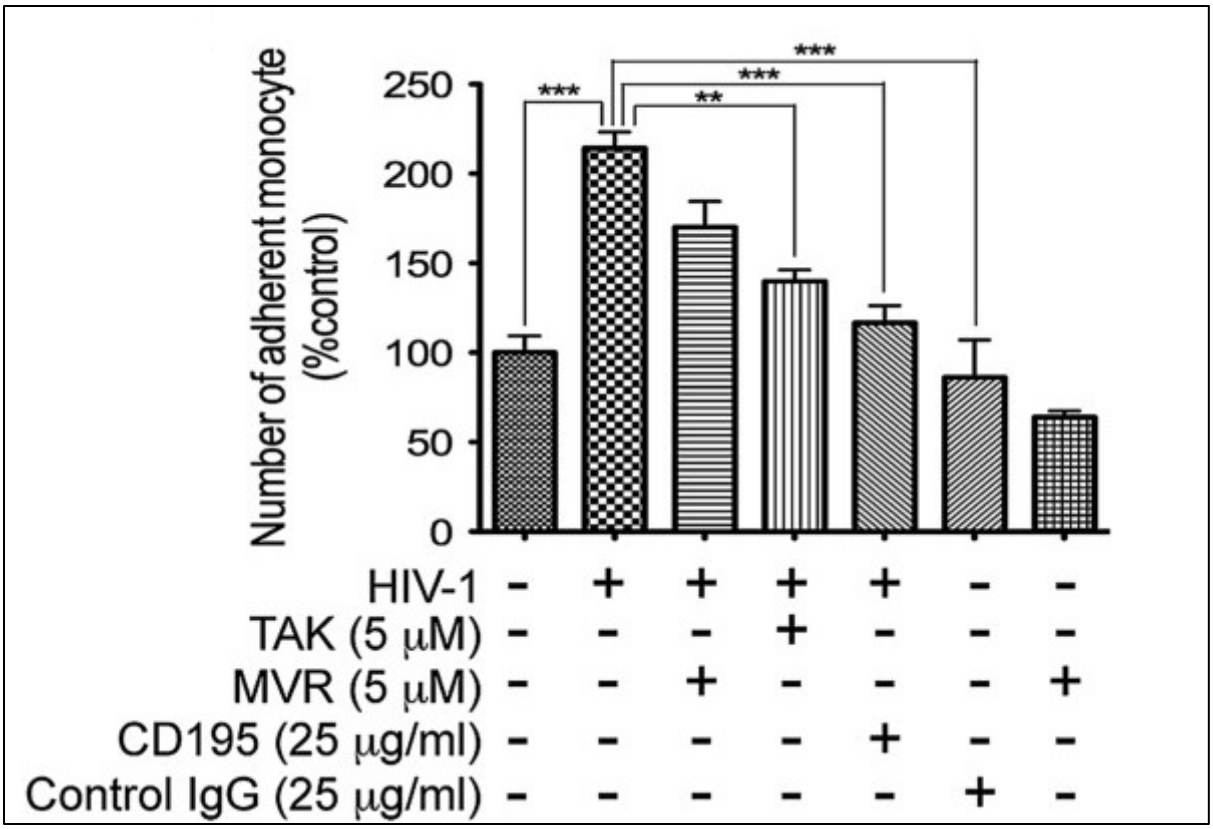

Figure 2-6: CCR5 blockers decrease HIV-1-induced monocyte adhesion. HMBEC were grown to confluency on clear-bottom 96-well black plates. Monocytes (2.5 x 10^5/condition) were treated with TAK or MVR (5 μM) or CD195, a CCR5 neutralizing antibody (25 μg/ml) prior to HIV-1 infection, stained with 10 μM CFDA, and co-cultured with HBMEC for 15 minutes. Monocytes adhesion to HBMEC was quantified by spectrophotometry (excitation: 492 nm, emission: 517 nm). Controls consisted of untreated uninfected cells and cells treated with isotyped-matched control IgG (25 μg/ml). HIV-1 increased monocyte adhesion to HBMEC. Treatment with CCR5 antagonists decreased viral-induced monocyte adhesion. One-way ANOVA followed by Tukey's multiple-comparisons tests was performed using GraphPad Prism 5.0b to determine significance. Threshold of significance level was 0.05. *$p < 0.01$; ***$p < 0.001$. Error bars represent SEM. Modified from Woollard, S.M., Li, H., Singh S., Yu F., and

Protein	HIV-1 vs. control fold change	p-value	HIV-1 vs. TAK fold change	p-value	Location
Src	3.05	5.09E-10	0.67	3.34E-05	Cytoplasm
MKK3/MAP2K3	2.78	3.62E-09	0.41	1.16E-11	Cytoplasm
PKC alpha	2.56	7.34E-08	0.57	6.81E-06	Cytoplasm
p130Cas	2.51	2.06E-08	0.54	1.16E-11	Plasma membrane
MKK7/MAP2K7	2.41	5.47E-09	0.45	1.16E-11	Cytoplasm
CaMK2-beta/gamma/delta	2.40	1.61E-09	0.69	3.61E-04	Nucleus
Ezrin	2.22	4.15E-10	0.50	1.16E-11	Plasma membrane
PLC beta3	2.17	3.62E-09	0.48	1.09E-06	Cytoplasm
c-Raf	2.07	1.99E-11	0.57	1.29E-11	Cytoplasm
PLC-beta	2.04	7.50E-07	0.53	2.09E-10	Cytoplasm
WAVE1	2.02	3.19E-06	1.17	1.61E-03	Nucleus
LIMK1	1.99	1.99E-11	0.46	3.08E-11	Cytoplasm
Myosin regulatory light chain 2	1.99	5.47E-09	0.63	7.03E-11	Cytoplasm

Table 2-2: Differentially expressed total proteins in HIV-1 infected-monocytes co-cultured with HBMEC. Table shows p-values adjusted using the Benjamini & Hochberg method. Src: v-src sarcoma viral oncogene homolog; MKK3/MAP2K3: mitogen-activated protein kinase kinase3; PKC: protein kinase C; p130Cas: breast cancer anti-estrogen resistance 1; MKK7/MAP2K7: mitogen-activated protein kinase kinase 7; CAMK2: calcium/calmodulin-dependent protein kinase-2; PLC: phospholipase C; c-raf: v-raf-1 murine leukemia viral oncogene homolog 1; WAVE1: WAS protein family 1; LIMK1: LIM domain kinase 1. Modified from Woollard, S.M., Li, H., Singh S., Yu F., and Kanmogne G.D. (2014) HIV-1 induces cytoskeletal alterations and Rac1 activation during monocyte-

blood-brain barrier interactions: modulatory role of CCR5. *Retrovirology. 11:20 [261].* Reprinted with permission under the Creative Commons Attribution License or equivalent.

	HIV-1 vs. CONTROL		HIV-1 + TAK vs. CONTROL		HIV-1 vs. HIV-1 + TAK	
Name	**Fold change**	**p-value**	**Fold change**	**p-value**	**Fold change**	**p-value**
Merlin (Phospho-Ser518)	4.47	8.13E-12	1.39	8.97E-05	0.31	1.45E-10
VASP (Phospho-Ser157)	4.05	8.13E-12	1.29	0.00047	0.32	1.84E-11
ERK1-p44/42 MAP Kinase (Phospho-Tyr204)	2.38	4.31E-08	1.14	0.10	0.48	3.68E-09
Rac1/cdc42 (Phospho-Ser71)	2.24	1.28E-05	0.85	0.17	0.38	1.76E-07
Cortactin (Phospho-Tyr421)	1.20	8.13E-12	0.63	1.53E-10	0.31	1.84E-11
CaMK1-a (Phospho-Thr177)	1.93	5.75E-05	1.47	0.0092	0.76	0.00013
ERK1-p44/42 MAP Kinase (Phospho-Thr202)	1.74	6.72E-08	1.15	1.13E-05	0.66	3.71E-06
ERK3 (Phospho-Ser189)	1.68	7.74E-05	1.10	0.556	0.65	0.0035
MEK1(Phospho-Ser217)	1.47	0.00017	0.83	0.00034	0.57	4.63E-06
MKK6 (Phospho-Ser207)	0.49	8.13E-12	0.49	1.53E-10	1.01	0.96
FAK (Phospho-Tyr397)	0.44	8.13E-12	0.87	0.0552	1.97	8.0E-09
MKK7/MAP2K7 (Phospho-Ser271)	0.30	8.13E-12	0.81	0.0344	2.65	1.5

Table 2-3: Phosphorylated proteins differentially expressed in HIV-1 infected-monocytes co-cultured with HBMEC, when normalized to total proteins. Table shows p-values adjusted using the Benjamini & Hochberg method. VASP: vasodilator-stimulated phosphoprotein; CaMK1: calcium/calmodulin-dependent protein kinase-1; ERK: extracellular signal-regulated kinases; MEK / MKK: mitogen-activated protein

kinase kinase; FAK: focal adhesion kinase. Modified from Woollard, S.M., Li, H., Singh S., Yu F., and Kanmogne G.D. (2014) HIV-1 induces cytoskeletal alterations and Rac1 activation during monocyte-blood-brain barrier interactions: modulatory role of CCR5. *Retrovirology. 11:20 [261].* Reprinted with permission under the Creative Commons Attribution License or equivalent.

	HIV-1 vs. CONTROL		HIV-1 + TAK vs. CONTROL		HIV-1 vs. HIV-1 + TAK	
Name	**Fold change**	**p-value**	**Fold change**	**p-value**	**Fold change**	**p-value**
Merlin (Phospho-Ser518)	6.24	1.95E-11	1.15	0.079	0.184	1.16E-11
VASP (Phospho-Ser157)	4.38	1.95E-11	0.88	0.088	0.20	1.16E-11
Rac1/cdc42 (Phospho-Ser71)	3.56	3.67E-08	0.83	0.14	0.23	6.98E-10
ERK1-p44/42 MAP Kinase (Phospho-Tyr204)	3.26	9.42E-10	0.88	0.13	0.27	1.16E-11
Cortactin (Phospho-Tyr421)	2.93	1.96E-11	0.73	7.19E-08	0.25	1.16E-11
ERK1-p44/42 MAP Kinase (Phospho-Thr202)	2.55	1.2E-10	0.92	0.0028	0.34	3.18E-11
MEK1(Phospho-Ser217)	2.23	2.06E-08	0.74	2.35E-06	0.33	7.81E-10
CaMK1-a (Phospho-Thr177)	1.67	0.00038	1.08	0.91	0.64	3.19E-07
ERK3 (Phospho-Ser189)	1.61	0.00011	1.06	0.91	0.65	0.0026
MKK7/MAP2K7 (Phospho-Ser271)	0.73	1.51E-06	0.87	0.23	1.18	0.038
FAK (Phospho-Tyr397)	0.61	1.96E-11	0.64	2.82E-06	1.05	0.63
MKK6 (Phospho-Ser207)	0.60	1.96E-11	0.71	2.27E-06	1.17	0.00089

Table 2-4: Phosphorylated proteins differentially expressed in HIV-1 infected-monocytes co-cultured with HBMEC, when normalized to actin levels. Table shows p-values adjusted using the Benjamini & Hochberg method. Modified from Woollard, S.M., Li, H., Singh S., Yu F., and Kanmogne G.D. (2014) HIV-1 induces cytoskeletal alterations and Rac1 activation during monocyte-blood-brain barrier interactions:

modulatory role of CCR5. *Retrovirology. 11:20 [261].* Reprinted with permission under the Creative Commons Attribution License or equivalent.

Differentially expressed total proteins		
Molecular and cellular functions	**p-value**	**N**
Cellular Assembly and Organization	9.10E-08 - 9.06E-03	11
Cellular Movement	1.75E-07 - 9.06E-03	11
Cell Morphology	2.35E-07 - 9.76E-03	11
Cellular Function and Maintenance	3.24E-07 - 9.06E-03	11
Cellular Development	3.74E-07 - 9.68E-03	9
Differentially expressed phospho-proteins		
Molecular and cellular functions	**p-value**	**N**
Cell Cycle	4.42E-11 - 5.12E-03	10
Cell Signaling	6.64E-10 - 5.07E-03	9
Cellular Movement	1.23E-09 - 5.24E-03	8
Cell Morphology	3.71E-09 - 5.12E-03	10
Post-translational Modification	4.87E-09 - 5.07E-03	10

Table 2-5: Molecular and cellular functions associated with differentially expressed total and phosphorylated proteins in HIV-1 infected monocytes following monocytes-endothelial interactions. N = number of associated proteins. Modified from Woollard, S.M., Li, H., Singh S., Yu F., and Kanmogne G.D. (2014) HIV-1 induces cytoskeletal alterations and Rac1 activation during monocyte-blood-brain barrier interactions: modulatory role of CCR5. *Retrovirology. 11:20 [261].* Reprinted with permission under the Creative Commons Attribution License or equivalent.

Differentially expressed total proteins		
Canonical pathways	**p-value**	**N**
Chemokine Signaling	3.08E-12	6
Melatonin Signaling	3.37E-12	6
Role of NFAT in Cardiac Hypertrophy	1.02E-11	7
Cholecystokinin/Gastrin-mediated Signaling	3.23E-11	6
GNRH Signaling	1.52E-10	6
Differentially expressed phospho-proteins		
Canonical pathways	**p-value**	**N**
GNRH Signaling	7.51E-11	6
Germ Cell-Sertoli Cell Junction Signaling	2.29E-10	6
Integrin Signaling	9.39E-10	6
HGMB1 Signaling	1.9E-09	5
HGF Signaling	2.74E-09	5

Table 2-6: Canonical pathways associated with differentially expressed total and phosphorylated proteins in HIV-1 infected monocytes following monocyte-endothelial interactions. N = number of associated proteins. Modified from Woollard, S.M., Li, H., Singh S., Yu F., and Kanmogne G.D. (2014) HIV-1 induces cytoskeletal alterations and Rac1 activation during monocyte-blood-brain barrier interactions: modulatory role of CCR5. *Retrovirology. 11:20 [261].* Reprinted with permission under the Creative Commons Attribution License or equivalent.

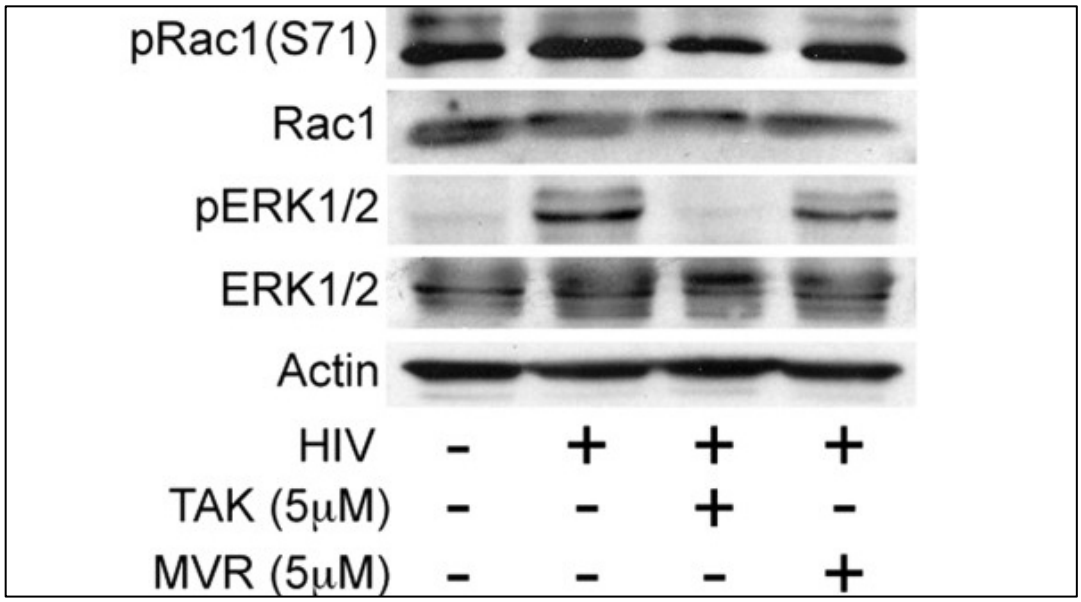

Figure 2-7: Increased levels of pRac1 (S71) and pERK1/2 (Thr202/Tyr204) in HIV-1 infected monocytes co-cultured with HBMEC. Monocytes were treated with 5 μM TAK or 5 μM MVR for 30 minutes prior to 12 hours infection with HIV-1. Following infection, monocytes were washed 3 times with PBS to remove free virus, and co-cultured with HBMEC for 2 hours. Protein was purified from monocytes and HBMEC separately. Monocyte protein was fractionated on an SDS-PAGE gel and transferred to a nitrocellulose membrane as described in the Methods (2.2.11). HIV-1-infected monocytes showed increased levels of pRac1 (S71) and pERK1 (Thr202/Tyr204) following monocyte-endothelial interactions, compared to non-infected monocytes co-cultured with HBMEC. TAK and MVR reduced HIV-1-induced phosphorylation of Rac1 and ERK1/2. Modified from Woollard, S.M., Li, H., Singh S., Yu F., and Kanmogne G.D. (2014) HIV-1 induces cytoskeletal alterations and Rac1 activation during monocyte-blood-brain barrier interactions: modulatory role of CCR5. *Retrovirology. 11:20 [261].* Reprinted with permission under the Creative Commons Attribution License or equivalent.

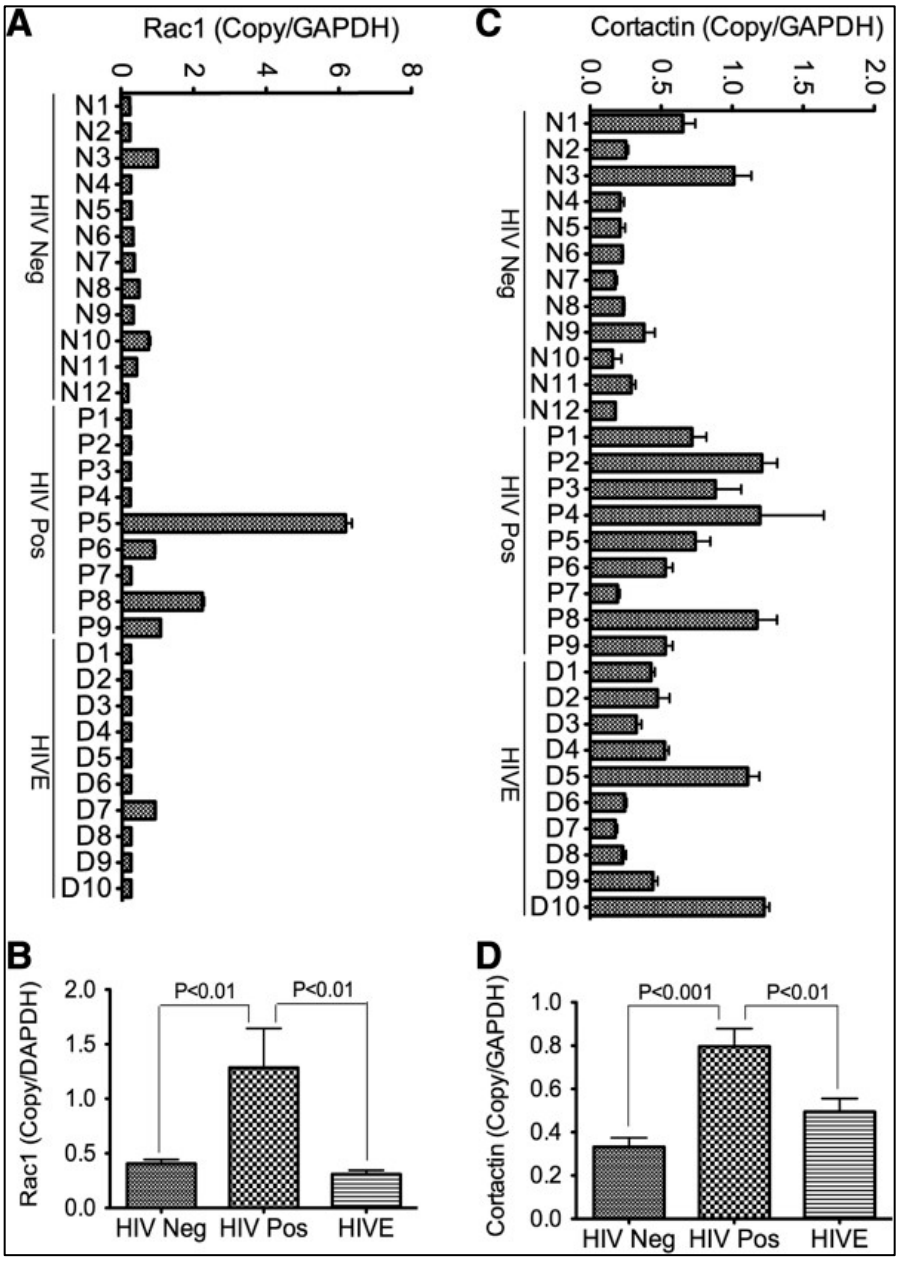

Figure 2-8: Increased transcription of RAC1 and CTTN in brain tissues of HIV-1-infected humans. Total RNA was extracted from the brains (cortex) of HIV-1-seronegative individuals or HIV-1-seropositive patients with or without neurocognitive impairment using Trizol followed by revere transcription as described in methods section 2.2.10. Quantitative real-time PCR was performed using the Taqman detection system using the Applied Biosystems StepOne Plus system. Data was quantified using the delta-delta Ct method. Quantitative real-time PCR show overall increase in Rac1 (A, B)

and cortactin (C, D) mRNA in brain tissues of HIV-1-positive individuals (HIV-1 Pos), compared to seronegative controls (HIV-1 Neg) and HIV-1-infected patients with encephalitis (HIVE). One-way ANOVA followed by Tukey's multiple-comparisons tests was performed using GraphPad Prism 5.0b to determine significance. Threshold of significance level was 0.05. Error bars represent SEM. Modified from Woollard, S.M., Li, H., Singh S., Yu F., and Kanmogne G.D. (2014) HIV-1 induces cytoskeletal alterations and Rac1 activation during monocyte-blood-brain barrier interactions: modulatory role of CCR5**.** ***Retrovirology.*** *11:20* ***[261].*** Reprinted with permission under the Creative Commons Attribution License or equivalent**.**

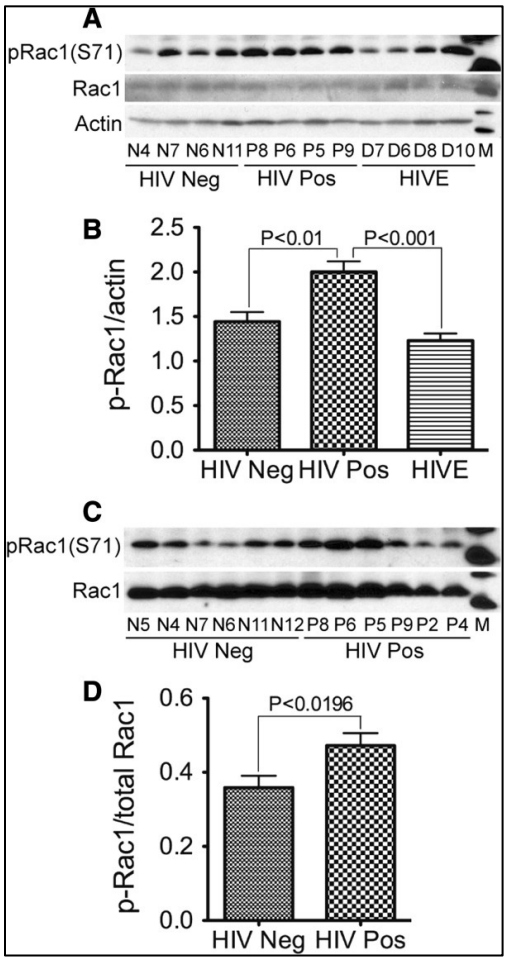

Figure 2-9: Increased phosphorylation of Rac1(S71) in brain tissues of HIV-1-infected humans. Protein was extracted from brains (cortex) of HIV-1-seronegative individuals or HIV-1-seropositive humans with or without neurocognitive impairment. Protein was fractionated on an SDS-PAGE gel, transferred to a nitrocellulose membrane, and analyzed as described in methods section 2.2.11. A and B: Western blot analysis of brain tissue show increased levels of pRac1 (S71) in brain tissues of HIV-1-seropositive individuals (HIV Pos; N=4) compared to HIV-1-infected patients with encephalitis (HIVE; N=4) and seronegative controls (HIV-1 Neg; N=4). C and D: Confirmation of pRac1 (s71) in the brain tissues of HIV-1-positive individuals (HIV Pos; N=6) compared to seronegative controls (HIV Neg; N=6). Statistical significance was determined by One-way ANOVA followed by Tukey's multiple-comparisons tests (B), or

a tow-tailed t-test (D), using GraphPad Prism 5.0b. Error bars represent SEM. Modified from Woollard, S.M., Li, H., Singh S., Yu F., and Kanmogne G.D. (2014) HIV-1 induces cytoskeletal alterations and Rac1 activation during monocyte-blood-brain barrier interactions: modulatory role of CCR5**.** ***Retrovirology.*** *11:20* ***[261].*** Reprinted with permission under the Creative Commons Attribution License or equivalent**.**

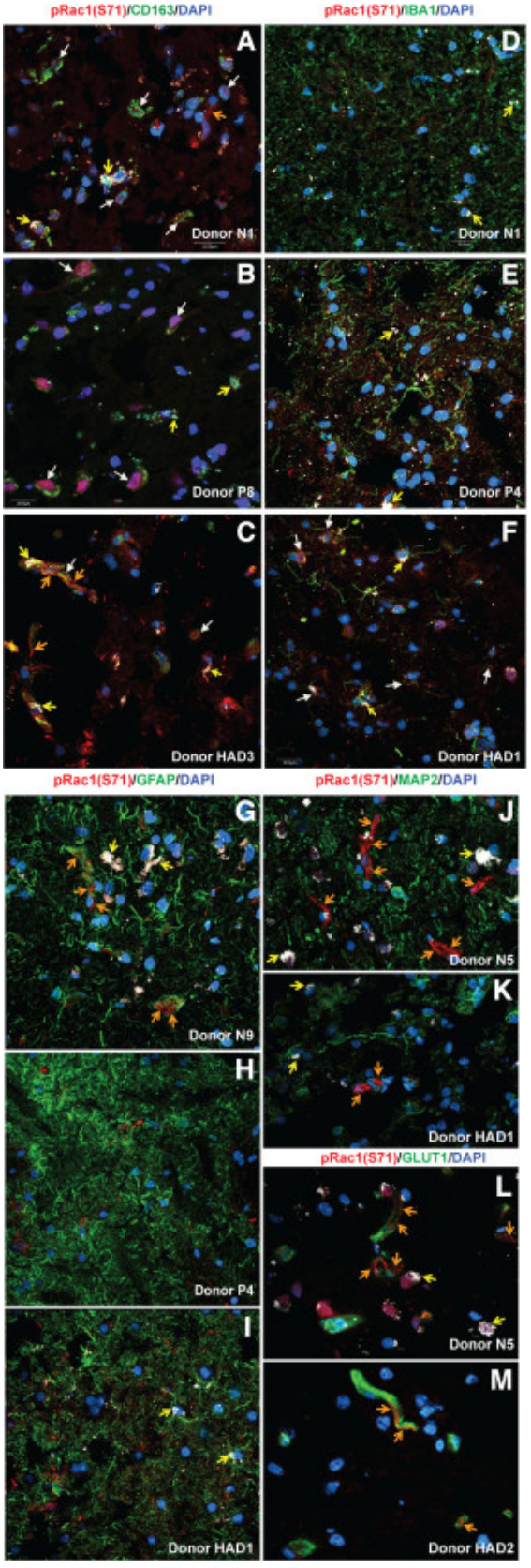
pRac1(S71)/CD163/DAPI
A
Donor N1
B
Donor P8
C
Donor HAD3
pRac1(S71)/IBA1/DAPI
D
Donor N1
E
Donor P4
F
Donor HAD1
pRac1(S71)/GFAP/DAPI
G
Donor N9
H
Donor P4
I
Donor HAD1
pRac1(S71)/MAP2/DAPI
J
Donor N5
K
Donor HAD1
pRac1(S71)/GLUT1/DAPI
L
Donor N5
M
Donor HAD2

Figure 2-10: Expression of pRac1 (S71) in human brain macrophages and blood vessels. Five-micrometer sections of brain tissue from HIV-1-seronegative individuals or HIV-1-seropositive humans with or without neurocognitive impairment, were mounted on glass slides, fixed, permeabilized, and incubated 1 hour in PBS containing 3% BSA to block for non-specific binding. Tissues were incubated overnight with antibodies to phospho-Rac1(S71) and CD163, IBA1, GFAP, MAP2, or GLUT1, followed by staining (1 hour in the dark at room temperature) with secondary antibodies coupled with Alexa Fluor-488 or −635, washed and mounted as described in section 2.2.12. Confocal microscopy showed expression of pRac1(S71) in human brain macrophages (A-C, white arrows) and blood vessels tight junction strands (A, C, G, J-M orange arrows). There was no significant expression of pRac1 (S71) in microglia in most brain tissues (D, E); but a few HIVE patients did show expression of pRac1(S71) in microglia (F, white arrows). There was no expression of pRac1 (S71) in astrocytes (G-I) or neurons (J, K). For all experiments, a 4th laser line was used to differentiate lipofuscin-like autofluorescent pigments from antibody staining (yellow arrows). Scale bar for all panels: 20 μM. Modified from Woollard, S.M., Li, H., Singh S., Yu F., and Kanmogne G.D. (2014) HIV-1 induces cytoskeletal alterations and Rac1 activation during monocyte-blood-brain barrier interactions: modulatory role of CCR5**.** ***Retrovirology.*** *11:20* ***[261].*** Reprinted with permission under the Creative Commons Attribution License or equivalent**.**

Chapter 3

Maraviroc reduces HIV-induced BBB injury and HIV CNS infection in Hu-PBL-NOD/SCID mice

3.1 Background

HIV-1 often enters the CNS before individuals are aware of infection, as early as 8-14 days post-infection [262, 263]. HIV-1 induces BBB breakdown, which results in viral entry into the CNS; productive viral infection and inflammation in the CNS further exacerbate BBB breakdown and increase the entry of HIV-1 virions and infected cells into the brain [152]. Post-mortem analysis of brain tissue samples from HIV-1-positive patients with HAD showed reduced expression of the tight junction proteins ZO-1, occludin, and claudin-5 [264]. Since the introduction of ART, the prevalence of the most severe stage of HAND, HAD, has decreased [158]. However, the prevalence of the milder stages, ANI and MND, have increased, and this appears to be related to the increasing life expectancy of HIV-1-infected patients on ART [158].

The role of MVR in preventing BBB dysfunction and CNS injury has not been previously investigated. Using an *in vitro* BBB model we showed that treatment of monocytes with CCR5 antagonists was associated with a decrease in HIV-1-induced adhesion to brain endothelial cells [261]. We further showed that CCR5 antagonists reduced HIV-1-induced expression and activation of cytoskeleton-associated proteins [261]. Others have found that MVR is detectable in the CSF of HIV-1-infected patients and is associated with decreased CSF viral loads [121, 123-125]. MVR was also shown to be neuroprotective in SIV-infected rhesus macaques [265] and is able to inhibit T-cell, monocyte, macrophage, and dendritic cell migration induced by chemokines *in vitro* [224, 225, 266]. However, it has not been determined if MVR can enter the CNS and reduce HIV-1 viral load in the CNS.

We hypothesized that blocking CCR5, through treatment with MVR, would prevent HIV-1-induced CNS injury and reduce infection levels in the brain. To test this

hypothesis, we used a Hu-PBL-NSG mouse model infected with HIV-1 and treated with a human-equivalent mouse dose of MVR, to analyze the effect of MVR treatment on engrafted human cells, blood and CNS viremia, and BBB integrity (Figure 4-1). We further quantified MVR levels in the brain to determine if MVR could enter into the CNS.

3.2 Materials and Methods

3.2.1 MVR preparation for injection

MVR (Selzentry; ViiV Healthcare) in 300 mg tablets was purchased from the Nebraska Medical Center pharmacy. To prepare stock concentrations of 75 mg/ml, 1 tablet was crushed using a mortar and pestle and dissolved in 4 ml of a 1:1 mixture of dimethyl sulfoxide (DMSO) and PBS. Stock solutions were stored at -80°C in 600 µl aliquots and used within 2 days of preparation. For animal injections, 500 µl of stock solution was further diluted in 2 ml PBS for a working concentration of 18.75 mg/ml. This solution was filtered using a 0.45 µM syringe filter to remove undissolvable drug excipients. Each mouse was injected intraperitoneally (I.P.) with 200 µl of working solution, for a final amount of 3 mg MVR per mouse. For untreated mice, solutions were prepared in a similar fashion: a stock solution of a 1:1 mixture of DMSO and PBS was prepared in 4 ml. This solution was frozen at -80°C in 600 µl aliquots. For injections, 500 µl of the PBS/DMSO solution was further diluted in 2 ml PBS, and each mouse received I.P. injections of 200 µl.

3.2.2 Hu-PBL-NOD/SCID mouse model

Four-week old male nonobese diabetic (NOD)/ severe combined immune deficiency (SCID), IL2 receptor gamma chain knockout mice: NOD.Cg-Prkdc^{scid}Il2rg^{tm1Wjl}/SzJ (NSG) mice were purchased from Jackson Laboratory (Bar Harbor, ME) and maintained in sterile microisolator cages under pathogen-free conditions in accordance with ethical

guidelines for care of laboratory animals at the University of Nebraska Medical Center and National Institutes of Health. Animals were injected I.P. with human PBL (30 $\times 10^6$ cells/mouse) at 4 to 6 weeks of age. At 1 to 2 weeks after engraftment, animals' blood was analyzed by flow cytometry to quantify PBL engraftment. Engrafted animals were infected by I.P. injection of 100 µl HIV- 1_{ADA} using a single dose of 10^4 tissue culture infectious doses ($TCID_{50}$). Twelve hours after infection, mice were injected (I.P.) with 3 mg MVR (in 200 µl solution) and from that point forward, mice were injected (I.P.) with 3 mg of MVR (in 200 µl solution) every 12 hours. Untreated mice were injected (I.P.) with 200 µl of DMSO/PBS solution every 12 hours. Treatment groups were: untreated, uninfected mice (group G1); treated, uninfected mice (group G2); untreated, infected mice (group G3); and treated, infected mice (group G4). Animals were bled weekly and the levels of human cells in animals' blood quantified by FACS. Animals were sacrificed at 3 weeks post-infection and tissues from each animal were divided into 3 parts. One part was used for paraffin embedding and immunohistochemical studies, the second part was stored in optimal cutting temperature compound for immunofluorescence experiments, and the third part was used for RNA extraction and qPCR. Uninfected mice injected with PBS or MVR served as controls.

3.2.3 Flow Cytometry/ Fluorescence-activated cell sorting (FACS)

To quantify human cells in mouse blood, blood samples (approximately 200 µl per mouse) were collected from the animal facial vein into ethylenediaminetetraacetic acid-coated tubes (BD Biosciences), using lancets (MEDIpoint, Inc., Mineola, NY), before infection and at 1, 2, and 3 weeks post-infection. Samples were centrifuged at 1800 rpm for 8 minutes at 4°C to remove serum. Blood samples were brought to a final volume of 50 µl using FACS buffer (PBS containing 2% FBS) and transferred to empty 5 ml polypropylene round-bottom tubes (BD Falcon, Franklin Lakes, NJ). Any leftover blood

was mixed in 5 ml polypropylene tubes and used for gating. Blood samples were lysed by re-suspending in 1 ml Red Blood Cell Lysing Buffer (Roche Diagnostics, Indianapolis, IN), followed by incubation at room temperature for 5 minutes, and centrifuged at 1500 RPM for 5 minutes. Following centrifugation, the supernatant was discarded and pelleted cells were resuspended in 1 ml FACS buffer. Fourty microliters of antibody mixture was then added to each sample and the samples incubated for 1 hour in the dark on ice. The antibody mixture contained the following fluorochrome-conjugated human monoclonal antibodies: PE-Cy7 anti-CD45 (Biolegend, San Diego, Ca; product number: 304016), APC anti-CD8 (Biolegend; 344722), PE anti-CD195 (Biolegend; 321406), Pacific Blue anti-CD3 (Biolegend; 300330), and FITC anti-CD4 (BD Biosciences; 555346). Following incubation with antibody, samples were washed twice with 1 ml of FACS buffer by centrifugation (1500 RPM for 10 minutes) and fixed by resuspension in 200 µl of 2% paraformaldehyde in PBS. For gating, samples were resuspended in 400 µl of 2% PFA. Samples were analyzed using a FACS DIVA (BD Immunocytometry Systems, Mountain View, CA). Results are expressed as percentages of total number of gated lymphocytes. The gating strategy was human CD45⇒CD3⇒CD4/CD8.

3.2.4 Immunohistochemistry

Following animal sacrifice, each tissue sample was put in a tissue cassette and fixed by overnight incubation at 4° C with PBS containing 4% paraformaldehyde. Tissues were processed using a Shandon Citadel 1000 automated tissue processor (Thermo Fisher). Processing consisted of three steps: tissue dehydration, tissue clearing, and tissue embedding. First, tissues were dehydrated in increasing concentrations of Flex buffer (Thermo Fisher), a dehydrating agent consisting of a blend of isopropyl and methyl alcohol. For dehydration, tissues were incubated for 1 hour in a container containing 70% Flex buffer before being transferred to a container containing 80% Flex buffer and

incubated for 1 hour. This process was repeated for concentrations of 95% and 100% Flex buffer. After dehydration, tissues were cleared of alcohol using xylene. For clearing, tissues were incubated in xylene for one hour, transferred to a container containing fresh xylene and incubated for 1 hour, and transferred once again to another container containing fresh xylene and incubated for 1 hour. Following dehydration and clearing, tissues were embedded in paraffin (Leica) by incubation in a container containing hot paraffin (58° C) for 1 hour, transferred to a new container with hot paraffin (58° C), and incubated again for 1 hour.

Tissues were embedded into blocks using a Histostar Embedding Workstation (Thermo Fisher). To prepare tissue blocks, tissues in cassettes and metal molds were placed in a 58 °C paraffin bath for 15 minutes. One at a time, a mold and a tissue cassette was removed from the bath. The mold was filled with a small amount of hot paraffin and placed on a cold spot for 10 seconds to let the wax harden slightly. With forceps, the tissue was removed from the cassette, placed into the mold cut side down, and placed back onto the cold spot. The cassette was placed on top of the mold and hot paraffin was added to cover the top of the cassette. The mold/cassette was placed on a cold surface for 30 minutes, more paraffin being added if it seeps below the cover. After 30 minutes the block was popped out of the mold and prepared for cutting.

Tissues were cut using a Leica RM2235 mictrotome. For cutting, paraffin tissue blocks were placed in the object clamp of the microtome. Excess paraffin was trimmed from the block at a setting of 20 µM until the tissue was reached. A wipe soaked with 30% ammonia water was placed over the tissue block for 1 minute to soften tissue and reduce cracking. Five-micrometer sections were cut from the paraffin tissue blocks and transferred to a 38° C water bath containing CitriSolv Hybrid Solvent and Clearing Agent (Fisher) for 10 to 20 seconds to expand tissue to its original dimensions and to remove wrinkles. Tissues were mounted onto Fisherbrand Superfrost/Plus microscope slides by

dipping a slide into the water bath at an angle and gently guiding the tissue onto the slide with a blunt metal tip. Slides were dried at room temperature overnight on a slide rack.

For antigen retrieval, slides were dried in an incubator at 60°C for 30 minutes and transferred into a staining dish containing the Trilogy solution (Cell Marque, Rocklin, CA). The staining dish containing Trilogy/slides along with a second staining dish containing only Trilogy solution was transferred into a Cuisinart CPC-600 pressure cooker (East Winsdor, NJ) that was filled with 700 ml water. Slides were incubated in the pressure cooker for 15 minutes at a pressure of 15 pounds per square inch. After 15 minutes the pressure was removed from the cooker and the slides were transferred to the second staining dish containing only Trilogy, gently agitated by hand for approximately 5 seconds, and incubated for 5 minutes while still in the pressure cooker. Slides were washed five times in a slide dish containing distilled water for 5 minutes each wash. Finally slides were transferred into a slide dish containing 10% Tween20/tris-buffered saline (TTBS).

For immunohistochemistry, samples were blocked with 10% normal goat serum (NGS; Vector, Burlingame, CA), diluted in TTBS for 30 minutes in a humidity chamber (Fisher). Excess NGS was flicked from slides and slides were incubated with a mouse monoclonal antibody for claudin-5 (1:100; Abcam) diluted in 10% NGS for 1 hour. Slides were washed 3 times with TTBS, 3 minutes each wash, and then incubated with 1-3 drops of polymer-based HRP-conjugated anti-mouse Dako EnVision secondary antibody (Carpinteria, CA) for 1 hour in a humidity chamber. Slides were washed 3 times with TTBS, 3 minutes each wash, and developed with a 3,3'-diaminobenzidine (DAB; Dako). DAB was prepared by adding 20 µl DAB (1 drop) to 1 ml of the substrate solution provided. During development, slides were monitored under the microscope for optimal development time and then rinsed 2 times with deionized water. Slides were

counterstained with 1:10 dilution of Mayer's hematoxylin, washed 3 times with water, dipped in 0.037 mol/l ammonia for 10 seconds, and rinsed with deionized water 3 times. Slides were dehydrated by incubating two times with 80% ethanol for 5 minutes each time, two times with 95% ethanol for 5 minutes each time, two times with 100% ethanol for 5 minutes each time, and three times with 100% xylene for 5 minutes each time. Slides were mounted by adding a drop of cytoseal 60 (Thermo Fisher) and slowing placing a coverslip over the tissue to reduce the presence of air bubbles. Omission of the primary antibodies or use of isotope-matched mouse IgG as primary antibody (Santa Cruz, Dallas Texas) served as controls. Images were acquired using a Nikon DS-Fi1 camera fixed to a Nikon Eclipse E800 (Nikon Instruments), using NIS Elements F3.0 software. Semi-quantitative analysis of claudin-5 expression (percentage of area occupied by immunostaining) was performed using computer-assisted image analysis with Image-Pro®Premier software (MediaCybernetics, Rockville, MD). Three images per mouse were analyzed.

3.2.5 Immunofluorescence

Mouse brain cortex sections were embedded with OCT in 22 mm X 22 mm X 20 mm Peel-A-Way embedding molds (Ted Pella Inc, Redding, CA) after sacrifice and stored at -80 °C until ready to cut. Prior to cutting, embedding molds were warmed slightly to remove OCT embedded tissue. Five-micrometer sections were cut from each mouse brain tissue using a Leica CM1860 cryostat and mounted on Fisherbrand Superfrost/Plus microscope slides. Tissue sections were fixed in 4% paraformaldehyde diluted in PBS for 20 minutes at room temperature in a humidity chamber, dried, washed with 1X PBS for 5 minutes at room temperature, and incubated 1 hour in a humidity chamber with PBS containing 3% BSA to block for non-specific binding. Mouse brain tissues were incubated overnight at 4 °C in a humidity chamber with ZO-2 antibody (Cell

Signaling) diluted in PBS containing 3% BSA (1:50 dilution). After incubation with the primary antibody, slides were washed with 1X PBS 3 times, 5 minutes each wash, and stained with anti-rabbit secondary antibody coupled with Alexa Fluor-594 (Life Technologies) diluted (1:500) in PBS containing 3% BSA, for 1 hour in the dark at room temperature in a humidity chamber. Stained tissues were washed 5 times with 1X PBS, 5 minutes each wash, and mounted with Prolong Gold anti-fade reagent containing DAPI (Molecular Probes, Grand Island, NY). Stained tissues were examined using an Eclipse TE20000-U fluorescent microscope (Nikon) with a Cy5 HYQ filter connected to a CoolSNAP EZ camera (Photometrics, Tucson, AZ). Semiquantitative analysis of ZO-2 expression (percentage of area occupied by immunostaining) was performed by computer-assisted image analysis using the Image-Pro®Premier software. Three images per slide were analyzed.

3.2.6 RNA extraction, reverse transcription, and qRT-PCR

Total RNA from mouse brains was extracted using the Trizol reagent. One-milliliter of Trizol reagent was added to 50 mg of brain tissue and tissues were homogenized using the TissueRuptor homogenizer (Qiagen, Valencia, CA). Homogenized samples were incubated at room temperature for 5 minutes and after incubation, 200 µl of chloroform was added to each sample, shaken by hand for 15 seconds, and incubated at room temperature for 15 minutes. Samples were centrifuged at 12,000 x g for 15 minutes at 4℃. During centrifugation the mixture separates into three layers: a bottom red phenol-chloroform phase, an interphase, and a colorless top aqueous phase. The aqueous phase was transferred to a new tube and mixed with 500 µl of 100% isopropanol to precipitate RNA. Samples were incubated at room temperature for 10 minutes followed by centrifugation at 12,000 x g for 10 minutes at 4℃. Supernatant was removed from the tubes and 1 ml of 75% ethanol was added to each sample, vortexed, and centrifuged at

7,500 x g for 5 minutes at 4 ℃. Supernatant was removed and samples were air dried for 5 minutes at room temperature. Pellets were re-dissolved in 30 µl of RNase-free water and incubated for 10 minutes on a heat block set at 55 ℃. RNA was further cleaned using Total RNA cleanup kit (Qiagen). RNA yield and quality were checked using a NanoDrop spectrophotometer (NanoDrop Technologies, Wilmington, DE) and for all samples absorbance ratio of 260/280 was ≥ 2.

Reverse transcription was performed using the Verso cDNA synthesis kit (Thermo Fisher). One-microgram of RNA in 11 µl of nuclease-free water was mixed with 4 µl 5X cDNA synthesis buffer, 2 µl dNTP mix (0.05 mM of each dNTP), 1 µl random hexamers (400 ng/µl), 1 µl RT enhancer, and 1 µl Verso enzyme mix. Cycling conditions were: 1 cycle of 42 °C for 30 minutes followed by 95 °C for 2 minutes with a final hold at 4 °C.

Quantitative real-time PCR was performed using a Roche LightCycler 480 II Roche) with a 384-well block. For each sample, the cDNA obtained was diluted in nuclease free water at a ratio of 1:20; a 20 µl reaction mixture containing 5 µl of each diluted cDNA sample, 10 µl of Roche LightCycler 480 Probes master mix (containing the polymerase enzyme, dNTPs and $MgCl_2$), 4 µl of nuclease free water, and 1 µl of primer-probe [containing 900 nM of each forward and reverse primer and 250 nM TaqMan minor groove binder (MGB) probe] was prepared. Twenty-microliters of the reaction mixture was added to the wells of a 384-well plate and loaded into the Roche LightCycler 480 II machine. Cycling conditions were: 95 °C for 5 minutes with a ramp rate of 4.8 ℃/second; followed by 45 cycles of 95 ℃ for 10 seconds with a ramp rate of 4.8 ℃/second, 60 ℃ for 15 seconds with a ramp rate of 2.5 ℃/second, and 72 ℃ for 1 second with a ramp rate of 4.8 ℃/second; and one hold at 40 ℃ for 10 seconds with a ramp rate of 2 ℃/second. Data was analyzed as described in **2.2.10**. All primers were obtained from Applied Biosytems. Primer-probe ID or sequences were GAPDH:

Hs99999905_m1; Long Terminal Repeat (LTR) forward primer: 5′ -GCCTCAATAAAGCTTGCCTTGA-3′ ; LTR reverse primer: 5′ -TCCACACTGACTAAAAGGGTCTGA-3′ ; LTR probe: 5′ -FAM-GCGAGTGCCCGTCTGTTGTGTGACTCTGGTAACTAGCTCGC-MGB-3′ ; Tat forward primer: 5′ -GGAGGAGGGTTGCTTTGATAGAG-3′ ; Tat reverse primer: 5′ -AAAGCCTTAGGCATCTCCTATGG-3′ ; and Tat probe: 5′ -FAM-CTTCGTCGCTGTCTCCGCTTCTTCC-MGB-3; Pol forward primer: 5′ -GCACTTTAAATTTTCCCATTAGTCCTA-3′ ; Pol reverse primer: 5′ -CAAATTTCTACTAATGCTTTTATTTTTTC-3′ ; Pol probe: 5′ -FAM-AAGCCAGGAATGGATGGCC-MGB-3′ .

3.2.7 Ultraperformance liquid chromatography tandem mass spectrometry (UPLC-MS/MS)

NSG mice not engrafted with human-PBL were used to quantify levels of MVR in mouse plasma and brain samples. Mice were mice were injected (I.P.) with 3 mg MVR (in 200 µl solution) every 12 hours for three weeks. After 3 weeks of treatment, mice were sacrificed and blood and tissue samples were collected as described in **3.2.2**. To quantify MVR levels in plasma, 50 µl of plasma was added to 10 µl of 1 µg/ml indinavir (IDV) free base as internal standard (IS) and 1 ml of ice-cold acetonitrile. For brain tissue, 100 mg of tissues was homogenized in 4 volumes of UPLC-grade water and then added to 10 µl of IS and 1 ml ice-cold acetonitrile. Both plasma and brain samples were vortexed for 3 minutes and centrifuged at 16,000 x g for 10 min at 4˚C. One milliliter of supernatant was evaporated to dryness under vacuum and dried samples were reconstituted in 100 µl of 50% UPLC-grade methanol diluted in water. The samples were

centrifuged for 10 min at 16,000 x g at 4˚C and 40 µl of supernatant was used for analysis.

Chromatographic separation was performed using a Waters ACQUITY UPLC (Milford, MA) system coupled with AB 4000 Q TRAP quadruple linear ion trap hybrid mass spectrometer, with an electrospray ionization source (Applied Biosystems/MDS Sciex, Foster City, CA). Separation was achieved using an Acquity BEH Shield RP18 column (1.7 µm, 2.1 x 100 mm) equipped with an Acquity VanGuard BEH Shield precolumn (1.7 µm, 2.1 x 5 mm) using a step-wise gradient of 7.5 mM ammonium acetate, pH 5 for mobile phase A and acetonitrile for mobile phase B. The gradient was held at 70% mobile phase A for 3 minutes, decreased to 40% mobile phase A over 1 minute and 30 seconds and held for 30 seconds, decreased to 5% mobile phase A over 30 seconds and held for 30 seconds, increased to 70% mobile phase A over 15 seconds and held for 1 minute and 45 seconds prior to next sample injection at a flow rate of 0.25 ml/min. The injection volume for all samples was 10 µl. Detection was achieved in the positive ionization mode using the following transitions: m/z MVC 514/280; m/z IDV 614/421. Calibration standards consisted of 0.2 to 2000 ng/ml MVR with 100 ng/ml IDV for both plasma and brain homogenates and the ratio of analyte to IS peak area was used for quantitation of unknowns.

3.2.8 Statistical analysis

Statistical analysis was performed as described in section **2.2.11**.

3.3 Results

3.3.1 MVR treatment or HIV-1 infection does not affect hu-PBL NSG mouse weights

To assess the effect of MVR treatment and HIV-1 infection on the weights of hu-PBL NSG mice, we weighed mice every four days during the course of the experiment. All groups: untreated, uninfected (G1; N=5); treated, uninfected (G2; N=10); untreated, infected (G3; N-12); and treated, infected (G4; N=12) lost weight during the treatment period, but weight changes during the course of treatment was not significantly different among the four groups of mice (Figure 3-2).

3.3.2 HIV-1 infection decreased human CD4+ cells and increased CD8+ cells in the blood of HIV-1-infected hu-PBL NSG mice and treatment with MVR attenuated these effects

HIV-1 infection is known to decrease the level of CD4+ cells and increase the levels of CD8+ [267]. To this end, we analyzed animal's blood samples at weeks 1, 2, and 3 p.i. by FACS to determine whether MVR treatment of infected mice could restore these cells to normal levels. There was no significant difference in human CD4+ or human CD8+ cell levels at week 1 p.i. between any of the 4 groups (Figure 3-3, 3-4). FACS analyses showed that human CD4+ cell levels decreased by 4.1-fold ($p<0.001$) and 14.4-fold ($p<0.001$) in placebo-treated infected mice compared to placebo-treated uninfected mice at weeks 2 and 3 p.i., respectively (Figure 3-3). Similar results were observed in placebo-treated infected mice compared to MVR-treated uninfected mice, with human CD4+ cell levels decreasing by 3.9-fold ($p<0.001$) and 14.7-fold ($p<0.001$) at weeks 2 and 3 p.i., respectively (Figure 3-3). MVR-treated infected mice showed an increase in human CD4+ cell levels by 2.3-fold ($p<0.05$) compared to placebo-treated infected mice at week 2 p.i. (Figure 3-3). There was no significant difference in human CD4+ cell levels

in MVR-treated infected mice compared to placebo-treated infected mice at week 3 p.i. (Figure 3-3).

Human CD8+ cell levels increased by 1.8-fold ($p<0.001$) and 3.0-fold ($p<0.001$) in placebo-treated infected mice compared to placebo-treated uninfected mice at weeks 2 and 3 p.i., respectively (Figured 3-4). Similar results were observed in placebo-treated infected mice compared to MVR-treated infected mice, with human CD8+ cell levels increasing by 1.7-fold ($p<0.001$) and 3.1-fold ($p<0.001$) at weeks 2 and 3 p.i. (Figure 3-4). MVR-treated infected mice showed a decrease in human CD8+ cell levels by 1.24-fold ($p<0.05$) compared to placebo-treated infected mice at week 3 p.i. (Figure 3-4). There was no significant difference in human CD8+ cell levels in MVR-treated infected mice compared to placebo-treated infected mice at week 3 p.i. (Figure 3-4).

3.3.3 HIV-1 infection decreases the levels of CD45+ cells in the blood of hu-PBL NSG mice and MVR treatment attenuates this effect

CD45 is a transmembrane protein found on the surface of all differentiated hematopoietic cells, except red blood cells and effector B cells [268]. We used FACS to estimate the levels of human CD45+ cells in animal's blood samples. There was no significant difference in human CD45+ cell levels at week-1 p.i. between any of the four groups (Figure 3-5). Human CD45+ cell levels decreased by 1.5-fold (NS) and 2.2-fold ($p<0.05$) in placebo-treated infected mice compared to placebo-treated uninfected mice at weeks 2 and 3 p.i., respectively (Figure-3-5). Similar results were observed in placebo-treated infected mice compared to MVR-treated uninfected mice, with human CD45+ cell levels decreasing by 1.5-fold (NS) and 2.1-fold ($p<0.05$) at weeks 2 and 3 p.i., respectively (Figure 3-3). MVR-treated infected mice showed a 2-fold increase in human CD45+ levels compared to placebo-treated infected mice at both weeks 2 and 3 p.i. ($p<0.01$, Figure 3-5).

3.2.4 HIV-1 infection disrupts claudin-5 and ZO-2 in the brain microvasculature of hu-PBL NSG mice and MVR prevents HIV-1-induced vascular damage

HIV-1 infection is associated with disruption of the BBB. Endothelial cells are a major component of the BBB. Endothelial cells are connected together by tight junctions that prevent the passive diffusion of materials between cells [154]. Claudin-5 is a major component of the BBB that plays a role in maintaining its integrity [269, 270]. ZO-2 is found at the cell membrane and acts as molecular scaffolds at the cytoplasmic side of tight junctions [271]. HIV-1 infection is associated with decreased expression of Claudin-5 and ZO-2 [272]. We have previously showed that CCR5 antibodies can partially prevent HIV-1-induced activation of STAT1 and STAT3 in HBMEC [215, 216]. Activation of STAT1 and STAT3 in HBMEC results in inflammation that leads to the loss of tight junctions [215, 216]. To determine whether blocking CCR5 *in vivo* in NSG mice attenuates HIV-1-induced vascular damage, we performed immunostaining for claudin-5 and ZO-2. HIV-1 infection resulted in injury to the brain endothelium, evidenced by loss of immunostaining for claudin-5 and ZO-2 (Figure 3-6A, B). Claudin-5 expression decreased by 1.7-fold in placebo-treated infected mice compared to placebo-treated uninfected mice and decreased by 1.3-fold in placebo-treated infected mice compared to MVR-treated uninfected mice (Figure 3-6A). MVR-treated infected mice showed a 2.3-fold increase in claudin-5 expression compared to placebo-treated infected mice ($p<0.05$, Figure 3-6A). ZO-2 expression decreased by 1.5-fold in placebo-treated infected mice compared to placebo-treated uninfected mice and decreased by 1.4-fold in placebo-treated infected mice compared to MVR-treated uninfected mice (Figure 3-6B). MVR-treated infected mice showed a 1.5-fold increase in ZO-2 expression compared to placebo-treated infected mice ($p<0.01$, Figure 3-6B).

3.3.5 MVR reduced HIV-1 levels in the brains of hu-PBL NSG mice

HIV-1-infected patients treated with MVR have decreased viral loads in their CSF [121, 124, 125, 273]. However, no study to date has investigated whether MVR can reduce viral loads in the CNS. To examine if MVR treatment could reduce HIV-1 levels in the brains of infected mice, we quantified HIV-1 Tat, LTR, and pol by real-time PCR using mRNA isolated from mice brains. Tat mRNA levels was increased by 6.9-fold ($p<0.01$) in the brains of infected mice compared to placebo-treated or MVR-treated uninfected mice and MVR treatment of infected mice decreased Tat mRNA levels by 3.5-fold ($p<0.05$) compared to placebo-treated infected mice (Figure 3-7A). HIV-1 infection increased LTR mRNA levels by 12,753-fold ($p<0.001$) compared to placebo-treated or MVR-treated uninfected mice and MVR treatment of infected mice decreased LTR mRNA levels by 11.5-fold ($p<0.05$) compared to placebo-treated infected mice (Figure 3-7B). Pol mRNA expression was increased by 10.6-fold ($p<0.001$) in infected mice compared to untreated or treated uninfected mice and MVR treatment of infected mice decreased pol mRNA levels by 10.8-fold ($p<0.001$) compared to placebo-treated infected mice (Figure 3-7C).

3.3.6 MVR is detectable in the CNS of NSG mice

Detectable levels of MVR in the CSF have been shown in multiple studies, with levels above the protein-adjusted inhibitory concentration (IC_{50}) of 0.57 ng/ml [121, 123-125]. However no studies have quantified MVR concentrations directly in the CNS. To this end, we quantified MVR concentrations in the brains of 8 mice treated with MVR twice daily for 3 weeks using UPLC-MS/MS. All mice had quantifiable CNS levels of MVR with a mean of 217 ng/g (range: 81 - 685 ng/g) (Table 3-1). MVR was also detectable in the plasma of all mice, with a mean plasma concentration of 117 ng/ml (range: 7.23 ng/ml – 294 ng/ml). There was a weak positive correlation ($r = 0.41$) between plasma and brain MVR concentrations.

3.4 Discussion

Using a mouse model of HIV/AIDS, we showed that HIV-1 decreased the levels of human CD4+ cells and CD45+ cells and increased the levels of CD8+ cells in the blood of engrafted mice. Treatment with MVR attenuated HIV-induced destruction of CD4+ and CD45+ cells. We further demonstrated that blocking CCR5, via the antagonist MVR, reduced HIV-1-induced BBB injury. We found reduced levels of claudin-5 and ZO-2 expression in the brain vasculature of HIV-1-infected mice and treatment with MVR diminished HIV-1-induced downregulation of claudin-5 and ZO-2. Lastly we showed that MVR treatment reduced HIV viral loads in the brain and that MVR was quantifiable in the CNS.

Tight junctions are components of the BBB that restrict the passage of molecules into the CNS [154]. Claudins are one of the most integral components of tight junctions and regulate the paracellular permeability of the barrier [274]. Claudin-5 is highly expressed in endothelial cells of the BBB and is the main structural transmembrane component of tight junctions [154, 275, 276]. Our results showing that HIV-1 infection decreases claudin-5 expression in the brain vasculature is consistent with other studies involving HIV-1 and/or HIV-1 proteins. Tat decreased claudin-5 expression and induced cellular redistribution of claudin-5 immunoreactivity in primary HBMEC, and this decrease was associated with monocyte infiltration into the brain tissues [174]. Claudin-5 expression was also decreased by direct exposure of HBMEC to HIV-1 [216]. Furthermore, Claudin-5 expression was decreased in brain microvessels of HIV-1-infected individuals with HAD [216]. Gp120 decreased claudin-5 expression when injected directly into the caudate putamen of rats [189].

ZO proteins act as scaffolding proteins to connect tight junction proteins to the actin cytoskeleton [154, 271]. ZOs bind directly to claudins on their N-terminal side via their PDZ domain and interact with actin on their C-terminal side [271]. ZO-2 is found in

brain endothelial cells [271]. In our mouse model of HIV/AIDS we showed that ZO-2 was decreased during HIV-1 infection. Studies have shown that Tat and gp120 exposure results in decreased ZO-2 expression in HBMEC [174, 178, 180].

HIV-1- and HIV-1 protein-induced decrease of claudin-5 and ZO-2 expression can occur via the Ras/ERK1/2 pathway through activation of vascular endothelial growth factor receptor type 2 (VEGFR-2) [36]. The PI3K/protein kinase B (PKB) pathway and STAT/janus kinase (JAK) pathway are also involved [216, 277]. In fact, there is cross talk between the PI3K/PKB pathway and STAT/JAK pathway in HIV-1-induced endothelial dysfunction and this is partially mediated by CCR5 [215, 278]. Post-translational modifications (PTMs) of tight junction proteins have been found to be associated with disruption of the BBB [279, 280]. Claudin-5 is phosphorylated by activation of the Rho GTPase, Rho, and its downstream enzyme Rho-associated protein kinase (RhoK), which leads to increased HIV-1-induced monocyte migration through HBMEC and BBB disruption [280]. It is therefore possible that HIV-1 binding to CD4 and/or CCR5 or CXCR4 can activate small GTPases, such as Ras and Rho, which in turn activate the PI3K/AKT, STAT/JNK, and/or ERK1/2 pathways, resulting in PTM of tight junction proteins and BBB dysfunction.

HBMEC express CCR5 and it has been suggested that gp120 can bind directly to CCR5 and induce BBB dysfunction [179]. Furthermore, our data showed that HIV-induced BBB disruption was reduced by MVR treatment. This suggests that MVR could not only attenuate HIV-induced BBB dysfunction by preventing HIV entry into monocytes/macrophages and T-cells, but also possibly by directly preventing the binding of HIV-1 proteins (i.e. Tat and gp120) to brain endothelial cells; reducing tight junction disruption by blocking the activation of VEGFR-2 and the PI3K/AKT and STAT/JAK pathways; or by reducing monocyte infiltration into brain tissues.

Many antiretroviral drugs are not able to penetrate the CNS, and thus, the brain remains an HIV reservoir [281, 282]. Therefore, drugs that are able to pass through the BBB could help in the elimination of viral reservoirs. The CNS HIV Antiretroviral Therapy Effects Research group ranks drugs on the basis of information from the literature on measured CSF concentrations, physiochemical drug characteristics, and effectiveness in the CNS (reflected by suppression of CSF viral load and improved neurocognitive performance) [10, 283]. Drugs are given a CNS penetration-effectiveness rank, with 4 having the highest estimated CNS penetration and 1 having the lowest [283]. MVR has a ranking of 3, suggesting that it is able to penetrate the CNS [283]. This ranking is based on several studies showing detectable levels of MVR in the CSF, with levels higher than the protein-adjusted IC50 of 0.57 ng/ml [121, 123-125, 273]. In agreement with these data, we found that mice had quantifiable CNS levels of MVR, with a mean of 217 ng/g (range: 81 ng/g - 685 ng/g).

MVR was first discovered to be a substrate for Pgp1, which suggested limited CNS penetration [97]. MVR was later found to be a substrate for organic anion transporting polypeptide 1B1 (OATP1B1) [284]. OATPs are a superfamily of influx transporters that generally transport large and hydrophobic organic anions [285]. All OATPs share a similar transmembrane domain organization, with 12 predicted transmembrane domains and a large fifth extracellular loop [286]. OATP1B1 is mainly expressed in the liver, but has also been detected in small intestinal enterocytes [287, 288]. It does not appear to be expressed in cells of the brain or cells of the BBB [289, 290]. It is possible that other OATPs could be involved in the transport of MVR into the brain, such as OATP1A2, which has been found be highly expressed in the brain [291, 292]. OATPs that are within the same family, such as the OATP1 family, share ≥40% amino acid sequence similarity and may share substrates; for example, HIV-1 protease inhibitors have been shown to be substrates for both OATP1A2 and OATP1B1 [291,

293]. In addition to OATPs, other families of influx transporters include organic anion transporters, organic cation transporters, and peptide transporters [285, 294].

In addition to showing that MVR can be quantified in the brain, we also showed that MVR reduced HIV-1 Tat, LTR, and pol levels in the brain. This is consistent with studies showing that MVR can reduce HIV-1 infection in the CSF [123, 124]. Additionally, MVR has been shown to reduce SIV RNA and DNA levels in the brains of rhesus macaques [265]. However, short-term MVR intensification in HIV-1-infected individuals on cART was not associated with improvements in neurologic assessments [295]. Conversely, patients with HIV-1-associated neurocognitive impairment treated with a combination of abacavir, lamivudine, and MVR for 48 weeks showed a trend towards neurocognitive improvement [217]. In another study, when MVR was added to patients cART regimens, patients showed significant cognitive improvements [296]. Our data showing that MVR can enter the CNS and reduce brain viral loads in mice, taken together with the above data showing that long term MVR treatment in humans is associated with neurocognitive improvements, provides evidence that MVR is a viable option for the treatment of HAND.

One of the hallmarks of HIV-1 infection is the loss of CD4+ T-cells and an initial increase of CD8+ T-cells [267, 297, 298]. Our data was consistent with these changes, as we saw a decrease in human CD4+ cells and an increase in human CD8+ cells in placebo-treated HIV-1-infected mice. HIV-1-infected mice that were treated with MVR had at least a partial attenuation of these changes. In HIV-1-infected patients, MVR has been associated with improvements in T-cell counts and our data is consistent with these reports [128]. In addition, we observed a decrease in the levels of human CD45+ cells in placebo-treated HIV-1-infected mice. HIV-1-infected mice that were treated with MVR had a partial increase in CD45+ cell levels. CD45 is a protein tyrosine phosphatase that is expressed on all nucleated hematopoietic cells and is involved in T-cell

development and signaling [268]. HIV-1 infection results in dysfunction of CD45 signaling [299]. These results suggest that MVR is able to at least partially restore balance to the immune system, which could help in further suppression of viral load.

Overall, MVR was safe, as observed by no significant differences in weights among animals groups. MVR restored the level of immune cells in infected animals, increasing CD4+ and CD45+ cells and decreasing CD8+ cell levels. Furthermore, MVR was able to reduce the severity of HIV-1-induced BBB injury by preventing the downregulation of the tight junction proteins claudin-5 and ZO-2. Finally, we showed that MVR can enter the CNS and can decrease infection in the brain. Our results suggest a potential role for MVR in decreasing viral reservoir in the brain and reducing the severity and prevalence of HAND.

3.5 Summary

To elucidate the role of CCR5 inhibition/MVR on HIV-1-induced BBB dysfunction and CNS infection we used a mouse model of HIV-1/AIDS. We used immunohistochemistry and immunofluorescence to show that HIV-1 infection results in disruption of the tight junction proteins, claudin-5 and ZO-2. Tight junction disruption was at least partially attenuated in infected mice treated with MVR. Using FACS analysis, we showed that HIV-1 infection of mice decreased CD4+ cells and CD45+ cells and increased CD8+ cells in blood plasma, and MVR treatment of infected mice had a partial attenuation of these changes. Quantitative real-time-PCR on mRNA isolated from brain tissue showed that MVR treatment reduced HIV-1 viral load in the CNS. MVR levels were quantified in the blood plasma and brains of mice using UPLC-MS/MS. Mice treated with MVR over the course of 3 weeks had detectable levels of MVR in their brains and plasma.

3.6 Figures and tables

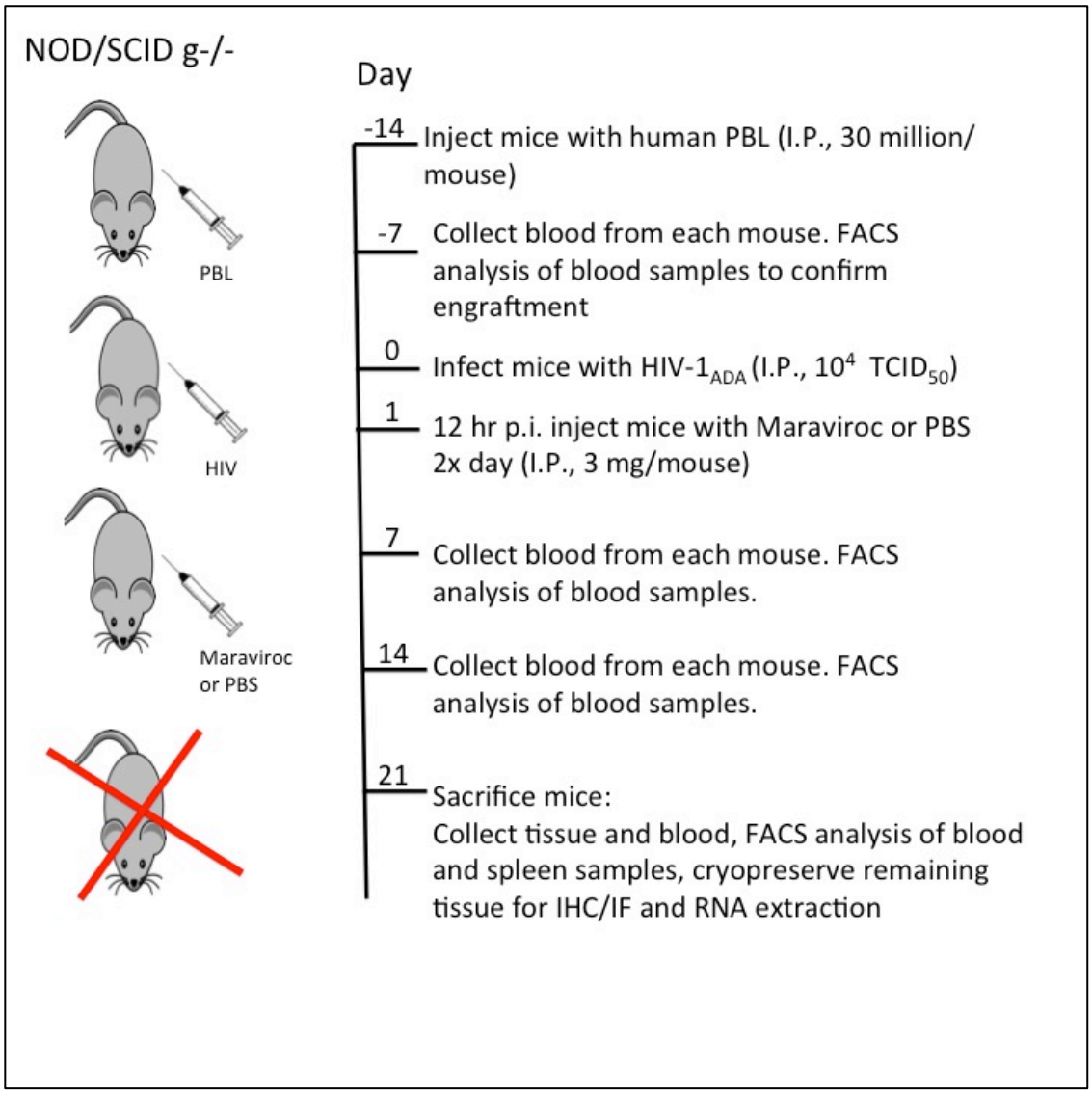

Figure 3-1: The Hu-PBL NSG mouse model. NSG mice (4 to 6 weeks old) were injected with 30 million of human PBL (Day -14). One week later, mice were bled through the facial vein and blood was analyzed by FACS to confirm engraftment of human immune cells (Day -7). At day 0, mice were infected with HIV-1_{ADA}, and 12 hours after infection injected with MVR (3 mg I.P.) or PBS. Mice were treated with MVR or PBS twice a day (about every 12 hours). Once a week mice were bled and blood samples

were analyzed by FACS to quantify the levels of human immune cells. At day 21, mice were sacrificed and tissue and blood samples collected for further analysis.

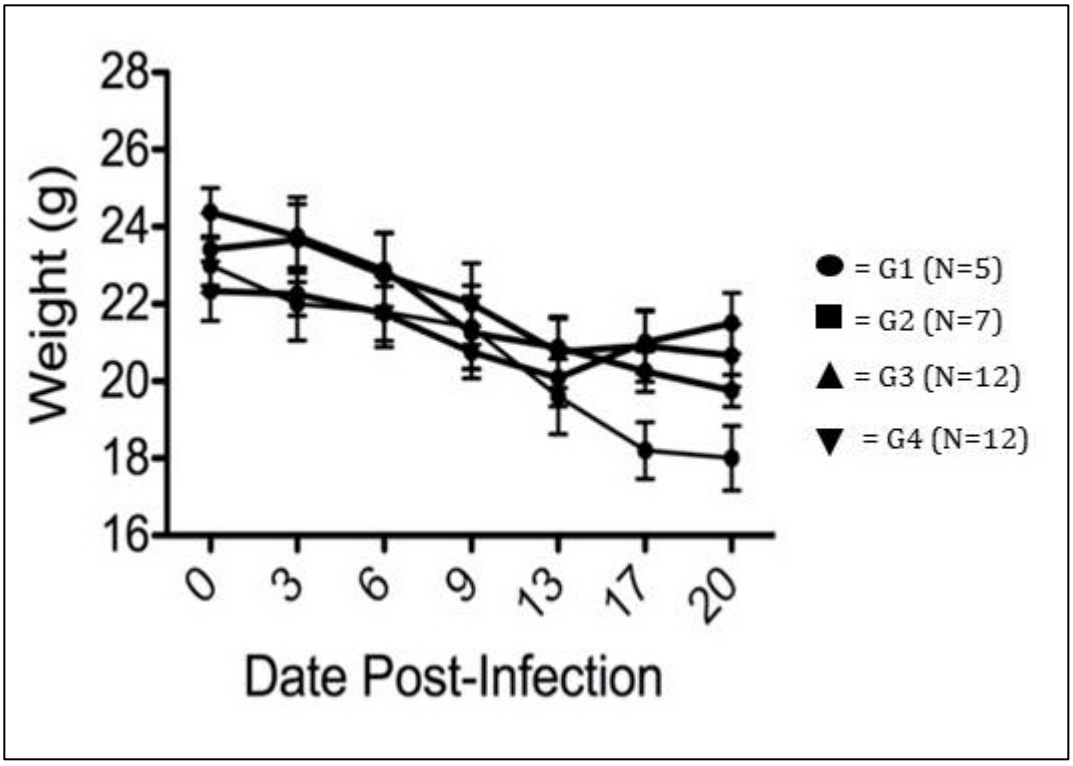

Figure 3-2: MVR or HIV-1 infection does not affect the weights of Hu-PBL NSG mice. NSG mice were engrafted with 30 million human PBL/mouse and infected with HIV-1_{ADA} (10^4 $TCID_{50}$). Mice were weighed every four days during the course of the experiment. The mean weight of each group from day 0 through day 20 is shown. Circles: control mice (G1), squares: uninfected mice treated with MVR (G2), triangles: HIV-1 infected mice (G3), upside-down triangles: HIV-1 infected mice treated with MVR (G4). Number of mice in each group: G1: 5, G2: 7, G3: 12, G4: 12. Two-way ANOVA followed by Bonferroni's correction for multiple-comparisons was performed using GraphPad Prism 5.0b to determine significance. Threshold of significance level was 0.05. Error bars represent mean ± SEM.

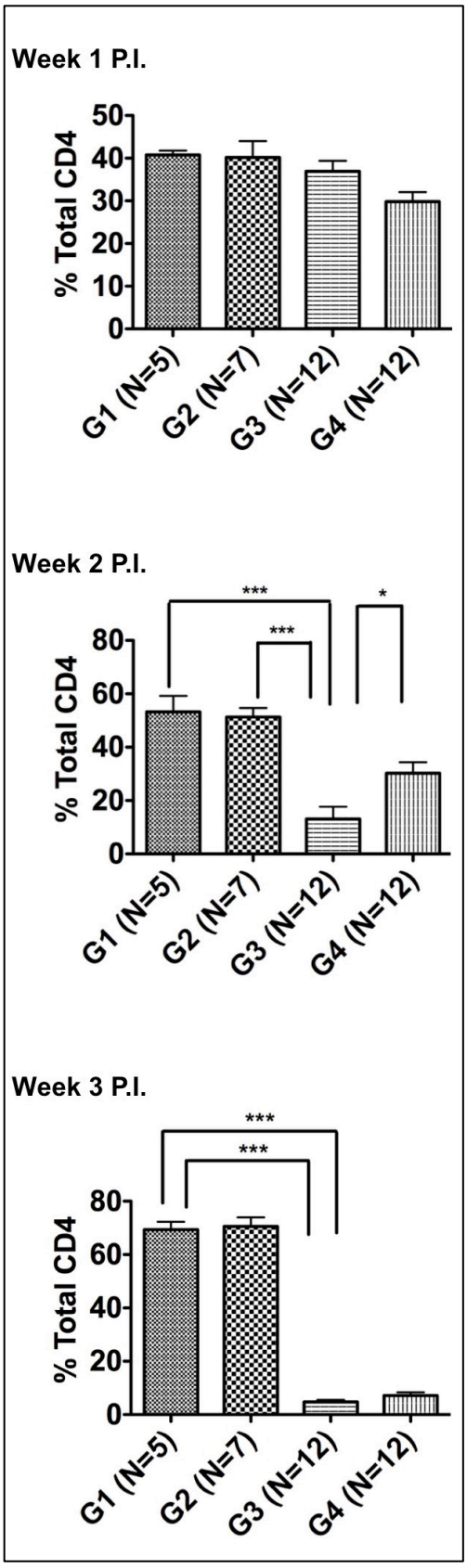
Week 1 P.I.
% Total CD4
50
40
30
20
10
0
G1 (N=5)
G2 (N=7)
G3 (N=12)
G4 (N=12)
Week 2 P.I.
***
***
*
% Total CD4
80
60
40
20
0
G1 (N=5)
G2 (N=7)
G3 (N=12)
G4 (N=12)
Week 3 P.I.
***
***
% Total CD4
80
60
40
20
0
G1 (N=5)
G2 (N=7)
G3 (N=12)
G4 (N=12)

Figure 3-3: Levels of CD4+ cells in the blood of HIV-1-infected Hu-PBL NSG mice. NSG mice were engrafted with 30 million human PBL/mouse and infected with HIV-1_{ADA} (10^4 $TCID_{50}$). Engrafted mice were treated with MVR (3 mg/mouse) or PBS twice daily. Mice were bled weekly and the levels of CD4+ in the blood were determined by FACS analysis. One-way ANOVA followed by Tukey's post-test for multiple-comparisons was performed using GraphPad Prism 5.0b to determine significance. Threshold of significance level was 0.05. Error bars represent mean ± SEM. *$p \leq 0.05$, ***$p \leq 0.001$. Number of mice in each group: G1 (uninfected mice): 5, G2 (uninfected mice treated with MVR): 7, G3 (infected mice): 12, G4 (infected mice treated with MVR): 12

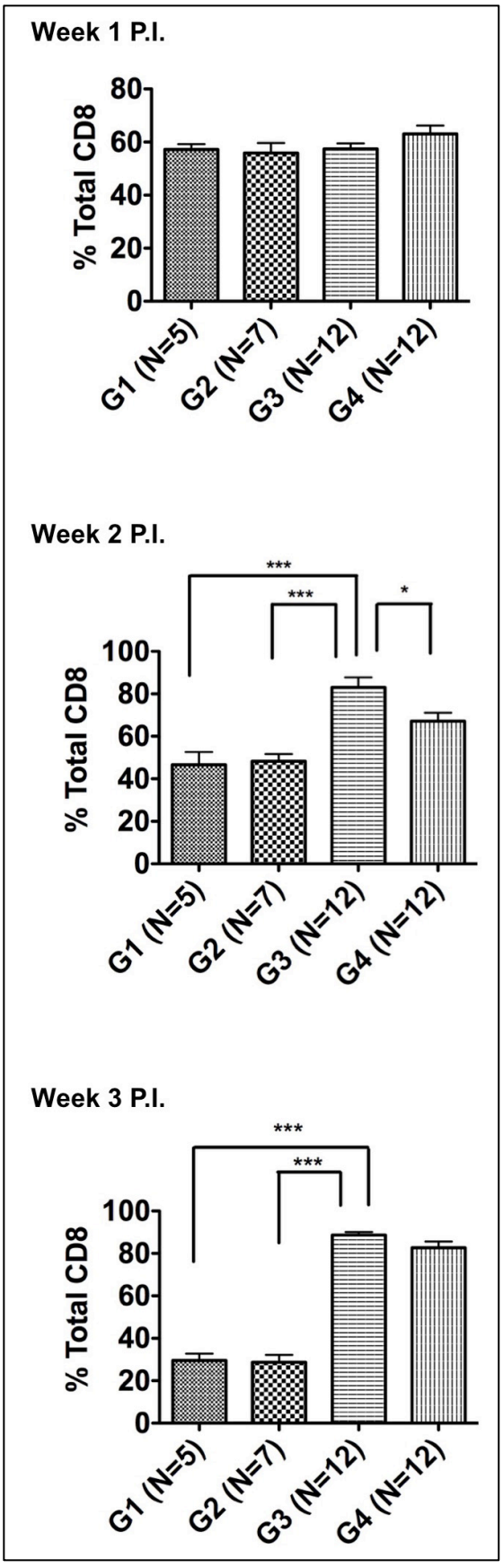
Week 1 P.I.
% Total CD8
80
60
40
20
0
G1 (N=5)
G2 (N=7)
G3 (N=12)
G4 (N=12)
Week 2 P.I.
***
***
*
% Total CD8
100
80
60
40
20
0
G1 (N=5)
G2 (N=7)
G3 (N=12)
G4 (N=12)
Week 3 P.I.
***
***
% Total CD8
100
80
60
40
20
0
G1 (N=5)
G2 (N=7)
G3 (N=12)
G4 (N=12)

Figure 3-4: Levels of CD8+ cells in the blood of HIV-1-infected Hu-PBL NSG mice. NSG mice were engrafted with 30 million human PBL/mouse and infected with HIV-1_{ADA} (10^4 $TCID_{50}$). Engrafted mice were treated with MVR (3 mg/mouse) or PBS twice daily. Mice were bled weekly and the levels of CD8+ in the blood was determined by FACS analysis. One-way ANOVA followed by Tukey's post-hoc test for multiple-comparisons was performed using GraphPad Prism 5.0b to determine significance. Threshold of significance level was 0.05. Error bars represent mean ± SEM.*$p \leq 0.05$, ***$p \leq 0.001$. Number of mice in each group: G1 (uninfected mice): 5, G2 (uninfected mice treated with MVR): 7, G3 (infected mice): 12, G4 (infected mice treated with MVR): 12

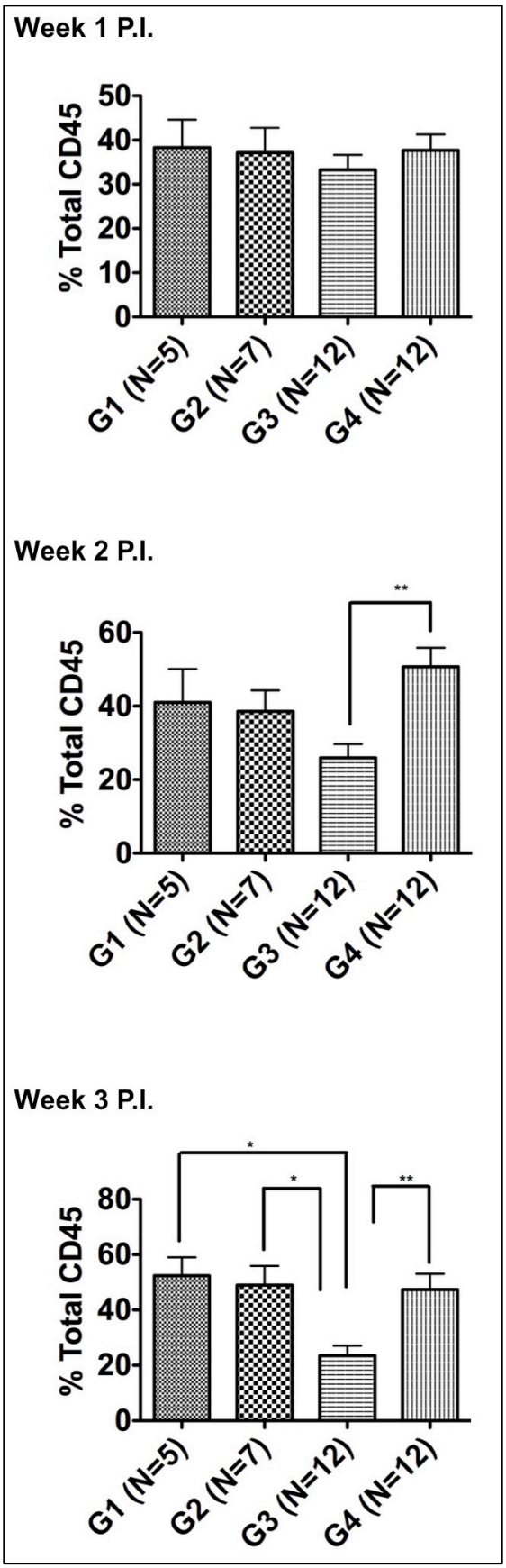
Week 1 P.I.
% Total CD45
50
40
30
20
10
0
G1 (N=5)
G2 (N=7)
G3 (N=12)
G4 (N=12)
Week 2 P.I.
**
% Total CD45
60
40
20
0
G1 (N=5)
G2 (N=7)
G3 (N=12)
G4 (N=12)
Week 3 P.I.
*
*
**
% Total CD45
80
60
40
20
0
G1 (N=5)
G2 (N=7)
G3 (N=12)
G4 (N=12)

Figure 3-5: Levels of CD45+ cells in the blood of HIV-1-infected of Hu-PBL NSG mice. NSG mice were engrafted with 30 million PBL/mouse and infected with HIV-1_{ADA} (10^4 $TCID_{50}$). Engrafted mice were treated with MVR (3 mg/mouse) or PBS twice daily. Mice were bled weekly and the levels of CD45+ in the blood was determined by FACS analysis. One-way ANOVA followed by Tukey's post-hoc test for multiple-comparisons was performed using GraphPad Prism 5.0b to determine significance. Threshold of significance level was 0.05. Error bars represent mean ± SEM. *$p \leq 0.05$, **$p \leq 0.01$. Number of mice in each group: G1 (uninfected mice): 5, G2 (uninfected mice treated with MVR): 7, G3 (infected mice): 12, G4 (infected mice treated with MVR): 12

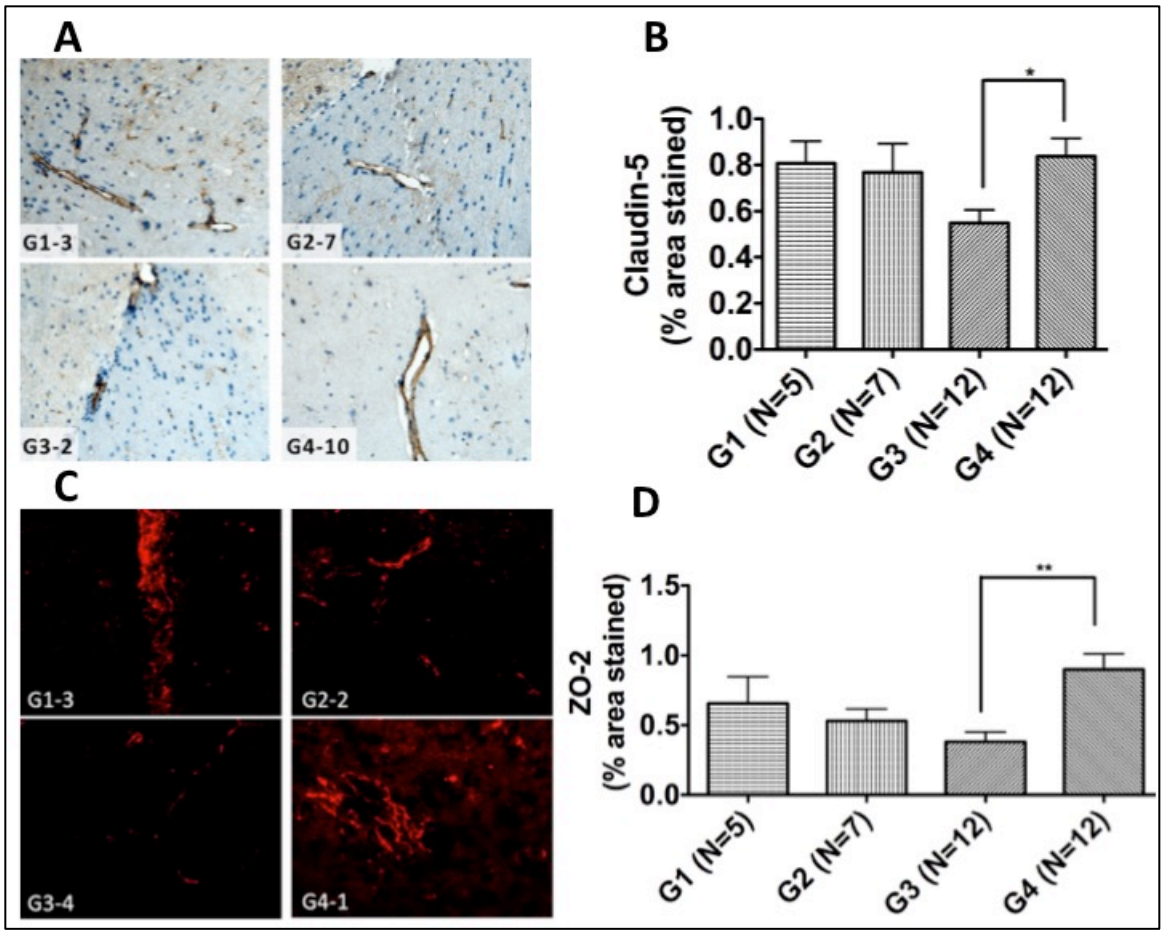

Figure 3-6. MVR treatment prevents HIV-1-induced disruption of CNS tight junctions in HIV-1-infected of Hu-PBL NSG mice. NSG mice were engrafted with 30 million human PBL/mouse. Engrafted mice were infected with HIV-1_{ADA} at 10^4 $TCID_{50}$. and/or treated with MVR (3 mg/mouse) twice daily, sacrificed at week-3 p.i., and brain tissues collected. To determine if MVR treatment could prevent HIV-1-induced CNS injury, tight junction protein expression on mice brain tissue sections was examined by immunohistochemistry and immunofluorescence, and three sections per sample were analyzed. Claudin-5 and ZO-2 expression was quantified by semi-quantitative analysis using the Image Pro-Premier software. **A**: immunohistochemistry of claudin-5, **B**: semi-quantitative analysis of claudin-5 staining, **C**: immunofluorescence of ZO-2. **D**: semi-quantitative analysis of ZO-2 staining. One-way ANOVA followed by Tukey's post-hoc

test for multiple-comparisons was performed using GraphPad Prism 5.0b to determine significance. Threshold of significance level was 0.05. Error bars represent mean ± SEM. Significance *p ≤ 0.05. Number of mice in each group: G1 (uninfected mice): 5, G2 (uninfected mice treated with MVR): 7, G3 (infected mice): 12, G4 (infected mice treated with MVR): 12

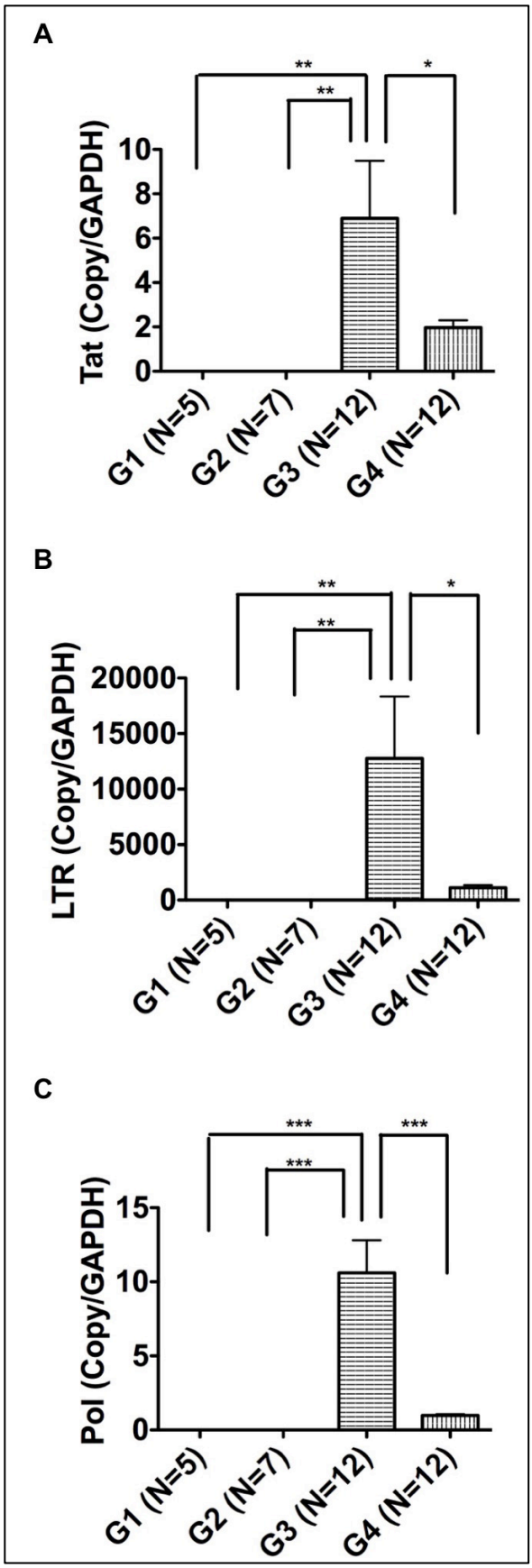
A
**
**
*
Tat (Copy/GAPDH)
10
8
6
4
2
0
G1 (N=5)
G2 (N=7)
G3 (N=12)
G4 (N=12)
B
**
**
*
LTR (Copy/GAPDH)
20000
15000
10000
5000
0
G1 (N=5)
G2 (N=7)
G3 (N=12)
G4 (N=12)
C
***
***
***
Pol (Copy/GAPDH)
15
10
5
0
G1 (N=5)
G2 (N=7)
G3 (N=12)
G4 (N=12)

Figure 3-7. MVR reduces HIV-1 levels in the brains of Hu-PBL NSG mice. NSG mice were engrafted with 30 million human PBL/mouse and infected with HIV-1_{ADA} (10^4 $TCID_{50}$)**.** Engrafted mice were treated with MVR (3 mg/mouse) or PBS twice daily, sacrificed at week-3 p.i., and brain tissues collected. RNA was extracted from brain tissues and used for real-time PCR to quantify the expression of HIV-1 genes. The levels of Tat (A), LTR (B) and pol (C) RNA in brains were quantified by real-time PCR using the delta Ct method, and normalized to each sample's human GAPDH. One-way ANOVA followed by Tukey's post-hoc test for multiple-comparisons was performed using GraphPad Prism 5.0b to determine significance. Threshold of significance level was 0.05. Error bars represent mean ± SEM. *$p \leq 0.05$, **$p \leq 0.01$, ***$p \leq 0.001$. Number of mice in each group: G1 (uninfected mice): 5, G2 (uninfected mice treated with MVR): 7, G3 (infected mice): 12, G4 (infected mice treated with MVR): 12.

Mouse	MVR Serum concentrations (ng/ml)	MVR Brain concentrations (ng/g)
1	7.23	91.5
2	31.2	89
3	17	81
4	49.6	98
5	52.8	96
6	294	105
7	254	487.5
8	234	685

Table 3-1: MVR concentrations in the serum and brains of mice.

Chapter 4

Conclusions

4.1 Conclusions and future directions

4.1.1 Chapter 2

In this study we used a combination of *in vivo* and *in vitro* techniques to help elucidate the role of CCR5 in HIV-1-induced BBB dysfunction and HAND. We found that CCR5 blockers could diminish HIV-1 infection in MDM and HIV-1-induced monocyte adhesion to the BBB. This is in agreement with other studies showing that treatment with MVR could prevent monocyte, macrophage, and HIV-1-induced T-cell chemotaxis *in vitro* [224, 266]. In addition, CCR5 blockers did not disrupt endothelial integrity. This suggests that they will not induce BBB dysfunction on their own.

We used a cytoskeleton-associated protein array and found that expression of cytoskeleton-associated proteins was upregulated in HIV-1-infected monocytes following monocyte-endothelial communications, including Rac1, cortactin, and ERK1/2. Treatment with CCR5 antagonists prevented these changes. We further found that Rac1 and cortactin mRNA expression is upregulated in the brains of HIV-1-infected individuals compared to seronegative controls and individuals with HIVE; and phosphorylation of Rac1 at S71 is upregulated in the brains of HIV-1-infected individuals compared to seronegative controls and individuals with HIVE. Since RAC1 and cortactin was upregulated in HIV-1-infected patients without evidence of encephalitis and not HIV-1-infected patients with encephalitis, we suggest that HIV-1-induced transcriptional regulation of Rac1 and cortactin likely occurs during the earlier stages of infection; this correlates with BBB breach and increased cell trafficking into the CNS. We used immunofluorescence analysis to determine the location of pRac1 (S71) in the human brain. We found that pRac1 (S71) is expressed mostly in brain macrophages and blood vessel tight junctions; expression in microglia was limited to a few samples from individuals with HIVE and there was no expression in astroglia and neurons.

Rac1 is involved in cellular adhesion and migration through the formation of membrane ruffles and lamellipodia [245, 300]. Therefore, it was not surprising to see Rac1 upregulated in monocytes during monocyte-endothelial communications. The possibility of Rac1's involvement in HIV-1-induced adhesion of monocytes to the BBB is in agreement with studies showing that activation of Rac1 in lymphocytes promotes adhesion by cell spreading [247]. Rac1 has already been implicated in HIV-1 pathogenesis. It can interact with Nef to cause cytoskeletal rearrangements and increased lamellipodia formation, it can help in translocating Tat through cell membranes, and can promote viral particles production [235-237, 253]. Furthermore, Rac1 can be activated through CCR5 to promote cytoskeletal rearrangements [221]. Future experiments will be to elucidate the pathway through which CCR5 induces Rac1 activation in HIV-1 infected monocytes. Other future experiments will include using a Rac1 inhibitor to determine whether Rac1 inhibition alone can prevent HIV-1-induced monocyte adhesion to the BBB.

4.1.2 Chapter 3

We next used a hu-PBL mouse model to examine the *in vivo* effects of CCR5 inhibitors during HIV-1 infection. We used the CCR5 antagonist MVR, since it is currently used to treat HIV-infected humans in clinical settings. As expected, we saw a loss of CD4+ cells and an increase in CD8+ cells in the blood of mice following HIV-1 infection. Treatment with MVR could partially attenuate these changes. This is in agreement with several studies showing that MVR treatment is associated with increases in CD4+ cell levels [128, 129, 301]. We also showed that HIV-1 infection reduced the levels of CD45+ cells in the blood and treatment with MVR helped restore these levels. These results suggest that MVR could help restore the immune cells and immune function in HIV-1 infection. Immune restoration in the periphery could be beneficial for the integrity of the BBB and

the prevention of HAND. By decreasing infection levels in the periphery there would be less infected cells entering into the CNS, thus decreasing the levels of CNS inflammation.

Next, using our mouse model we examined the expression of tight junction proteins in the brain following HIV-1 infection and MVR treatment. Using immunofluorescence and immunohistochemistry analyses, we showed that the levels of claudin-5 and ZO-2 were reduced in the brains of HIV-1-infected mice. These results are in agreement with several studies showing that HIV-1 infection and HIV-1 proteins can diminish the expression of tight junction proteins [176, 178, 180, 272, 277, 302]. MVR treatment was able to partially attenuate the loss of claudin-5 and ZO-2. It is not known whether this attenuation was through the inhibition of HIV-1 infection or if MVR can directly prevent these changes. It is likely a combination of both. It has been shown that gp120 can bind to CCR5 without binding CD4 on HBMEC and that this resulted in BBB dysfunction [179, 215]. Therefore it is likely that MVR could prevent viral protein binding to endothelial cells, thus preventing viral-induced endothelial dysfunction. Pathways that are involved in BBB disruption, such as ERK1/2 pathway, PI3K pathway, and the STAT pathway, have been found to be activated by CCR5 [215, 216, 303]. Furthermore, PTM of tight junction proteins are associated with BBB dysfunction and these PTM occurred through activation of Rho GTPases [279, 280]. Future studies will include further elucidating the role of CCR5 in HIV-1-induced BBB dysfunction, and determine whether this involves PTM of tight junction proteins. We will also determine if Rac1 activation during HIV-1 infection is associated with BBB dysfunction.

We showed that MVR treatment of HIV-1-infected mice decreased Tat, LTR, and pol mRNA in the brain. This is in agreement with studies showing that MVR treatment decreases viral load in the CSF [123, 125]. We then showed, using UPLC-MS/MS, that MVR was detectable in the brains of mice. This is in agreement with studies showing

that MVR is detectable in the CSF at levels higher than its IC_{50} [121, 123-125, 273]. Future studies will elucidate how MVR enters the brain. MVR is a known substrate of Pgp1, which is involved in drug efflux [97, 304]. Pgp1 is a substrate for many antiretrovirals and can prevent the accumulation of these drugs into sanctuary sites, such as the brain [305]. MVR has also been shown to be a substrate for OATP1B1, which is involved in drug influx [284, 285]. However, this transporter does not appear to be expressed in the brain or in cells of the BBB [285]. It is possible that MVR could be transported across the BBB through another member of the OATP1 family that is expressed in cells of the BBB.

4.2 Overall summary

Our data suggest that MVR could reduce HAND by reducing viral infection of macrophages, decreasing monocyte infiltration into the brain, reducing brain viral loads, and preventing HIV-induced tight junction down-regulation. However, our studies did not examine neurocognitive impairment in animals. A few studies have looked at the effect of MVR on neurocognitive impairment using both simian models and human patients. Fourteen-day treatment intensification with 150 mg/kg of MVR twice daily in HIV-infected neurologically asymptomatic adults resulted in a small increase in markers of neuronal integrity [122]. SIV-infected rhesus macaques treated with MVR showed decreased CNS levels of SIV RNA and DNA, decreased inflammation, macrophage activation, and amyloid precursor protein [265]. Neurocognitively impaired HIV-infected patients receiving MVR trended towards improvements in neurocognitive status and showed reduced CNS inflammation [217]. MVR intensification was associated with significant improvements in neuropsychological performance in patients with mild to moderate neurocognitive impairment [296].

Our studies suggest a role for CCR5 in HIV-1-induced BBB disruption. We propose the following overall mechanism for the possible role of CCR5 in HIV-1-induced BBB disruption: HIV-1 infection of monocytes results in cytoskeleton changes, via activation of cytoskeletal-associated proteins, such as Rac1 and cortactin, that leads to increased adhesion and migration of these infected monocytes through the brain endothelium. Increased migration of infected cells results in BBB injury and CNS infection; and inflammation in the brain results in reduced expression of BBB tight junctions, which further increases the infiltration on infected cells into the CNS, as well as allowing free viral particles to enter the CNS. Free virus infiltrating into the CNS leads to increased levels of infection and inflammation in the brain, resulting in neuronal damage and eventual neuronal death.

One must consider the possible negative consequences of blocking CCR5. CCR5 has a neuroprotective role during infection with West Nile Virus, as it enhanced the leukocytes trafficking into the CNS and helped in WNV clearance [42]. In addition to its role in HIV CNS infection and subsequent neurocognitive impairment, CCR5 has also been shown to have some neuroprotective effects during HIV-1 infection. CCL4 and CCL5 can out-compete gp120 for binding to CCR5 activation of CCR5 can activate the AKT pathway in microglia, neurons, and astrocytes, and provide protection against HIV-induced neurotoxicity and neuronal death [197, 306, 307]. One must also consider the effects of aging and other antiretrovirals on neuronal health. Low, but otherwise detectable, levels of HIV RNA can be found in the CSF in 10% of patients on long-term cART with undetectable plasma viral load [308]. The effect of this low level of RNA remains unforeseen. In addition, long-term use of ART is associated with numerous adverse effects, including hepatic steatosis, neuropathy, and cardiomyopathy [309].

In conclusion, in this study, we determined that CCR5 inhibition could prevent MDM infection and HIV-1-induced monocyte adhesion to the BBB. This was associated

with increased expression and phosphorylation of the cytoskeleton-associated protein Rac1, which is involved in cellular adhesion and migration, in monocytes. CCR5 inhibition also prevented these changes. Rac1 mRNA expression was increased in the brains of HIV-1-infected individuals compared to seronegative controls and individuals with HAND. There was also increased expression of pRac1 (S71) in the brains of infected individuals compared to seronegative controls and individuals with HAND. Expression of pRac1 (S71) in the brain is limited mainly to brain macrophages and blood vessel tight junctions. MVR treatment in HIV-1-infected hu-PBL NSG mice partially prevented HIV-1-induced decreases of CD4+ levels and CD45+ levels and HIV-1-induced increase of CD8+ cells. MVR partially attenuated the loss of tight junction proteins in infected mice. MVR decreased viral loads in the brain of infected mice and MVR could be quantified in the brains of mice. Taken together, these results suggest a role for CCR5 in the pathogenesis of BBB dysfunction during HIV-1 infection and HAND.

References

1. Organization, W.H. *GHO data HIV/AIDS*. 2015 5/28/15]; Available from: http://www.who.int/gho/hiv/en/.

2. CDC. *HIV/AIDS basics*. 2015 5/28/15]; Available from: http://www.cdc.gov/hiv/basics/whatishiv.html.

3. Lucas, S. and A.M. Nelson, *HIV and the spectrum of human disease.* J Pathol, 2015. **235**(2): p. 229-41.

4. Tang, H., K.L. Kuhen, and F. Wong-Staal, *Lentivirus replication and regulation.* Annu Rev Genet, 1999. **33**: p. 133-70.

5. Frankel, A.D. and J.A. Young, *HIV-1: fifteen proteins and an RNA.* Annu Rev Biochem, 1998. **67**: p. 1-25.

6. Vella, S., B. Schwartlander, S.P. Sow, S.P. Eholie, and R.L. Murphy, *The history of antiretroviral therapy and of its implementation in resource-limited areas of the world.* AIDS, 2012. **26**(10): p. 1231-41.

7. Marin, B., R. Thiebaut, H.C. Bucher, V. Rondeau, D. Costagliola, M. Dorrucci, . . . G. Chene, *Non-AIDS-defining deaths and immunodeficiency in the era of combination antiretroviral therapy.* AIDS, 2009. **23**(13): p. 1743-53.

8. Spudich, S., *HIV and neurocognitive dysfunction.* Curr HIV/AIDS Rep, 2013. **10**(3): p. 235-43.

9. Meulendyke, K.A., J.D. Croteau, and M.C. Zink, *HIV life cycle, innate immunity and autophagy in the central nervous system.* Curr Opin HIV AIDS, 2014. **9**(6): p. 565-71.

10. Letendre, S., J. Marquie-Beck, E. Capparelli, B. Best, D. Clifford, A.C. Collier, . . . C. Group, *Validation of the CNS Penetration-Effectiveness rank for quantifying*

antiretroviral penetration into the central nervous system. Arch Neurol, 2008. **65**(1): p. 65-70.

11. Rottman, J.B., K.P. Ganley, K. Williams, L. Wu, C.R. Mackay, and D.J. Ringler, *Cellular localization of the chemokine receptor CCR5. Correlation to cellular targets of HIV-1 infection.* Am J Pathol, 1997. **151**(5): p. 1341-51.
12. Liu, R., W.A. Paxton, S. Choe, D. Ceradini, S.R. Martin, R. Horuk, . . . N.R. Landau, *Homozygous defect in HIV-1 coreceptor accounts for resistance of some multiply-exposed individuals to HIV-1 infection.* Cell, 1996. **86**(3): p. 367-77.
13. Mummidi, S., S.S. Ahuja, B.L. McDaniel, and S.K. Ahuja, *The human CC chemokine receptor 5 (CCR5) gene. Multiple transcripts with 5'-end heterogeneity, dual promoter usage, and evidence for polymorphisms within the regulatory regions and noncoding exons.* J Biol Chem, 1997. **272**(49): p. 30662-71.
14. Liu, R., X. Zhao, T.A. Gurney, and N.R. Landau, *Functional analysis of the proximal CCR5 promoter.* AIDS Res Hum Retroviruses, 1998. **14**(17): p. 1509-19.
15. Sorce, S., R. Myburgh, and K.H. Krause, *The chemokine receptor CCR5 in the central nervous system.* Prog Neurobiol, 2011. **93**(2): p. 297-311.
16. Kobilka, B.K., *G protein coupled receptor structure and activation.* Biochim Biophys Acta, 2007. **1768**(4): p. 794-807.
17. Paterlini, M.G., *Structure modeling of the chemokine receptor CCR5: implications for ligand binding and selectivity.* Biophys J, 2002. **83**(6): p. 3012-31.
18. Barmania, F., M. Potgieter, and M.S. Pepper, *Mutations in C-C chemokine receptor type 5 (CCR5) in South African individuals.* Int J Infect Dis, 2013. **17**(12): p. e1148-53.

19. Combadiere, C., S.K. Ahuja, H.L. Tiffany, and P.M. Murphy, *Cloning and functional expression of CC CKR5, a human monocyte CC chemokine receptor selective for MIP-1(alpha), MIP-1(beta), and RANTES.* J Leukoc Biol, 1996. **60**(1): p. 147-52.

20. Raport, C.J., J. Gosling, V.L. Schweickart, P.W. Gray, and I.F. Charo, *Molecular cloning and functional characterization of a novel human CC chemokine receptor (CCR5) for RANTES, MIP-1beta, and MIP-1alpha.* J Biol Chem, 1996. **271**(29): p. 17161-6.

21. Samson, M., O. Labbe, C. Mollereau, G. Vassart, and M. Parmentier, *Molecular cloning and functional expression of a new human CC-chemokine receptor gene.* Biochemistry, 1996. **35**(11): p. 3362-7.

22. Oppermann, M., *Chemokine receptor CCR5: insights into structure, function, and regulation.* Cell Signal, 2004. **16**(11): p. 1201-10.

23. Mueller, A. and P.G. Strange, *CCL3, acting via the chemokine receptor CCR5, leads to independent activation of Janus kinase 2 (JAK2) and Gi proteins.* FEBS Lett, 2004. **570**(1-3): p. 126-32.

24. Berro, R., A. Yasmeen, R. Abrol, B. Trzaskowski, S. Abi-Habib, A. Grunbeck, . . . J.P. Moore, *Use of G-protein-coupled and -uncoupled CCR5 receptors by CCR5 inhibitor-resistant and -sensitive human immunodeficiency virus type 1 variants.* J Virol, 2013. **87**(12): p. 6569-81.

25. Aramori, I., S.S. Ferguson, P.D. Bieniasz, J. Zhang, B. Cullen, and M.G. Cullen, *Molecular mechanism of desensitization of the chemokine receptor CCR-5: receptor signaling and internalization are dissociable from its role as an HIV-1 co-receptor.* EMBO J, 1997. **16**(15): p. 4606-16.

26. Zhao, J., L. Ma, Y.L. Wu, P. Wang, W. Hu, and G. Pei, *Chemokine receptor CCR5 functionally couples to inhibitory G proteins and undergoes desensitization.* J Cell Biochem, 1998. **71**(1): p. 36-45.

27. Harmon, B. and L. Ratner, *Induction of the Galpha(q) signaling cascade by the human immunodeficiency virus envelope is required for virus entry.* J Virol, 2008. **82**(18): p. 9191-205.

28. Mellado, M., J.M. Rodriguez-Frade, A.J. Vila-Coro, S. Fernandez, A. Martin de Ana, D.R. Jones, . . . A.C. Martinez, *Chemokine receptor homo- or heterodimerization activates distinct signaling pathways.* EMBO J, 2001. **20**(10): p. 2497-507.

29. Del Corno, M., Q.H. Liu, D. Schols, E. de Clercq, S. Gessani, B.D. Freedman, and R.G. Collman, *HIV-1 gp120 and chemokine activation of Pyk2 and mitogen-activated protein kinases in primary macrophages mediated by calcium-dependent, pertussis toxin-insensitive chemokine receptor signaling.* Blood, 2001. **98**(10): p. 2909-16.

30. Ganju, R.K., P. Dutt, L. Wu, W. Newman, H. Avraham, S. Avraham, and J.E. Groopman, *Beta-chemokine receptor CCR5 signals via the novel tyrosine kinase RAFTK.* Blood, 1998. **91**(3): p. 791-7.

31. Misse, D., P.O. Esteve, B. Renneboog, M. Vidal, M. Cerutti, Y. St Pierre, . . . F. Veas, *HIV-1 glycoprotein 120 induces the MMP-9 cytopathogenic factor production that is abolished by inhibition of the p38 mitogen-activated protein kinase signaling pathway.* Blood, 2001. **98**(3): p. 541-7.

32. Wong, M., S. Uddin, B. Majchrzak, T. Huynh, A.E. Proudfoot, L.C. Platanias, and E.N. Fish, *Rantes activates Jak2 and Jak3 to regulate engagement of multiple signaling pathways in T cells.* J Biol Chem, 2001. **276**(14): p. 11427-31.

33. Burgering, B.M. and P.J. Coffer, *Protein kinase B (c-Akt) in phosphatidylinositol-3-OH kinase signal transduction.* Nature, 1995. **376**(6541): p. 599-602.

34. Mueller, A., E. Kelly, and P.G. Strange, *Pathways for internalization and recycling of the chemokine receptor CCR5.* Blood, 2002. **99**(3): p. 785-91.

35. Zhou, Y., T. Kurihara, R.P. Ryseck, Y. Yang, C. Ryan, J. Loy, . . . R. Bravo, *Impaired macrophage function and enhanced T cell-dependent immune response in mice lacking CCR5, the mouse homologue of the major HIV-1 coreceptor.* J Immunol, 1998. **160**(8): p. 4018-25.

36. Tyner, J.W., O. Uchida, N. Kajiwara, E.Y. Kim, A.C. Patel, M.P. O'Sullivan, . . . M.J. Holtzman, *CCL5-CCR5 interaction provides antiapoptotic signals for macrophage survival during viral infection.* Nat Med, 2005. **11**(11): p. 1180-7.

37. Molon, B., G. Gri, M. Bettella, C. Gomez-Mouton, A. Lanzavecchia, A.C. Martinez, . . . A. Viola, *T cell costimulation by chemokine receptors.* Nat Immunol, 2005. **6**(5): p. 465-71.

38. Dean, M., M. Carrington, C. Winkler, G.A. Huttley, M.W. Smith, R. Allikmets, . . . S.J. O'Brien, *Genetic restriction of HIV-1 infection and progression to AIDS by a deletion allele of the CKR5 structural gene. Hemophilia Growth and Development Study, Multicenter AIDS Cohort Study, Multicenter Hemophilia Cohort Study, San Francisco City Cohort, ALIVE Study.* Science, 1996. **273**(5283): p. 1856-62.

39. Samson, M., F. Libert, B.J. Doranz, J. Rucker, C. Liesnard, C.M. Farber, . . . M. Parmentier, *Resistance to HIV-1 infection in caucasian individuals bearing mutant alleles of the CCR-5 chemokine receptor gene.* Nature, 1996. **382**(6593): p. 722-5.

40. Dragic, T., V. Litwin, G.P. Allaway, S.R. Martin, Y. Huang, K.A. Nagashima, . . . W.A. Paxton, *HIV-1 entry into CD4+ cells is mediated by the chemokine receptor CC-CKR-5.* Nature, 1996. **381**(6584): p. 667-73.

41. Deng, H., R. Liu, W. Ellmeier, S. Choe, D. Unutmaz, M. Burkhart, . . . N.R. Landau, *Identification of a major co-receptor for primary isolates of HIV-1.* Nature, 1996. **381**(6584): p. 661-6.

42. Glass, W.G., D.H. McDermott, J.K. Lim, S. Lekhong, S.F. Yu, W.A. Frank, . . . P.M. Murphy, *CCR5 deficiency increases risk of symptomatic West Nile virus infection.* J Exp Med, 2006. **203**(1): p. 35-40.

43. Glass, W.G., J.K. Lim, R. Cholera, A.G. Pletnev, J.L. Gao, and P.M. Murphy, *Chemokine receptor CCR5 promotes leukocyte trafficking to the brain and survival in West Nile virus infection.* J Exp Med, 2005. **202**(8): p. 1087-98.

44. Kindberg, E., A. Mickiene, C. Ax, B. Akerlind, S. Vene, L. Lindquist, . . . L. Svensson, *A deletion in the chemokine receptor 5 (CCR5) gene is associated with tickborne encephalitis.* J Infect Dis, 2008. **197**(2): p. 266-9.

45. Galvani, A.P. and M. Slatkin, *Evaluating plague and smallpox as historical selective pressures for the CCR5-Delta 32 HIV-resistance allele.* Proc Natl Acad Sci U S A, 2003. **100**(25): p. 15276-9.

46. Zimmermann, T., M. Moehler, I. Gockel, G.G. Sgourakis, S. Biesterfeld, M. Muller, . . . C.C. Schimanski, *Low expression of chemokine receptor CCR5 in human colorectal cancer correlates with lymphatic dissemination and reduced CD8+ T-cell infiltration.* Int J Colorectal Dis, 2010. **25**(4): p. 417-24.

47. van Deventer, H.W., W. O'Connor, Jr., W.J. Brickey, R.M. Aris, J.P. Ting, and J.S. Serody, *C-C chemokine receptor 5 on stromal cells promotes pulmonary metastasis.* Cancer Res, 2005. **65**(8): p. 3374-9.

48. Tang, C.H., A. Yamamoto, Y.T. Lin, Y.C. Fong, and T.W. Tan, *Involvement of matrix metalloproteinase-3 in CCL5/CCR5 pathway of chondrosarcomas metastasis.* Biochem Pharmacol, 2010. **79**(2): p. 209-17.

49. Chuang, J.Y., W.H. Yang, H.T. Chen, C.Y. Huang, T.W. Tan, Y.T. Lin, . . . C.H. Tang, *CCL5/CCR5 axis promotes the motility of human oral cancer cells.* J Cell Physiol, 2009. **220**(2): p. 418-26.

50. Cao, Z., X. Xu, X. Luo, L. Li, B. Huang, X. Li, . . . J. Gong, *Role of RANTES and its receptor in gastric cancer metastasis.* J Huazhong Univ Sci Technolog Med Sci, 2011. **31**(3): p. 342-7.

51. Mencarelli, A., L. Graziosi, B. Renga, S. Cipriani, C. D'Amore, D. Francisci, . . . S. Fiorucci, *CCR5 Antagonism by Maraviroc Reduces the Potential for Gastric Cancer Cell Dissemination.* Transl Oncol, 2013. **6**(6): p. 784-93.

52. Wilen, C.B., J.C. Tilton, and R.W. Doms, *HIV: cell binding and entry.* Cold Spring Harb Perspect Med, 2012. **2**(8).

53. Garg, H. and R. Blumenthal, *Role of HIV Gp41 mediated fusion/hemifusion in bystander apoptosis.* Cell Mol Life Sci, 2008. **65**(20): p. 3134-44.

54. McDougal, J.S., M.S. Kennedy, J.M. Sligh, S.P. Cort, A. Mawle, and J.K. Nicholson, *Binding of HTLV-III/LAV to T4+ T cells by a complex of the 110K viral protein and the T4 molecule.* Science, 1986. **231**(4736): p. 382-5.

55. Gibbings, D. and A.D. Befus, *CD4 and CD8: an inside-out coreceptor model for innate immune cells.* J Leukoc Biol, 2009. **86**(2): p. 251-9.

56. Luckheeram, R.V., R. Zhou, A.D. Verma, and B. Xia, *CD4(+)T cells: differentiation and functions.* Clin Dev Immunol, 2012. **2012**: p. 925135.

57. Leahy, D.J., *A structural view of CD4 and CD8.* FASEB J, 1995. **9**(1): p. 17-25.

58. Hartley, O., P.J. Klasse, Q.J. Sattentau, and J.P. Moore, *V3: HIV's switch-hitter.* AIDS Res Hum Retroviruses, 2005. **21**(2): p. 171-89.

59. Wilen, C.B., J.C. Tilton, and R.W. Doms, *Molecular mechanisms of HIV entry.* Adv Exp Med Biol, 2012. **726**: p. 223-42.

60. Da, L.T., J.M. Quan, and Y.D. Wu, *Understanding of the bridging sheet formation of HIV-1 glycoprotein gp120.* J Phys Chem B, 2009. **113**(43): p. 14536-43.

61. White, J.M., S.E. Delos, M. Brecher, and K. Schornberg, *Structures and mechanisms of viral membrane fusion proteins: multiple variations on a common theme.* Crit Rev Biochem Mol Biol, 2008. **43**(3): p. 189-219.

62. Tran, E.E., M.J. Borgnia, O. Kuybeda, D.M. Schauder, A. Bartesaghi, G.A. Frank, . . . S. Subramaniam, *Structural mechanism of trimeric HIV-1 envelope glycoprotein activation.* PLoS Pathog, 2012. **8**(7): p. e1002797.

63. Chan, D.C., D. Fass, J.M. Berger, and P.S. Kim, *Core structure of gp41 from the HIV envelope glycoprotein.* Cell, 1997. **89**(2): p. 263-73.

64. Ji, H., W. Shu, F.T. Burling, S. Jiang, and M. Lu, *Inhibition of human immunodeficiency virus type 1 infectivity by the gp41 core: role of a conserved hydrophobic cavity in membrane fusion.* J Virol, 1999. **73**(10): p. 8578-86.

65. Chan, D.C. and P.S. Kim, *HIV entry and its inhibition.* Cell, 1998. **93**(5): p. 681-4.

66. Melikyan, G.B., R.M. Markosyan, H. Hemmati, M.K. Delmedico, D.M. Lambert, and F.S. Cohen, *Evidence that the transition of HIV-1 gp41 into a six-helix bundle, not the bundle configuration, induces membrane fusion.* J Cell Biol, 2000. **151**(2): p. 413-23.

67. Melikyan, G.B., *HIV entry: a game of hide-and-fuse?* Curr Opin Virol, 2014. **4**: p. 1-7.

68. Pauza, C.D. and T.M. Price, *Human immunodeficiency virus infection of T cells and monocytes proceeds via receptor-mediated endocytosis.* J Cell Biol, 1988. **107**(3): p. 959-68.

69. Marechal, V., M.C. Prevost, C. Petit, E. Perret, J.M. Heard, and O. Schwartz, *Human immunodeficiency virus type 1 entry into macrophages mediated by macropinocytosis.* J Virol, 2001. **75**(22): p. 11166-77.

70. Fredericksen, B.L., B.L. Wei, J. Yao, T. Luo, and J.V. Garcia, *Inhibition of endosomal/lysosomal degradation increases the infectivity of human immunodeficiency virus.* J Virol, 2002. **76**(22): p. 11440-6.

71. Miyauchi, K., Y. Kim, O. Latinovic, V. Morozov, and G.B. Melikyan, *HIV enters cells via endocytosis and dynamin-dependent fusion with endosomes.* Cell, 2009. **137**(3): p. 433-44.

72. von Kleist, L., W. Stahlschmidt, H. Bulut, K. Gromova, D. Puchkov, M.J. Robertson, . . . V. Haucke, *Role of the clathrin terminal domain in regulating coated pit dynamics revealed by small molecule inhibition.* Cell, 2011. **146**(3): p. 471-84.

73. Zaitseva, M., K. Peden, and H. Golding, *HIV coreceptors: role of structure, posttranslational modifications, and internalization in viral-cell fusion and as targets for entry inhibitors.* Biochim Biophys Acta, 2003. **1614**(1): p. 51-61.

74. Alkhatib, G., E.A. Berger, P.M. Murphy, and J.E. Pease, *Determinants of HIV-1 coreceptor function on CC chemokine receptor 3. Importance of both extracellular and transmembrane/cytoplasmic regions.* J Biol Chem, 1997. **272**(33): p. 20420-6.

75. He, J., Y. Chen, M. Farzan, H. Choe, A. Ohagen, S. Gartner, . . . D. Gabuzda, *CCR3 and CCR5 are co-receptors for HIV-1 infection of microglia.* Nature, 1997. **385**(6617): p. 645-9.

76. Lee, B., B.J. Doranz, S. Rana, Y. Yi, M. Mellado, J.M. Frade, . . . R.W. Doms, *Influence of the CCR2-V64I polymorphism on human immunodeficiency virus type 1 coreceptor activity and on chemokine receptor function of CCR2b, CCR3, CCR5, and CXCR4.* J Virol, 1998. **72**(9): p. 7450-8.

77. Lee, S., H.L. Tiffany, L. King, P.M. Murphy, H. Golding, and M.B. Zaitseva, *CCR8 on human thymocytes functions as a human immunodeficiency virus type 1 coreceptor.* J Virol, 2000. **74**(15): p. 6946-52.

78. Calado, M., P. Matoso, Q. Santos-Costa, M. Espirito-Santo, J. Machado, L. Rosado, . . . J.M. Azevedo-Pereira, *Coreceptor usage by HIV-1 and HIV-2 primary isolates: the relevance of CCR8 chemokine receptor as an alternative coreceptor.* Virology, 2010. **408**(2): p. 174-82.

79. Blanpain, C., F. Libert, G. Vassart, and M. Parmentier, *CCR5 and HIV infection.* Receptors Channels, 2002. **8**(1): p. 19-31.

80. Vicenzi, E., P. Lio, and G. Poli, *The puzzling role of CXCR4 in human immunodeficiency virus infection.* Theranostics, 2013. **3**(1): p. 18-25.

81. Schuitemaker, H., A.B. van 't Wout, and P. Lusso, *Clinical significance of HIV-1 coreceptor usage.* J Transl Med, 2011. **9 Suppl 1**: p. S5.

82. Peters, P.J., W.M. Sullivan, M.J. Duenas-Decamp, J. Bhattacharya, C. Ankghuambom, R. Brown, . . . P.R. Clapham, *Non-macrophage-tropic human immunodeficiency virus type 1 R5 envelopes predominate in blood, lymph nodes, and semen: implications for transmission and pathogenesis.* J Virol, 2006. **80**(13): p. 6324-32.

83. Musich, T., O. O'Connell, M.P. Gonzalez-Perez, C.A. Derdeyn, P.J. Peters, and P.R. Clapham, *HIV-1 non-macrophage-tropic R5 envelope glycoproteins are not more tropic for entry into primary CD4+ T-cells than envelopes highly adapted for macrophages.* Retrovirology, 2015. **12**: p. 25.

84. Valentin, A., H. Trivedi, W. Lu, L.G. Kostrikis, and G.N. Pavlakis, *CXCR4 mediates entry and productive infection of syncytia-inducing (X4) HIV-1 strains in primary macrophages.* Virology, 2000. **269**(2): p. 294-304.

85. Penn, M.L., J.C. Grivel, B. Schramm, M.A. Goldsmith, and L. Margolis, *CXCR4 utilization is sufficient to trigger CD4+ T cell depletion in HIV-1-infected human lymphoid tissue.* Proc Natl Acad Sci U S A, 1999. **96**(2): p. 663-8.

86. Berger, E.A., P.M. Murphy, and J.M. Farber, *Chemokine receptors as HIV-1 coreceptors: roles in viral entry, tropism, and disease.* Annu Rev Immunol, 1999. **17**: p. 657-700.

87. Jensen, M.A. and A.B. van 't Wout, *Predicting HIV-1 coreceptor usage with sequence analysis.* AIDS Rev, 2003. **5**(2): p. 104-12.

88. Brumme, Z.L., W.W. Dong, B. Yip, B. Wynhoven, N.G. Hoffman, R. Swanstrom, . . . P.R. Harrigan, *Clinical and immunological impact of HIV envelope V3 sequence variation after starting initial triple antiretroviral therapy.* AIDS, 2004. **18**(4): p. F1-9.

89. Delobel, P., K. Sandres-Saune, M. Cazabat, C. Pasquier, B. Marchou, P. Massip, and J. Izopet, *R5 to X4 switch of the predominant HIV-1 population in cellular reservoirs during effective highly active antiretroviral therapy.* J Acquir Immune Defic Syndr, 2005. **38**(4): p. 382-92.

90. Yi, Y., A. Singh, F. Shaheen, A. Louden, C. Lee, and R.G. Collman, *Contrasting use of CCR5 structural determinants by R5 and R5X4 variants within a human immunodeficiency virus type 1 primary isolate quasispecies.* J Virol, 2003. **77**(22): p. 12057-66.

91. Lin, G., F. Baribaud, J. Romano, R.W. Doms, and J.A. Hoxie, *Identification of gp120 binding sites on CXCR4 by using CD4-independent human immunodeficiency virus type 2 Env proteins.* J Virol, 2003. **77**(2): p. 931-42.

92. Clapham, P.R. and A. McKnight, *HIV-1 receptors and cell tropism.* Br Med Bull, 2001. **58**: p. 43-59.

93. Low, A.J., R.A. McGovern, and P.R. Harrigan, *Trofile HIV co-receptor usage assay.* Expert Opin Med Diagn, 2009. **3**(2): p. 181-91.

94. Whitcomb, J.M., W. Huang, S. Fransen, K. Limoli, J. Toma, T. Wrin, . . . C.J. Petropoulos, *Development and characterization of a novel single-cycle recombinant-virus assay to determine human immunodeficiency virus type 1 coreceptor tropism.* Antimicrob Agents Chemother, 2007. **51**(2): p. 566-75.

95. Sanchez, V., M. Masia, C. Robledano, S. Padilla, J.M. Ramos, and F. Gutierrez, *Performance of genotypic algorithms for predicting HIV-1 tropism measured against the enhanced-sensitivity Trofile coreceptor tropism assay.* J Clin Microbiol, 2010. **48**(11): p. 4135-9.

96. Ashkenazi, A., Y. Wexler-Cohen, and Y. Shai, *Multifaceted action of Fuzeon as virus-cell membrane fusion inhibitor.* Biochim Biophys Acta, 2011. **1808**(10): p. 2352-8.

97. Walker, D.K., S. Abel, P. Comby, G.J. Muirhead, A.N. Nedderman, and D.A. Smith, *Species differences in the disposition of the CCR5 antagonist, UK-427,857, a new potential treatment for HIV.* Drug Metab Dispos, 2005. **33**(4): p. 587-95.

98. Daar, E.S., X.L. Li, T. Moudgil, and D.D. Ho, *High concentrations of recombinant soluble CD4 are required to neutralize primary human immunodeficiency virus type 1 isolates.* Proc Natl Acad Sci U S A, 1990. **87**(17): p. 6574-8.

99. Haqqani, A.A. and J.C. Tilton, *Entry inhibitors and their use in the treatment of HIV-1 infection.* Antiviral Res, 2013. **98**(2): p. 158-70.

100. Lalezari, J., G.H. Latiff, C. Brinson, J. Echevarria, S. Trevino-Perez, J.R. Bogner, . . . M. Lataillade, *Safety profile of HIV-1 attachment inhibitor prodrug BMS-663068 in antiretroviral-experienced subjects: week 24 analysis.* J Int AIDS Soc, 2014. **17**(4 Suppl 3): p. 19530.

101. Song, R., D. Franco, C.Y. Kao, F. Yu, Y. Huang, and D.D. Ho, *Epitope mapping of ibalizumab, a humanized anti-CD4 monoclonal antibody with anti-HIV-1 activity in infected patients.* J Virol, 2010. **84**(14): p. 6935-42.

102. Wild, C., T. Greenwell, and T. Matthews, *A synthetic peptide from HIV-1 gp41 is a potent inhibitor of virus-mediated cell-cell fusion.* AIDS Res Hum Retroviruses, 1993. **9**(11): p. 1051-3.

103. Lalezari, J.P., K. Henry, M. O'Hearn, J.S. Montaner, P.J. Piliero, B. Trottier, . . . T.S. Group, *Enfuvirtide, an HIV-1 fusion inhibitor, for drug-resistant HIV infection in North and South America.* N Engl J Med, 2003. **348**(22): p. 2175-85.

104. Donzella, G.A., D. Schols, S.W. Lin, J.A. Este, K.A. Nagashima, P.J. Maddon, . . . J.P. Moore, *AMD3100, a small molecule inhibitor of HIV-1 entry via the CXCR4 co-receptor.* Nat Med, 1998. **4**(1): p. 72-7.

105. Hendrix, C.W., A.C. Collier, M.M. Lederman, D. Schols, R.B. Pollard, S. Brown, . . . A.H.S. Group, *Safety, pharmacokinetics, and antiviral activity of AMD3100, a selective CXCR4 receptor inhibitor, in HIV-1 infection.* J Acquir Immune Defic Syndr, 2004. **37**(2): p. 1253-62.

106. Uy, G.L., M.P. Rettig, and A.F. Cashen, *Plerixafor, a CXCR4 antagonist for the mobilization of hematopoietic stem cells.* Expert Opin Biol Ther, 2008. **8**(11): p. 1797-804.

107. Cocchi, F., A.L. DeVico, A. Garzino-Demo, S.K. Arya, R.C. Gallo, and P. Lusso, *Identification of RANTES, MIP-1 alpha, and MIP-1 beta as the major HIV-suppressive factors produced by CD8+ T cells.* Science, 1995. **270**(5243): p. 1811-5.

108. Kiss, D.L., J. Longden, G.A. Fechner, and V.M. Avery, *The functional antagonist Met-RANTES: a modified agonist that induces differential CCR5 trafficking.* Cell Mol Biol Lett, 2009. **14**(4): p. 537-47.

109. Elsner, J., M. Mack, H. Bruhl, Y. Dulkys, D. Kimmig, G. Simmons, . . . A.E. Proudfoot, *Differential activation of CC chemokine receptors by AOP-RANTES.* J Biol Chem, 2000. **275**(11): p. 7787-94.

110. Kuritzkes, D.R., *HIV-1 entry inhibitors: an overview.* Curr Opin HIV AIDS, 2009. **4**(2): p. 82-7.

111. Nichols, W.G., H.M. Steel, T. Bonny, K. Adkison, L. Curtis, J. Millard, . . . N. Clumeck, *Hepatotoxicity observed in clinical trials of aplaviroc (GW873140).* Antimicrob Agents Chemother, 2008. **52**(3): p. 858-65.

112. Pfizer. *Selzentry*. 2/25/15]; Available from: http://www.viivhealthcare.com/media/70429/us_selzentry.pdf.

113. Bayes, M., X. Rabasseda, and J.R. Prous, *Gateways to clinical trials.* Methods Find Exp Clin Pharmacol, 2004. **26**(8): p. 639-63.

114. Dorr, P., M. Westby, S. Dobbs, P. Griffin, B. Irvine, M. Macartney, . . . M. Perros, *Maraviroc (UK-427,857), a potent, orally bioavailable, and selective small-molecule inhibitor of chemokine receptor CCR5 with broad-spectrum anti-human immunodeficiency virus type 1 activity.* Antimicrob Agents Chemother, 2005. **49**(11): p. 4721-32.

115. Abel, S., D. Russell, L.A. Whitlock, C.E. Ridgway, A.N. Nedderman, and D.K. Walker, *Assessment of the absorption, metabolism and absolute bioavailability of maraviroc in healthy male subjects.* Br J Clin Pharmacol, 2008. **65 Suppl 1**: p. 60-7.

116. Brown, K.C., K.B. Patterson, S.A. Malone, N.J. Shaheen, H.M. Prince, J.B. Dumond, . . . A.D. Kashuba, *Single and multiple dose pharmacokinetics of maraviroc in saliva, semen, and rectal tissue of healthy HIV-negative men.* J Infect Dis, 2011. **203**(10): p. 1484-90.

117. Tiraboschi, J.M., J. Niubo, J. Curto, and D. Podzamczer, *Maraviroc concentrations in seminal plasma in HIV-infected patients.* J Acquir Immune Defic Syndr, 2010. **55**(5): p. e35-6.

118. Massud, I., W. Aung, A. Martin, S. Bachman, J. Mitchell, R. Aubert, . . . J.G. Garcia-Lerma, *Lack of prophylactic efficacy of oral maraviroc in macaques despite high drug concentrations in rectal tissues.* J Virol, 2013. **87**(16): p. 8952-61.

119. Dumond, J.B., K.B. Patterson, A.L. Pecha, R.E. Werner, E. Andrews, B. Damle, . . . A.D. Kashuba, *Maraviroc concentrates in the cervicovaginal fluid and vaginal tissue of HIV-negative women.* J Acquir Immune Defic Syndr, 2009. **51**(5): p. 546-53.

120. Malcolm, R.K., C.J. Forbes, L. Geer, R.S. Veazey, L. Goldman, P.J. Klasse, and J.P. Moore, *Pharmacokinetics and efficacy of a vaginally administered maraviroc gel in rhesus macaques.* J Antimicrob Chemother, 2013. **68**(3): p. 678-83.

121. Croteau, D., B.M. Best, S. Letendre, S.S. Rossi, R.J. Ellis, D.B. Clifford, . . . C. Group, *Lower than expected maraviroc concentrations in cerebrospinal fluid exceed the wild-type CC chemokine receptor 5-tropic HIV-1 50% inhibitory concentration.* AIDS, 2012. **26**(7): p. 890-3.

122. Garvey, L., M. Nelson, N. Latch, O.W. Erlwein, J.M. Allsop, A. Mitchell, . . . A. Winston, *CNS effects of a CCR5 inhibitor in HIV-infected subjects: a pharmacokinetic and cerebral metabolite study.* J Antimicrob Chemother, 2012. **67**(1): p. 206-12.

123. Melica, G., A. Canestri, G. Peytavin, J.D. Lelievre, M. Bouvier-Alias, C. Clavel, . . . Y. Levy, *Maraviroc-containing regimen suppresses HIV replication in the cerebrospinal fluid of patients with neurological symptoms.* AIDS, 2010. **24**(13): p. 2130-3.

124. Tiraboschi, J.M., J. Niubo, J. Curto, and D. Podzamczer, *Maraviroc concentrations in cerebrospinal fluid in HIV-infected patients.* J Acquir Immune Defic Syndr, 2010. **55**(5): p. 606-9.

125. Yilmaz, A., V. Watson, L. Else, and M. Gisslen, *Cerebrospinal fluid maraviroc concentrations in HIV-1 infected patients.* AIDS, 2009. **23**(18): p. 2537-40.

126. Fatkenheuer, G., A.L. Pozniak, M.A. Johnson, A. Plettenberg, S. Staszewski, A.I. Hoepelman, . . . E. van der Ryst, *Efficacy of short-term monotherapy with maraviroc, a new CCR5 antagonist, in patients infected with HIV-1.* Nat Med, 2005. **11**(11): p. 1170-2.

127. Gulick, R.M., J. Lalezari, J. Goodrich, N. Clumeck, E. DeJesus, A. Horban, . . . M.S. Teams, *Maraviroc for previously treated patients with R5 HIV-1 infection.* N Engl J Med, 2008. **359**(14): p. 1429-41.

128. Asmuth, D.M., J. Goodrich, D.A. Cooper, R. Haubrich, N. Rajicic, B. Hirschel, . . . H. Valdez, *CD4+ T-cell restoration after 48 weeks in the maraviroc treatment-experienced trials MOTIVATE 1 and 2.* J Acquir Immune Defic Syndr, 2010. **54**(4): p. 394-7.

129. Pulido, I., K. Machmach, M.C. Romero-Sanchez, M. Genebat, G. Mendez-Lagares, E. Ruiz-Mateos, and M. Leal, *T-cell changes after a short-term exposure to maraviroc in HIV-infected patients are related to antiviral activity.* J Infect, 2012. **64**(4): p. 417-23.

130. Kawana-Tachikawa, A., J.M. Llibre, I. Bravo, R. Escrig, B. Mothe, J. Puig, . . . M. Investigators, *Effect of maraviroc intensification on HIV-1-specific T cell immunity in recently HIV-1-infected individuals.* PLoS One, 2014. **9**(1): p. e87334.

131. Beliakova-Bethell, N., S. Jain, C.H. Woelk, M.D. Witt, X. Sun, S.M. Lada, . . . M.P. Dube, *Maraviroc intensification in patients with suppressed HIV viremia has*

limited effects on CD4+ T cell recovery and gene expression. Antiviral Res, 2014. **107**: p. 42-9.

132. Pozo-Balado, M.M., M. Martinez-Bonet, I. Rosado, E. Ruiz-Mateos, G. Mendez-Lagares, M.M. Rodriguez-Mendez, . . . M. Leal, *Maraviroc reduces the regulatory T-cell frequency in antiretroviral-naive HIV-infected subjects.* J Infect Dis, 2014. **210**(6): p. 890-8.

133. Reuter, S., P. Braken, B. Jensen, S. Sierra-Aragon, M. Oette, M. Balduin, . . . D. Haussinger, *Maraviroc in treatment-experienced patients with HIV-1 infection - experience from routine clinical practice.* Eur J Med Res, 2010. **15**(6): p. 231-7.

134. Babiker, Z.O., S.T. Douthwaite, L.E. Collier, A. Pennell, A.J. Uriel, and E. Wilkins, *Real-life outcomes of maraviroc-based regimens in HIV-1-infected individuals.* J Int Assoc Provid AIDS Care, 2013. **12**(1): p. 12-4.

135. Bon, I., A. Clo, M. Borderi, V. Colangeli, L. Calza, S. Morini, . . . M.C. Re, *Prevalence of R5 strains in multi-treated HIV subjects and impact of new regimens including maraviroc in a selected group of patients with CCR5-tropic HIV-1 infection.* Int J Infect Dis, 2013. **17**(10): p. e875-82.

136. Raymond, S., A. Maillard, C. Amiel, G. Peytavin, M.A. Trabaud, D. Desbois, . . . A.A.C.R.S.G. on behalf the, *Virological failure of patients on maraviroc-based antiretroviral therapy.* J Antimicrob Chemother, 2015.

137. Neff, C.P., T. Ndolo, A. Tandon, Y. Habu, and R. Akkina, *Oral pre-exposure prophylaxis by anti-retrovirals raltegravir and maraviroc protects against HIV-1 vaginal transmission in a humanized mouse model.* PLoS One, 2010. **5**(12): p. e15257.

138. Neff, C.P., T. Kurisu, T. Ndolo, K. Fox, and R. Akkina, *A topical microbicide gel formulation of CCR5 antagonist maraviroc prevents HIV-1 vaginal transmission in humanized RAG-hu mice.* PLoS One, 2011. **6**(6): p. e20209.

139. Matsuzawa, T., T. Kawamura, Y. Ogawa, M. Takahashi, R. Aoki, K. Moriishi, . . . S. Shimada, *Oral administration of the CCR5 inhibitor, maraviroc, blocks HIV ex vivo infection of Langerhans cells within the epithelium.* J Invest Dermatol, 2013. **133**(12): p. 2803-5.

140. Mechai, F., Y. Quertainmont, S. Sahali, J.F. Delfraissy, and J. Ghosn, *Post-exposure prophylaxis with a maraviroc-containing regimen after occupational exposure to a multi-resistant HIV-infected source person.* J Med Virol, 2008. **80**(1): p. 9-10.

141. Taiwo, B., E.P. Acosta, P. Ryscavage, B. Berzins, D. Lu, J. Lalezari, . . . S. Swindells, *Virologic response, early HIV-1 decay, and maraviroc pharmacokinetics with the nucleos(t)ide-free regimen of maraviroc plus darunavir/ritonavir in a pilot study.* J Acquir Immune Defic Syndr, 2013. **64**(2): p. 167-73.

142. Macias, J., M.M. Viloria, A. Rivero, I. de los Santos, M. Marquez, J. Portilla, . . . F.s. group, *Lack of short-term increase in serum mediators of fibrogenesis and in non-invasive markers of liver fibrosis in HIV/hepatitis C virus-coinfected patients starting maraviroc-based antiretroviral therapy.* Eur J Clin Microbiol Infect Dis, 2012. **31**(8): p. 2083-8.

143. Nozza, S., L. Galli, F. Visco, A. Soria, F. Canducci, S. Salpietro, . . . A. Castagna, *Raltegravir, maraviroc, etravirine: an effective protease inhibitor and nucleoside reverse transcriptase inhibitor-sparing regimen for salvage therapy in HIV-infected patients with triple-class experience.* AIDS, 2010. **24**(6): p. 924-8.

144. Nozza, S., L. Galli, A. Bigoloni, N. Gianotti, V. Spagnuolo, A. Carbone, . . . A. Castagna, *Four-year outcome of a PI and NRTI-sparing salvage regimen: maraviroc, raltegravir, etravirine.* New Microbiol, 2014. **37**(2): p. 145-51.

145. Martin-Blondel, G., L. Cuzin, P. Delobel, V. Cuvinciuc, H. Dumas, M. Alvarez, . . . B. Marchou, *Is maraviroc beneficial in paradoxical progressive multifocal leukoencephalopathy-immune reconstitution inflammatory syndrome management?* AIDS, 2009. **23**(18): p. 2545-6.

146. Giacomini, P.S., A. Rozenberg, I. Metz, D. Araujo, N. Arbour, A. Bar-Or, and P.M.L.I.G. Maraviroc in Multiple Sclerosis-Associated, *Maraviroc and JC virus-associated immune reconstitution inflammatory syndrome.* N Engl J Med, 2014. **370**(5): p. 486-8.

147. Velasco-Velazquez, M., X. Jiao, M. De La Fuente, T.G. Pestell, A. Ertel, M.P. Lisanti, and R.G. Pestell, *CCR5 antagonist blocks metastasis of basal breast cancer cells.* Cancer Res, 2012. **72**(15): p. 3839-50.

148. Ochoa-Callejero, L., L. Perez-Martinez, S. Rubio-Mediavilla, J.A. Oteo, A. Martinez, and J.R. Blanco, *Maraviroc, a CCR5 antagonist, prevents development of hepatocellular carcinoma in a mouse model.* PLoS One, 2013. **8**(1): p. e53992.

149. Choi, S.W., G.C. Hildebrandt, K.M. Olkiewicz, D.A. Hanauer, M.N. Chaudhary, I.A. Silva, . . . K.R. Cooke, *CCR1/CCL5 (RANTES) receptor-ligand interactions modulate allogeneic T-cell responses and graft-versus-host disease following stem-cell transplantation.* Blood, 2007. **110**(9): p. 3447-55.

150. Reshef, R., S.M. Luger, E.O. Hexner, A.W. Loren, N.V. Frey, S.D. Nasta, . . . D.L. Porter, *Blockade of lymphocyte chemotaxis in visceral graft-versus-host disease.* N Engl J Med, 2012. **367**(2): p. 135-45.

151. Amsellem, V., L. Lipskaia, S. Abid, L. Poupel, A. Houssaini, R. Quarck, . . . S. Adnot, *CCR5 as a treatment target in pulmonary arterial hypertension.* Circulation, 2014. **130**(11): p. 880-91.

152. Persidsky, Y., S.H. Ramirez, J. Haorah, and G.D. Kanmogne, *Blood-brain barrier: structural components and function under physiologic and pathologic conditions.* J Neuroimmune Pharmacol, 2006. **1**(3): p. 223-36.

153. Bergers, G. and S. Song, *The role of pericytes in blood-vessel formation and maintenance.* Neuro Oncol, 2005. **7**(4): p. 452-64.

154. Bauer, H.C., I.A. Krizbai, H. Bauer, and A. Traweger, *"You Shall Not Pass"-tight junctions of the blood brain barrier.* Front Neurosci, 2014. **8**: p. 392.

155. Mineta, K., Y. Yamamoto, Y. Yamazaki, H. Tanaka, Y. Tada, K. Saito, . . . S. Tsukita, *Predicted expansion of the claudin multigene family.* FEBS Lett, 2011. **585**(4): p. 606-12.

156. Krause, G., L. Winkler, S.L. Mueller, R.F. Haseloff, J. Piontek, and I.E. Blasig, *Structure and function of claudins.* Biochim Biophys Acta, 2008. **1778**(3): p. 631-45.

157. Garrido-Urbani, S., P.F. Bradfield, and B.A. Imhof, *Tight junction dynamics: the role of junctional adhesion molecules (JAMs).* Cell Tissue Res, 2014. **355**(3): p. 701-15.

158. del Palacio, M., S. Alvarez, and M.A. Munoz-Fernandez, *HIV-1 infection and neurocognitive impairment in the current era.* Rev Med Virol, 2012. **22**(1): p. 33-45.

159. Heaton, R.K., D.B. Clifford, D.R. Franklin, Jr., S.P. Woods, C. Ake, F. Vaida, . . . C. Group, *HIV-associated neurocognitive disorders persist in the era of potent antiretroviral therapy: CHARTER Study.* Neurology, 2010. **75**(23): p. 2087-96.

160. Wright, E.J., M. Nunn, J. Joseph, K. Robertson, L. Lal, and B.J. Brew, *NeuroAIDS in the Asia Pacific Region.* J Neurovirol, 2008. **14**(6): p. 465-73.

161. Heaton, R.K., L.A. Cysique, H. Jin, C. Shi, X. Yu, S. Letendre, . . . H. group, *Neurobehavioral effects of human immunodeficiency virus infection among former plasma donors in rural China.* J Neurovirol, 2010. **16**(2): p. 185-8.

162. McArthur, J.C., *HIV dementia: an evolving disease.* J Neuroimmunol, 2004. **157**(1-2): p. 3-10.

163. Robertson, K.R., M. Smurzynski, T.D. Parsons, K. Wu, R.J. Bosch, J. Wu, . . . R.J. Ellis, *The prevalence and incidence of neurocognitive impairment in the HAART era.* AIDS, 2007. **21**(14): p. 1915-21.

164. Sacktor, N., R.H. Lyles, R. Skolasky, C. Kleeberger, O.A. Selnes, E.N. Miller, . . . A.C.S. Multicenter, *HIV-associated neurologic disease incidence changes:: Multicenter AIDS Cohort Study, 1990-1998.* Neurology, 2001. **56**(2): p. 257-60.

165. Cysique, L.A., P. Maruff, and B.J. Brew, *Prevalence and pattern of neuropsychological impairment in human immunodeficiency virus-infected/acquired immunodeficiency syndrome (HIV/AIDS) patients across pre- and post-highly active antiretroviral therapy eras: a combined study of two cohorts.* J Neurovirol, 2004. **10**(6): p. 350-7.

166. Simioni, S., M. Cavassini, J.M. Annoni, A. Rimbault Abraham, I. Bourquin, V. Schiffer, . . . R.A. Du Pasquier, *Cognitive dysfunction in HIV patients despite long-standing suppression of viremia.* AIDS, 2010. **24**(9): p. 1243-50.

167. Rao, V.R., A.P. Ruiz, and V.R. Prasad, *Viral and cellular factors underlying neuropathogenesis in HIV associated neurocognitive disorders (HAND).* AIDS Res Ther, 2014. **11**: p. 13.

168. Eugenin EA, B.J., *Mechanisms of Viral and Cell Entry into the Central Nervous System*, in *The Neurology of AIDS. 3*, G.I. Gendelman HE, Everall IP, Fox HS, Gelbard HA, Lipton SA, Swindells S, Editor. 2012, Oxford University Press: New York. p. 231–245.

169. An, S.F., M. Groves, F. Gray, and F. Scaravilli, *Early entry and widespread cellular involvement of HIV-1 DNA in brains of HIV-1 positive asymptomatic individuals.* J Neuropathol Exp Neurol, 1999. **58**(11): p. 1156-62.

170. Meltzer, M.S., D.R. Skillman, P.J. Gomatos, D.C. Kalter, and H.E. Gendelman, *Role of mononuclear phagocytes in the pathogenesis of human immunodeficiency virus infection.* Annu Rev Immunol, 1990. **8**: p. 169-94.

171. Chaudhuri, A., F. Duan, B. Morsey, Y. Persidsky, and G.D. Kanmogne, *HIV-1 activates proinflammatory and interferon-inducible genes in human brain microvascular endothelial cells: putative mechanisms of blood-brain barrier dysfunction.* J Cereb Blood Flow Metab, 2008. **28**(4): p. 697-711.

172. Sharief, M.K., M. Ciardi, E.J. Thompson, F. Sorice, F. Rossi, V. Vullo, and A. Cirelli, *Tumour necrosis factor-alpha mediates blood-brain barrier damage in HIV-1 infection of the central nervous system.* Mediators Inflamm, 1992. **1**(3): p. 191-6.

173. Ivey, N.S., A.G. MacLean, and A.A. Lackner, *Acquired immunodeficiency syndrome and the blood-brain barrier.* J Neurovirol, 2009. **15**(2): p. 111-22.

174. Andras, I.E., H. Pu, M.A. Deli, A. Nath, B. Hennig, and M. Toborek, *HIV-1 Tat protein alters tight junction protein expression and distribution in cultured brain endothelial cells.* J Neurosci Res, 2003. **74**(2): p. 255-65.

175. Xu, R., X. Feng, X. Xie, J. Zhang, D. Wu, and L. Xu, *HIV-1 Tat protein increases the permeability of brain endothelial cells by both inhibiting occludin expression and cleaving occludin via matrix metalloproteinase-9.* Brain Res, 2012. **1436**: p. 13-9.

176. Pu, H., K. Hayashi, I.E. Andras, S.Y. Eum, B. Hennig, and M. Toborek, *Limited role of COX-2 in HIV Tat-induced alterations of tight junction protein expression and disruption of the blood-brain barrier.* Brain Res, 2007. **1184**: p. 333-44.

177. Kim, T.A., H.K. Avraham, Y.H. Koh, S. Jiang, I.W. Park, and S. Avraham, *HIV-1 Tat-mediated apoptosis in human brain microvascular endothelial cells.* J Immunol, 2003. **170**(5): p. 2629-37.

178. Kanmogne, G.D., C. Primeaux, and P. Grammas, *HIV-1 gp120 proteins alter tight junction protein expression and brain endothelial cell permeability: implications for the pathogenesis of HIV-associated dementia.* J Neuropathol Exp Neurol, 2005. **64**(6): p. 498-505.

179. Kanmogne, G.D., K. Schall, J. Leibhart, B. Knipe, H.E. Gendelman, and Y. Persidsky, *HIV-1 gp120 compromises blood-brain barrier integrity and enhances monocyte migration across blood-brain barrier: implication for viral neuropathogenesis.* J Cereb Blood Flow Metab, 2007. **27**(1): p. 123-34.

180. Nakamuta, S., H. Endo, Y. Higashi, A. Kousaka, H. Yamada, M. Yano, and H. Kido, *Human immunodeficiency virus type 1 gp120-mediated disruption of tight junction proteins by induction of proteasome-mediated degradation of zonula occludens-1 and -2 in human brain microvascular endothelial cells.* J Neurovirol, 2008. **14**(3): p. 186-95.

181. Avraham, H.K., S. Jiang, T.H. Lee, O. Prakash, and S. Avraham, *HIV-1 Tat-mediated effects on focal adhesion assembly and permeability in brain microvascular endothelial cells.* J Immunol, 2004. **173**(10): p. 6228-33.

182. Toborek, M., Y.W. Lee, H. Pu, A. Malecki, G. Flora, R. Garrido, . . . A. Nath, *HIV-Tat protein induces oxidative and inflammatory pathways in brain endothelium.* J Neurochem, 2003. **84**(1): p. 169-79.

183. Annunziata, P., C. Cioni, S. Toneatto, and E. Paccagnini, *HIV-1 gp120 increases the permeability of rat brain endothelium cultures by a mechanism involving substance P.* AIDS, 1998. **12**(18): p. 2377-85.

184. Banks, W.A. and A.J. Kastin, *Characterization of lectin-mediated brain uptake of HIV-1 GP120.* J Neurosci Res, 1998. **54**(4): p. 522-9.

185. Banks, W.A., A.J. Kastin, J.M. Brennan, and K.L. Vallance, *Adsorptive endocytosis of HIV-1gp120 by blood-brain barrier is enhanced by lipopolysaccharide.* Exp Neurol, 1999. **156**(1): p. 165-71.

186. Ren, Z., Q. Yao, and C. Chen, *HIV-1 envelope glycoprotein 120 increases intercellular adhesion molecule-1 expression by human endothelial cells.* Lab Invest, 2002. **82**(3): p. 245-55.

187. Stins, M.F., D. Pearce, F. Di Cello, A. Erdreich-Epstein, C.A. Pardo, and K. Sik Kim, *Induction of intercellular adhesion molecule-1 on human brain endothelial cells by HIV-1 gp120: role of CD4 and chemokine coreceptors.* Lab Invest, 2003. **83**(12): p. 1787-98.

188. Stins, M.F., Y. Shen, S.H. Huang, F. Gilles, V.K. Kalra, and K.S. Kim, *Gp120 activates children's brain endothelial cells via CD4.* J Neurovirol, 2001. **7**(2): p. 125-34.

189. Louboutin, J.P., L. Agrawal, B.A. Reyes, E.J. Van Bockstaele, and D.S. Strayer, *HIV-1 gp120-induced injury to the blood-brain barrier: role of metalloproteinases 2 and 9 and relationship to oxidative stress.* J Neuropathol Exp Neurol, 2010. **69**(8): p. 801-16.

190. Ranki, A., M. Nyberg, V. Ovod, M. Haltia, I. Elovaara, R. Raininko, . . . K. Krohn, *Abundant expression of HIV Nef and Rev proteins in brain astrocytes in vivo is associated with dementia.* AIDS, 1995. **9**(9): p. 1001-8.

191. Masanetz, S. and M.H. Lehmann, *HIV-1 Nef increases astrocyte sensitivity towards exogenous hydrogen peroxide.* Virol J, 2011. **8**: p. 35.

192. Sporer, B., U. Koedel, R. Paul, B. Kohleisen, V. Erfle, A. Fontana, and H.W. Pfister, *Human immunodeficiency virus type-1 Nef protein induces blood-brain*

barrier disruption in the rat: role of matrix metalloproteinase-9. J Neuroimmunol, 2000. **102**(2): p. 125-30.

193. Schmidtmayerova, H., H.S. Nottet, G. Nuovo, T. Raabe, C.R. Flanagan, L. Dubrovsky, . . . B. Sherry, *Human immunodeficiency virus type 1 infection alters chemokine beta peptide expression in human monocytes: implications for recruitment of leukocytes into brain and lymph nodes.* Proc Natl Acad Sci U S A, 1996. **93**(2): p. 700-4.

194. Leonoudakis, D., S.P. Braithwaite, M.S. Beattie, and E.C. Beattie, *TNFalpha-induced AMPA-receptor trafficking in CNS neurons; relevance to excitotoxicity?* Neuron Glia Biol, 2004. **1**(3): p. 263-73.

195. Lannuzel, A., P.M. Lledo, H.O. Lamghitnia, J.D. Vincent, and M. Tardieu, *HIV-1 envelope proteins gp120 and gp160 potentiate NMDA-induced [Ca2+]i increase, alter [Ca2+]i homeostasis and induce neurotoxicity in human embryonic neurons.* Eur J Neurosci, 1995. **7**(11): p. 2285-93.

196. Hesselgesser, J., D. Taub, P. Baskar, M. Greenberg, J. Hoxie, D.L. Kolson, and R. Horuk, *Neuronal apoptosis induced by HIV-1 gp120 and the chemokine SDF-1 alpha is mediated by the chemokine receptor CXCR4.* Curr Biol, 1998. **8**(10): p. 595-8.

197. Meucci, O., A. Fatatis, A.A. Simen, T.J. Bushell, P.W. Gray, and R.J. Miller, *Chemokines regulate hippocampal neuronal signaling and gp120 neurotoxicity.* Proc Natl Acad Sci U S A, 1998. **95**(24): p. 14500-5.

198. Ronaldson, P.T. and R. Bendayan, *HIV-1 viral envelope glycoprotein gp120 produces oxidative stress and regulates the functional expression of multidrug resistance protein-1 (Mrp1) in glial cells.* J Neurochem, 2008. **106**(3): p. 1298-313.

199. Shah, A., S. Kumar, S.D. Simon, D.P. Singh, and A. Kumar, *HIV gp120- and methamphetamine-mediated oxidative stress induces astrocyte apoptosis via cytochrome P450 2E1.* Cell Death Dis, 2013. **4**: p. e850.

200. Pocernich, C.B., R. Sultana, H. Mohmmad-Abdul, A. Nath, and D.A. Butterfield, *HIV-dementia, Tat-induced oxidative stress, and antioxidant therapeutic considerations.* Brain Res Brain Res Rev, 2005. **50**(1): p. 14-26.

201. Kim, S.H., A.J. Smith, J. Tan, R.D. Shytle, and B. Giunta, *MSM ameliorates HIV-1 Tat induced neuronal oxidative stress via rebalance of the glutathione cycle.* Am J Transl Res, 2015. **7**(2): p. 328-38.

202. Kruman, II, A. Nath, and M.P. Mattson, *HIV-1 protein Tat induces apoptosis of hippocampal neurons by a mechanism involving caspase activation, calcium overload, and oxidative stress.* Exp Neurol, 1998. **154**(2): p. 276-88.

203. Albright, A.V., S.S. Soldan, and F. Gonzalez-Scarano, *Pathogenesis of human immunodeficiency virus-induced neurological disease.* J Neurovirol, 2003. **9**(2): p. 222-7.

204. Williams, K.C., S. Corey, S.V. Westmoreland, D. Pauley, H. Knight, C. deBakker, . . . A.A. Lackner, *Perivascular macrophages are the primary cell type productively infected by simian immunodeficiency virus in the brains of macaques: implications for the neuropathogenesis of AIDS.* J Exp Med, 2001. **193**(8): p. 905-15.

205. Shiramizu, B., J. Ananworanich, T. Chalermchai, U. Siangphoe, D. Troelstrup, C. Shikuma, . . . S.S. Group, *Failure to clear intra-monocyte HIV infection linked to persistent neuropsychological testing impairment after first-line combined antiretroviral therapy.* J Neurovirol, 2012. **18**(1): p. 69-73.

206. Glass, J.D., H. Fedor, S.L. Wesselingh, and J.C. McArthur, *Immunocytochemical quantitation of human immunodeficiency virus in the brain: correlations with dementia.* Ann Neurol, 1995. **38**(5): p. 755-62.

207. Williams, D.W., M. Veenstra, P.J. Gaskill, S. Morgello, T.M. Calderon, and J.W. Berman, *Monocytes mediate HIV neuropathogenesis: mechanisms that contribute to HIV associated neurocognitive disorders.* Curr HIV Res, 2014. **12**(2): p. 85-96.

208. Burdo, T.H., A. Lackner, and K.C. Williams, *Monocyte/macrophages and their role in HIV neuropathogenesis.* Immunol Rev, 2013. **254**(1): p. 102-13.

209. Jaeger, L.B. and A. Nath, *Modeling HIV-associated neurocognitive disorders in mice: new approaches in the changing face of HIV neuropathogenesis.* Dis Model Mech, 2012. **5**(3): p. 313-22.

210. Rosenstiel, P., A. Gharavi, V. D'Agati, and P. Klotman, *Transgenic and infectious animal models of HIV-associated nephropathy.* J Am Soc Nephrol, 2009. **20**(11): p. 2296-304.

211. Gorantla, S., H. Sneller, L. Walters, J.G. Sharp, S.J. Pirruccello, J.T. West, . . . L. Poluektova, *Human immunodeficiency virus type 1 pathobiology studied in humanized BALB/c-Rag2-/-gammac-/- mice.* J Virol, 2007. **81**(6): p. 2700-12.

212. Gorantla, S., H.E. Gendelman, and L.Y. Poluektova, *Can humanized mice reflect the complex pathobiology of HIV-associated neurocognitive disorders?* J Neuroimmune Pharmacol, 2012. **7**(2): p. 352-62.

213. Albright, A.V., J.T. Shieh, T. Itoh, B. Lee, D. Pleasure, M.J. O'Connor, . . . F. Gonzalez-Scarano, *Microglia express CCR5, CXCR4, and CCR3, but of these, CCR5 is the principal coreceptor for human immunodeficiency virus type 1 dementia isolates.* J Virol, 1999. **73**(1): p. 205-13.

214. Shah, M., T.K. Smit, S. Morgello, W. Tourtellotte, B. Gelman, B.J. Brew, and N.K. Saksena, *Env gp120 sequence analysis of HIV type 1 strains from diverse areas of the brain shows preponderance of CCR5 usage.* AIDS Res Hum Retroviruses, 2006. **22**(2): p. 177-81.

215. Yang, B., S. Singh, R. Bressani, and G.D. Kanmogne, *Cross-talk between STAT1 and PI3K/AKT signaling in HIV-1-induced blood-brain barrier dysfunction: role of CCR5 and implications for viral neuropathogenesis.* J Neurosci Res, 2010. **88**(14): p. 3090-101.

216. Chaudhuri, A., B. Yang, H.E. Gendelman, Y. Persidsky, and G.D. Kanmogne, *STAT1 signaling modulates HIV-1-induced inflammatory responses and leukocyte transmigration across the blood-brain barrier.* Blood, 2008. **111**(4): p. 2062-72.

217. Tiraboschi, J.M., J.A. Munoz-Moreno, M.C. Puertas, C. Alonso-Villaverde, A. Prats, E. Ferrer, . . . D. Podzamczer, *Viral and inflammatory markers in cerebrospinal fluid of patients with HIV-1-associated neurocognitive impairment during antiretroviral treatment switch.* HIV Med, 2015.

218. Banks, W.A., N. Ercal, and T.O. Price, *The blood-brain barrier in neuroAIDS.* Current HIV research, 2006. **4**(3): p. 259-66.

219. Vicente-Manzanares, M., D. Sancho, M. Yanez-Mo, and F. Sanchez-Madrid, *The leukocyte cytoskeleton in cell migration and immune interactions.* Int Rev Cytol, 2002. **216**: p. 233-89.

220. Schweneker, M., A.S. Bachmann, and K. Moelling, *The HIV-1 co-receptor CCR5 binds to alpha-catenin, a component of the cellular cytoskeleton.* Biochem Biophys Res Commun, 2004. **325**(3): p. 751-7.

221. Di Marzio, P., W.W. Dai, G. Franchin, A.Y. Chan, M. Symons, and B. Sherry, *Role of Rho family GTPases in CCR1- and CCR5-induced actin reorganization in macrophages.* Biochem Biophys Res Commun, 2005. **331**(4): p. 909-16.

222. Cossarini, F., A. Galli, L. Galli, A. Bigoloni, S. Salpietro, C. Vinci, . . . S. Nozza, *Immune recovery and T cell subset analysis during effective treatment with maraviroc.* J Antimicrob Chemother, 2012. **67**(10): p. 2474-8.

223. Dentone, C., A. Di Biagio, A. Parodi, F. Bozzano, P. Fraccaro, A. Signori, . . . D. Fenoglio, *Innate immunity cell activation in virologically suppressed HIV-infected maraviroc-treated patients.* AIDS, 2014. **28**(7): p. 1071-4.

224. Rossi, R., M. Lichtner, A. De Rosa, I. Sauzullo, F. Mengoni, A.P. Massetti, . . . V. Vullo, *In vitro effect of anti-human immunodeficiency virus CCR5 antagonist maraviroc on chemotactic activity of monocytes, macrophages and dendritic cells.* Clin Exp Immunol, 2011. **166**(2): p. 184-90.

225. Rossi, R., M. Lichtner, I. Sauzullo, F. Mengoni, R. Marocco, A.P. Massetti, . . . V. Vullo, *Downregulation of leukocyte migration after treatment with CCR5 antagonist maraviroc.* J Acquir Immune Defic Syndr, 2010. **54**(5): p. e13-4.

226. Hardy, W.D., R.M. Gulick, H. Mayer, G. Fatkenheuer, M. Nelson, J. Heera, . . . J. Goodrich, *Two-year safety and virologic efficacy of maraviroc in treatment-experienced patients with CCR5-tropic HIV-1 infection: 96-week combined analysis of MOTIVATE 1 and 2.* J Acquir Immune Defic Syndr, 2010. **55**(5): p. 558-64.

227. Sierra-Madero, J., G. Di Perri, R. Wood, M. Saag, I. Frank, C. Craig, . . . H. Mayer, *Efficacy and safety of maraviroc versus efavirenz, both with zidovudine/lamivudine: 96-week results from the MERIT study.* HIV Clin Trials, 2010. **11**(3): p. 125-32.

228. Shiraishi, M., Y. Aramaki, M. Seto, H. Imoto, Y. Nishikawa, N. Kanzaki, . . . M. Fujino, *Discovery of novel, potent, and selective small-molecule CCR5 antagonists as anti-HIV-1 agents: synthesis and biological evaluation of anilide derivatives with a quaternary ammonium moiety.* J Med Chem, 2000. **43**(10): p. 2049-63.

229. Baba, M., O. Nishimura, N. Kanzaki, M. Okamoto, H. Sawada, Y. Iizawa, . . . M. Fujino, *A small-molecule, nonpeptide CCR5 antagonist with highly potent and selective anti-HIV-1 activity.* Proc Natl Acad Sci U S A, 1999. **96**(10): p. 5698-703.

230. Manda, K.R., A. Banerjee, W.A. Banks, and N. Ercal, *Highly active antiretroviral therapy drug combination induces oxidative stress and mitochondrial dysfunction in immortalized human blood-brain barrier endothelial cells.* Free Radic Biol Med, 2011. **50**(7): p. 801-10.

231. Jones, G.E., *Cellular signaling in macrophage migration and chemotaxis.* J Leukoc Biol, 2000. **68**(5): p. 593-602.

232. Fenteany, G. and M. Glogauer, *Cytoskeletal remodeling in leukocyte function.* Curr Opin Hematol, 2004. **11**(1): p. 15-24.

233. Bustelo, X.R., V. Sauzeau, and I.M. Berenjeno, *GTP-binding proteins of the Rho/Rac family: regulation, effectors and functions in vivo.* Bioessays, 2007. **29**(4): p. 356-70.

234. Borges, G., E. Berrocoso, J.A. Mico, and F. Neto, *ERK1/2: Function, signaling and implication in pain and pain-related anxio-depressive disorders.* Prog Neuropsychopharmacol Biol Psychiatry, 2015. **60**: p. 77-92.

235. Carter, G.C., L. Bernstone, D. Baskaran, and W. James, *HIV-1 infects macrophages by exploiting an endocytic route dependent on dynamin, Rac1 and Pak1.* Virology, 2011. **409**(2): p. 234-50.

236. Cook, J.A., L. Albacker, A. August, and A.J. Henderson, *CD28-dependent HIV-1 transcription is associated with Vav, Rac, and NF-kappa B activation.* J Biol Chem, 2003. **278**(37): p. 35812-8.

237. Lu, X., X. Wu, A. Plemenitas, H. Yu, E.T. Sawai, A. Abo, and B.M. Peterlin, *CDC42 and Rac1 are implicated in the activation of the Nef-associated kinase and replication of HIV-1.* Curr Biol, 1996. **6**(12): p. 1677-84.

238. Song, H.Y., S.M. Ju, W.Y. Seo, A.R. Goh, J.K. Lee, Y.S. Bae, . . . J. Park, *Nox2-based NADPH oxidase mediates HIV-1 Tat-induced up-regulation of VCAM-1/ICAM-1 and subsequent monocyte adhesion in human astrocytes.* Free Radic Biol Med, 2011. **50**(5): p. 576-84.

239. MacGrath, S.M. and A.J. Koleske, *Cortactin in cell migration and cancer at a glance.* J Cell Sci, 2012. **125**(Pt 7): p. 1621-6.

240. Vidal, C., B. Geny, J. Melle, M. Jandrot-Perrus, and M. Fontenay-Roupie, *Cdc42/Rac1-dependent activation of the p21-activated kinase (PAK) regulates human platelet lamellipodia spreading: implication of the cortical-actin binding protein cortactin.* Blood, 2002. **100**(13): p. 4462-9.

241. Schnell, S.A., W.A. Staines, and M.W. Wessendorf, *Reduction of lipofuscin-like autofluorescence in fluorescently labeled tissue.* J Histochem Cytochem, 1999. **47**(6): p. 719-30.

242. Ma, A.D. and C.S. Abrams, *Pleckstrin induces cytoskeletal reorganization via a Rac-dependent pathway.* J Biol Chem, 1999. **274**(40): p. 28730-5.

243. Zhao, X., K.A. Carnevale, and M.K. Cathcart, *Human monocytes use Rac1, not Rac2, in the NADPH oxidase complex.* J Biol Chem, 2003. **278**(42): p. 40788-92.

244. Price, L.S., J. Leng, M.A. Schwartz, and G.M. Bokoch, *Activation of Rac and Cdc42 by integrins mediates cell spreading.* Mol Biol Cell, 1998. **9**(7): p. 1863-71.

245. Ma, A.D., A. Metjian, S. Bagrodia, S. Taylor, and C.S. Abrams, *Cytoskeletal reorganization by G protein-coupled receptors is dependent on phosphoinositide 3-kinase gamma, a Rac guanosine exchange factor, and Rac.* Mol Cell Biol, 1998. **18**(8): p. 4744-51.

246. Tan, T.L., N. Fang, T.L. Neo, P. Singh, J. Zhang, R. Zhou, . . . W.N. Chen, *Rac1 GTPase is activated by hepatitis B virus replication--involvement of HBX.* Biochim Biophys Acta, 2008. **1783**(3): p. 360-74.

247. D'Souza-Schorey, C., B. Boettner, and L. Van Aelst, *Rac regulates integrin-mediated spreading and increased adhesion of T lymphocytes.* Mol Cell Biol, 1998. **18**(7): p. 3936-46.

248. Abel, S., J.D. Davis, C.E. Ridgway, J.C. Hamlin, and M. Vourvahis, *Pharmacokinetics, safety and tolerability of a single oral dose of maraviroc in HIV-negative subjects with mild and moderate hepatic impairment.* Antivir Ther, 2009. **14**(6): p. 831-7.

249. Chen, B.C., J.C. Kang, Y.T. Lu, M.J. Hsu, C.C. Liao, W.T. Chiu, . . . C.H. Lin, *Rac1 regulates peptidoglycan-induced nuclear factor-kappaB activation and cyclooxygenase-2 expression in RAW 264.7 macrophages by activating the phosphatidylinositol 3-kinase/Akt pathway.* Mol Immunol, 2009. **46**(6): p. 1179-88.

250. Hordijk, P.L., *Regulation of NADPH oxidases: the role of Rac proteins.* Circ Res, 2006. **98**(4): p. 453-62.

251. Fackler, O.T., X. Lu, J.A. Frost, M. Geyer, B. Jiang, W. Luo, . . . B.M. Peterlin, *p21-activated kinase 1 plays a critical role in cellular activation by Nef.* Mol Cell Biol, 2000. **20**(7): p. 2619-27.

252. Fackler, O.T., W. Luo, M. Geyer, A.S. Alberts, and B.M. Peterlin, *Activation of Vav by Nef induces cytoskeletal rearrangements and downstream effector functions.* Mol Cell, 1999. **3**(6): p. 729-39.

253. Lu, T.C., J.C. He, Z.H. Wang, X. Feng, T. Fukumi-Tominaga, N. Chen, . . . P.E. Klotman, *HIV-1 Nef disrupts the podocyte actin cytoskeleton by interacting with diaphanous interacting protein.* J Biol Chem, 2008. **283**(13): p. 8173-82.

254. Imamura, J., Y. Suzuki, K. Gonda, C.N. Roy, H. Gatanaga, N. Ohuchi, and H. Higuchi, *Single particle tracking confirms that multivalent Tat protein transduction domain-induced heparan sulfate proteoglycan cross-linkage activates Rac1 for internalization.* J Biol Chem, 2011. **286**(12): p. 10581-92.

255. Thomas, A., C. Mariani-Floderer, M.R. Lopez-Huertas, N. Gros, E. Hamard-Peron, C. Favard, . . . D. Muriaux, *Involvement of the Rac1-IRSp53-Wave2-Arp2/3 signaling pathway in HIV-1 Gag particle release in CD4 T cells.* J Virol, 2015.

256. Pontow, S.E., N.V. Heyden, S. Wei, and L. Ratner, *Actin cytoskeletal reorganizations and coreceptor-mediated activation of rac during human immunodeficiency virus-induced cell fusion.* J Virol, 2004. **78**(13): p. 7138-47.

257. Iyengar, S., J.E. Hildreth, and D.H. Schwartz, *Actin-dependent receptor colocalization required for human immunodeficiency virus entry into host cells.* J Virol, 1998. **72**(6): p. 5251-5.

258. Kirkbride, K.C., B.H. Sung, S. Sinha, and A.M. Weaver, *Cortactin: a multifunctional regulator of cellular invasiveness.* Cell Adh Migr, 2011. **5**(2): p. 187-98.

259. Toborek, M., Y.W. Lee, G. Flora, H. Pu, I.E. Andras, E. Wylegala, . . . A. Nath, *Mechanisms of the blood-brain barrier disruption in HIV-1 infection.* Cell Mol Neurobiol, 2005. **25**(1): p. 181-99.

260. van Wetering, S., N. van den Berk, J.D. van Buul, F.P. Mul, I. Lommerse, R. Mous, . . . P.L. Hordijk, *VCAM-1-mediated Rac signaling controls endothelial cell-cell contacts and leukocyte transmigration.* Am J Physiol Cell Physiol, 2003. **285**(2): p. C343-52.

261. Woollard, S.M., H. Li, S. Singh, F. Yu, and G.D. Kanmogne, *HIV-1 induces cytoskeletal alterations and Rac1 activation during monocyte-blood-brain barrier interactions: modulatory role of CCR5.* Retrovirology, 2014. **11**: p. 20.

262. Davis, L.E., B.L. Hjelle, V.E. Miller, D.L. Palmer, A.L. Llewellyn, T.L. Merlin, . . . C.A. Wiley, *Early viral brain invasion in iatrogenic human immunodeficiency virus infection.* Neurology, 1992. **42**(9): p. 1736-9.

263. Valcour, V., T. Chalermchai, N. Sailasuta, M. Marovich, S. Lerdlum, D. Suttichom, . . . J. Ananworanich, *Central nervous system viral invasion and inflammation during acute HIV infection.* The Journal of infectious diseases, 2012. **206**(2): p. 275-82.

264. Dallasta, L.M., L.A. Pisarov, J.E. Esplen, J.V. Werley, A.V. Moses, J.A. Nelson, and C.L. Achim, *Blood-brain barrier tight junction disruption in human immunodeficiency virus-1 encephalitis.* The American journal of pathology, 1999. **155**(6): p. 1915-27.

265. Kelly, K.M., S.E. Beck, K.A. Metcalf Pate, S.E. Queen, J.L. Dorsey, R.J. Adams, . . . J.L. Mankowski, *Neuroprotective maraviroc monotherapy in simian immunodeficiency virus-infected macaques: reduced replicating and latent SIV in the brain.* AIDS, 2013. **27**(18): p. F21-8.

266. Arberas, H., A.C. Guardo, M.E. Bargallo, M.J. Maleno, M. Calvo, J.L. Blanco, . . . M. Plana, *In vitro effects of the CCR5 inhibitor maraviroc on human T cell function.* J Antimicrob Chemother, 2013. **68**(3): p. 577-86.

267. Margolick, J.B., A. Munoz, A.D. Donnenberg, L.P. Park, N. Galai, J.V. Giorgi, . . . J. Ferbas, *Failure of T-cell homeostasis preceding AIDS in HIV-1 infection. The Multicenter AIDS Cohort Study.* Nat Med, 1995. **1**(7): p. 674-80.

268. Hermiston, M.L., Z. Xu, and A. Weiss, *CD45: a critical regulator of signaling thresholds in immune cells.* Annu Rev Immunol, 2003. **21**: p. 107-37.

269. Neuhaus, W., M. Wirth, V.E. Plattner, B. Germann, F. Gabor, and C.R. Noe, *Expression of Claudin-1, Claudin-3 and Claudin-5 in human blood-brain barrier mimicking cell line ECV304 is inducible by glioma-conditioned media.* Neurosci Lett, 2008. **446**(2-3): p. 59-64.

270. Cooper, I., K. Cohen-Kashi-Malina, and V.I. Teichberg, *Claudin-5 expression in in vitro models of the blood-brain barrier.* Methods Mol Biol, 2011. **762**: p. 347-54.

271. Traweger, A., S. Toepfer, R.N. Wagner, J. Zweimueller-Mayer, R. Gehwolf, C. Lehner, . . . H. Bauer, *Beyond cell-cell adhesion: Emerging roles of the tight junction scaffold ZO-2.* Tissue Barriers, 2013. **1**(2): p. e25039.

272. Andras, I.E. and M. Toborek, *HIV-1-induced alterations of claudin-5 expression at the blood-brain barrier level.* Methods Mol Biol, 2011. **762**: p. 355-70.

273. Peluso, M.J., D.J. Meyerhoff, R.W. Price, J. Peterson, E. Lee, A.C. Young, . . . S. Spudich, *Cerebrospinal fluid and neuroimaging biomarker abnormalities suggest early neurological injury in a subset of individuals during primary HIV infection.* The Journal of infectious diseases, 2013. **207**(11): p. 1703-12.

274. Angelow, S., R. Ahlstrom, and A.S. Yu, *Biology of claudins.* Am J Physiol Renal Physiol, 2008. **295**(4): p. F867-76.

275. Tsukita, S. and M. Furuse, *The structure and function of claudins, cell adhesion molecules at tight junctions.* Ann N Y Acad Sci, 2000. **915**: p. 129-35.

276. Nitta, T., M. Hata, S. Gotoh, Y. Seo, H. Sasaki, N. Hashimoto, . . . S. Tsukita, *Size-selective loosening of the blood-brain barrier in claudin-5-deficient mice.* J Cell Biol, 2003. **161**(3): p. 653-60.

277. Andras, I.E., H. Pu, J. Tian, M.A. Deli, A. Nath, B. Hennig, and M. Toborek, *Signaling mechanisms of HIV-1 Tat-induced alterations of claudin-5 expression in brain endothelial cells.* J Cereb Blood Flow Metab, 2005. **25**(9): p. 1159-70.

278. Frank, D.A., S. Mahajan, and J. Ritz, *Fludarabine-induced immunosuppression is associated with inhibition of STAT1 signaling.* Nat Med, 1999. **5**(4): p. 444-7.

279. Yamamoto, M., S.H. Ramirez, S. Sato, T. Kiyota, R.L. Cerny, K. Kaibuchi, . . . T. Ikezu, *Phosphorylation of claudin-5 and occludin by rho kinase in brain endothelial cells.* Am J Pathol, 2008. **172**(2): p. 521-33.

280. Persidsky, Y., D. Heilman, J. Haorah, M. Zelivyanskaya, R. Persidsky, G.A. Weber, . . . T. Ikezu, *Rho-mediated regulation of tight junctions during monocyte migration across the blood-brain barrier in HIV-1 encephalitis (HIVE).* Blood, 2006. **107**(12): p. 4770-80.

281. Alexaki, A., Y. Liu, and B. Wigdahl, *Cellular reservoirs of HIV-1 and their role in viral persistence.* Curr HIV Res, 2008. **6**(5): p. 388-400.

282. McArthur, J.C., J. Steiner, N. Sacktor, and A. Nath, *Human immunodeficiency virus-associated neurocognitive disorders: Mind the gap.* Annals of neurology, 2010. **67**(6): p. 699-714.

283. Letendre, S.L., R.J. Ellis, B.M. Ances, and J.A. McCutchan, *Neurologic complications of HIV disease and their treatment.* Top HIV Med, 2010. **18**(2): p. 45-55.

284. Siccardi, M., A. D'Avolio, S. Nozza, M. Simiele, L. Baietto, F.R. Stefani, . . . A. Owen, *Maraviroc is a substrate for OATP1B1 in vitro and maraviroc plasma*

concentrations are influenced by SLCO1B1 521 T>C polymorphism. Pharmacogenet Genomics, 2010. **20**(12): p. 759-65.

285. Roth, M., A. Obaidat, and B. Hagenbuch, *OATPs, OATs and OCTs: the organic anion and cation transporters of the SLCO and SLC22A gene superfamilies.* Br J Pharmacol, 2012. **165**(5): p. 1260-87.

286. Hagenbuch, B. and P.J. Meier, *The superfamily of organic anion transporting polypeptides.* Biochim Biophys Acta, 2003. **1609**(1): p. 1-18.

287. Hua, W.J., W.X. Hua, and H.J. Fang, *The role of OATP1B1 and BCRP in pharmacokinetics and DDI of novel statins.* Cardiovasc Ther, 2012. **30**(5): p. e234-41.

288. Glaeser, H., D.G. Bailey, G.K. Dresser, J.C. Gregor, U.I. Schwarz, J.S. McGrath, . . . R.B. Kim, *Intestinal drug transporter expression and the impact of grapefruit juice in humans.* Clin Pharmacol Ther, 2007. **81**(3): p. 362-70.

289. Bronger, H., J. Konig, K. Kopplow, H.H. Steiner, R. Ahmadi, C. Herold-Mende, . . . A.T. Nies, *ABCC drug efflux pumps and organic anion uptake transporters in human gliomas and the blood-tumor barrier.* Cancer Res, 2005. **65**(24): p. 11419-28.

290. Ji, C., W.R. Tschantz, N.D. Pfeifer, M. Ullah, and N. Sadagopan, *Development of a multiplex UPLC-MRM MS method for quantification of human membrane transport proteins OATP1B1, OATP1B3 and OATP2B1 in in vitro systems and tissues.* Anal Chim Acta, 2012. **717**: p. 67-76.

291. Hagenbuch, B. and P.J. Meier, *Organic anion transporting polypeptides of the OATP/ SLC21 family: phylogenetic classification as OATP/ SLCO superfamily, new nomenclature and molecular/functional properties.* Pflugers Arch, 2004. **447**(5): p. 653-65.

292. Kullak-Ublick, G.A., B. Hagenbuch, B. Stieger, C.D. Schteingart, A.F. Hofmann, A.W. Wolkoff, and P.J. Meier, *Molecular and functional characterization of an organic anion transporting polypeptide cloned from human liver.* Gastroenterology, 1995. **109**(4): p. 1274-82.

293. Hartkoorn, R.C., W.S. Kwan, V. Shallcross, A. Chaikan, N. Liptrott, D. Egan, . . . A. Owen, *HIV protease inhibitors are substrates for OATP1A2, OATP1B1 and OATP1B3 and lopinavir plasma concentrations are influenced by SLCO1B1 polymorphisms.* Pharmacogenet Genomics, 2010. **20**(2): p. 112-20.

294. Rubio-Aliaga, I. and H. Daniel, *Peptide transporters and their roles in physiological processes and drug disposition.* Xenobiotica, 2008. **38**(7-8): p. 1022-42.

295. Yilmaz, A., C. Verhofstede, A. D'Avolio, V. Watson, L. Hagberg, D. Fuchs, . . . M. Gisslen, *Treatment intensification has no effect on the HIV-1 central nervous system infection in patients on suppressive antiretroviral therapy.* J Acquir Immune Defic Syndr, 2010. **55**(5): p. 590-6.

296. Ndhlovu, L.C., T. Umaki, G.M. Chew, D.C. Chow, M. Agsalda, K.J. Kallianpur, . . . C.M. Shikuma, *Treatment intensification with maraviroc (CCR5 antagonist) leads to declines in CD16-expressing monocytes in cART-suppressed chronic HIV-infected subjects and is associated with improvements in neurocognitive test performance: implications for HIV-associated neurocognitive disease (HAND).* J Neurovirol, 2014. **20**(6): p. 571-82.

297. Okoye, A.A. and L.J. Picker, *CD4(+) T-cell depletion in HIV infection: mechanisms of immunological failure.* Immunol Rev, 2013. **254**(1): p. 54-64.

298. Catalfamo, M., C. Wilhelm, L. Tcheung, M. Proschan, T. Friesen, J.H. Park, . . . C. Lane, *CD4 and CD8 T cell immune activation during chronic HIV infection:*

roles of homeostasis, HIV, type I IFN, and IL-7. J Immunol, 2011. **186**(4): p. 2106-16.

299. Guntermann, C., N. Amft, B.J. Murphy, and K.E. Nye, *Impaired CD45-associated tyrosine phosphatase activity during HIV-1 infection: implications for CD3 and CD4 receptor signalling.* Biochem Biophys Res Commun, 1998. **252**(1): p. 69-77.
300. Wittchen, E.S., J.D. van Buul, K. Burridge, and R.A. Worthylake, *Trading spaces: Rap, Rac, and Rho as architects of transendothelial migration.* Curr Opin Hematol, 2005. **12**(1): p. 14-21.
301. Cuzin, L., S. Trabelsi, P. Delobel, C. Barbuat, J. Reynes, C. Allavena, . . . A.M.S. group, *Maraviroc intensification of stable antiviral therapy in HIV-1-infected patients with poor immune restoration: MARIMUNO-ANRS 145 study.* J Acquir Immune Defic Syndr, 2012. **61**(5): p. 557-64.
302. Boven, L.A., J. Middel, J. Verhoef, C.J. De Groot, and H.S. Nottet, *Monocyte infiltration is highly associated with loss of the tight junction protein zonula occludens in HIV-1-associated dementia.* Neuropathol Appl Neurobiol, 2000. **26**(4): p. 356-60.
303. Popik, W., J.E. Hesselgesser, and P.M. Pitha, *Binding of human immunodeficiency virus type 1 to CD4 and CXCR4 receptors differentially regulates expression of inflammatory genes and activates the MEK/ERK signaling pathway.* J Virol, 1998. **72**(8): p. 6406-13.
304. Lin, J.H. and M. Yamazaki, *Role of P-glycoprotein in pharmacokinetics: clinical implications.* Clin Pharmacokinet, 2003. **42**(1): p. 59-98.
305. Sankatsing, S.U., J.H. Beijnen, A.H. Schinkel, J.M. Lange, and J.M. Prins, *P glycoprotein in human immunodeficiency virus type 1 infection and therapy.* Antimicrob Agents Chemother, 2004. **48**(4): p. 1073-81.

306. Kaul, M. and S.A. Lipton, *Chemokines and activated macrophages in HIV gp120-induced neuronal apoptosis.* Proc Natl Acad Sci U S A, 1999. **96**(14): p. 8212-6.

307. Kaul, M., Q. Ma, K.E. Medders, M.K. Desai, and S.A. Lipton, *HIV-1 coreceptors CCR5 and CXCR4 both mediate neuronal cell death but CCR5 paradoxically can also contribute to protection.* Cell Death Differ, 2007. **14**(2): p. 296-305.

308. Eden, A., D. Fuchs, L. Hagberg, S. Nilsson, S. Spudich, B. Svennerholm, . . . M. Gisslen, *HIV-1 viral escape in cerebrospinal fluid of subjects on suppressive antiretroviral treatment.* J Infect Dis, 2010. **202**(12): p. 1819-25.

309. Robertson, K., J. Liner, and R.B. Meeker, *Antiretroviral neurotoxicity.* J Neurovirol, 2012. **18**(5): p. 388-99.